Chapter 6
Handling of Road Cars

Ordinary road cars are by far the most common type of motor vehicle. Almost all of them share the following features relevant to handling:

1. four wheels (two axles);
2. two-wheel drive;
3. open differential;
4. no wings (and hence, no significant aerodynamic downforces);
5. no intervention by electronic active safety systems like ABS or ESP under ordinary operating conditions.

Moreover, in the mathematical models it is also typically assumed that the vehicle moves on a *flat* road at almost *constant* forward speed u, thus requiring small longitudinal forces by the tires.

The handling analysis of this kind of vehicles is somehow the simplest that can be envisaged.[1] That does not mean that it is simple at all.

The vehicle model developed in Chap. 3 is employed. However, owing to the above listed features of road cars, several additional simplifications can be made, which first lead to the *double track model* and eventually to the celebrated *single track model*. All the steps that lead to the single track model are thoroughly discussed to clarify when it is a suitable model for vehicle dynamics.

[1] Some sports cars and all race cars have a limited-slip differential. Several race cars also have wings that provide fairly high aerodynamic downforces at high speed. The handling of these vehicles is somehow more involved than that of ordinary road cars and will be addressed in Chap. 7.

The original version of this chapter was revised: Belated corrections have been incorporated. The correction to this chapter is available at https://doi.org/10.1007/978-3-319-73220-6_12

M. Guiggiani, *The Science of Vehicle Dynamics*,
https://doi.org/10.1007/978-3-319-73220-6_6

6.1 Additional Simplifying Assumptions for Road Car Modeling

The vehicle model introduced in Chap. 3, and whose equations were collected in Sect. 3.15, is simplified hereafter, taking into account the distinguishing features relevant to handling of road cars (Fig. 6.1).

6.1.1 Negligible Vertical Aerodynamic Loads

Aerodynamics of road cars is mostly concerned with attaining low drag, because of its impact on fuel consumption. Therefore, road cars normally do not have aerodynamic devices to generate significant vertical loads, that is $Z_1^a \simeq 0$ and $Z_2^a \simeq 0$. Basically, this means that the handling features of a road car are (almost) speed insensitive.

6.1.2 Almost Constant Forward Speed

Moreover, if the forward speed u is almost constant ($\dot{u} \simeq 0$, and hence $a_x \simeq 0$), and the aerodynamic drag is not very high (like in ordinary cars, but not in a Formula 1

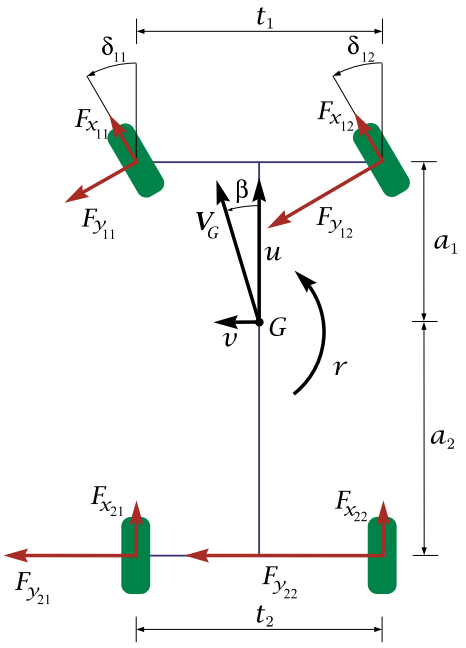

Fig. 6.1 Vehicle basic scheme (double track model)

car, which, however, does not have an open differential),[2] the tire longitudinal forces are quite small (Fig. 6.1). That means that also the *longitudinal slips are small and can be neglected*. Therefore,

$$\begin{aligned} F_{x_{ij}} &\simeq 0 \\ \sigma_{x_{ij}} &\simeq 0 \end{aligned} \tag{6.1}$$

which means that all wheels are almost under longitudinal pure rolling conditions.

6.1.3 Open Differential

The main simplification is that the vehicle is equipped with an *open differential*. Since there is almost no friction inside an open differential mechanism, in (3.169) we have that its internal efficiency $\eta_h \simeq 1$, and hence $M_l \simeq M_r$. In other words, both driving wheels receive always the same torque from the engine. Therefore, in the global equilibrium equations (3.91), the tire longitudinal forces $F_{x_{ij}}$ (Fig. 6.1) are such that $F_{x_{11}} = F_{x_{12}}$ and $F_{x_{21}} = F_{x_{22}}$, and hence do not contribute to the yaw moment N applied to the vehicle. Summing up, in (3.85)

$$\begin{aligned} \Delta X_1 &= -[F_{y_{12}} \sin(\delta_{12}) - F_{y_{11}} \sin(\delta_{11})]/2 \\ \Delta X_2 &= 0 \end{aligned} \tag{6.2}$$

Basically, this means that the handling features of a road car are (almost) insensitive to the radius of curvature of its trajectory, provided the radius is not too small.

A look at Fig. 3.26 can be useful to better understand $\Delta X_1 = (X_{12} - X_{11})/2$.

6.2 Mathematical Model for Road Car Handling

The equations collected in Sect. 3.15 for the fairly general vehicle model described in Chap. 3 are now tailored to the case of road cars with open differential, no wings, and almost constant forward speed.

The general definitions (3.84) for the horizontal (in-plane) forces acting on the vehicle now become (Figs. 6.1 and 6.2)

[2] The left and right wheels of the same axle are normally equipped with the same kind of brake. Therefore, the braking torque is pretty much the same under ordinary operating conditions, and, again, (6.2) holds true. However, there are important exceptions. The left and right braking forces can be different if: (a) the grip is different and at least one wheel is locked; (b) the friction coefficients inside the two brakes is different (for instance, because of different temperatures, which is often the case in racing cars); (c) some electronic stability system, like ESP or ABS, has been activated.

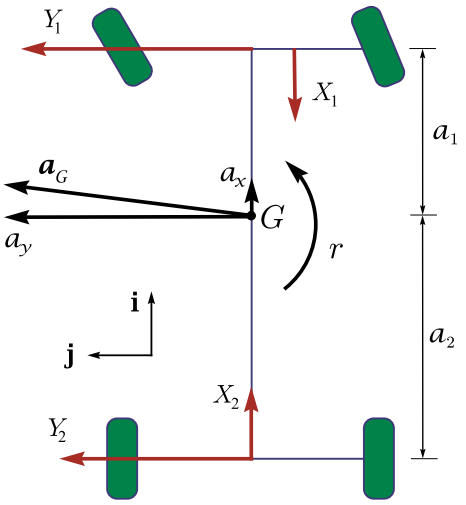

Fig. 6.2 Global dynamics of the double track model

$$
\begin{aligned}
X_1 &= F_{x_{11}}\cos(\delta_{11}) + F_{x_{12}}\cos(\delta_{12}) - [F_{y_{11}}\sin(\delta_{11}) + F_{y_{12}}\sin(\delta_{12})] \\
X_2 &= F_{x_{21}} + F_{x_{22}} \\
Y_1 &= F_{y_{11}}\cos(\delta_{11}) + F_{y_{12}}\cos(\delta_{12}) \\
Y_2 &= F_{y_{21}} + F_{y_{22}} \\
\Delta X_1 &= -[F_{y_{12}}\sin(\delta_{12}) - F_{y_{11}}\sin(\delta_{11})]/2 \\
\Delta X_2 &= 0
\end{aligned}
\tag{6.3}
$$

6.2.1 Global Equilibrium

Since the forward speed u in (3.91) is given, the vehicle has basically only *lateral* and *yaw* dynamics (often simply called lateral dynamics), described by the following system of two differential equations (Fig. 6.2)

$$
\begin{aligned}
ma_y &= m(\dot{v} + ur) = Y = Y_1 + Y_2 \\
J_z\dot{r} &= N = Y_1 a_1 - Y_2 a_2 + \Delta X_1 t_1
\end{aligned}
\tag{6.4}
$$

while

$$
ma_x = m(\dot{u} - vr) = X = X_1 + X_2 - \frac{1}{2}\rho_a S_a C_x u^2 \tag{6.5}
$$

is now an algebraic equation, the unknown being the sum $X_1 + X_2$ of the tire longitudinal forces (see (6.3)).

We recall that u is the longitudinal velocity, v is the lateral velocity of G, r is the vehicle yaw rate, a_x is the longitudinal acceleration, while a_y is the lateral acceleration. The vehicle has mass m and moment of inertia J_z with respect to a vertical axis located at G.

6.2.2 Approximate Lateral Forces

In all two-axle vehicles with an open differential, it is possible to solve (6.4) with respect to the front and rear lateral forces (cf. (3.97))

$$\begin{aligned} Y_1 &= \frac{ma_2}{l}\, a_y + \frac{J_z\dot{r} - \Delta X_1 t_1}{l} \simeq \frac{ma_2}{l}\, a_y \\ Y_2 &= \frac{ma_1}{l}\, a_y - \frac{J_z\dot{r} - \Delta X_1 t_1}{l} \simeq \frac{ma_1}{l}\, a_y \end{aligned} \tag{6.6}$$

where, in the last terms, we took into account that $|J_z\dot{r}| \ll |ma_y a_i|$, since in a car $J_z < ma_1a_2$ and $|\dot{r}a_i| \ll |a_y|$. The other term $\Delta X_1 t_1$ becomes relevant if the wheel steer angle is at least 15°. It is common practice to ignore this contribution. In most cases it is hardly mentioned, and almost always neglected, although it can be far from negligible. The main reason for this "ostracism" is that the analysis is much simpler if $\Delta X_1 t_1$ is set to zero.

Moreover, under ordinary operating conditions $|\dot{v}| \ll |ur|$ (Fig. 3.7), and we can use

$$\tilde{a}_y = ur = u^2\rho \tag{6.7}$$

already defined in (3.28), instead of the full expression $a_y = \dot{v} + ur$ of the lateral acceleration, to approximately evaluate the axle lateral forces (cf. (3.97))

$$Y_1 \simeq \frac{ma_2}{l}\, \tilde{a}_y \qquad \text{and} \qquad Y_2 \simeq \frac{ma_1}{l}\, \tilde{a}_y \tag{6.8}$$

Therefore, in a *two-axle* vehicle with *open differential*, the axle lateral forces are approximately *linear* functions of the lateral acceleration $\tilde{a}_y$. This is a simple, yet fundamental result in vehicle dynamics of road cars, which greatly impacts on the whole vehicle model.

Equation (6.8) hold true only when $\dot{v} = \dot{r} = 0$, that is when the vehicle is in steady-state conditions. However, they are sufficiently accurate when employed to estimate lateral load transfers and roll angles, as will be shown. Actually, we should never forget that in the present analysis there is no roll dynamics (except in Chap. 9). Therefore, the roll angle is always assumed to be the angle at steady state.

6.2.3 Lateral Load Transfers and Vertical Loads

According to (3.148) and (3.152), both lateral load transfers ΔZ_1 and ΔZ_2 are *linear* functions of both lateral forces Y_1 and Y_2.

Inserting (6.8) into (3.148), we obtain the following simplified equations for the lateral load transfers in vehicles with open differential and linear springs

$$\begin{aligned}\Delta Z_1 &\simeq \frac{k_{\phi_1}k_{\phi_2}}{t_1 k_\phi}\left(\frac{h-q}{k_{\phi_2}}+\frac{a_2q_1}{lk^s_{\phi_1}}+\frac{a_2q_1}{lk^s_{\phi_2}}+\frac{a_2q_1+a_1q_2}{lk^p_{\phi_2}}\right)m\tilde{a}_y=\eta_1 m\tilde{a}_y\\ \Delta Z_2 &\simeq \frac{k_{\phi_1}k_{\phi_2}}{t_2 k_\phi}\left(\frac{h-q}{k_{\phi_1}}+\frac{a_1q_2}{lk^s_{\phi_1}}+\frac{a_1q_2}{lk^s_{\phi_2}}+\frac{a_2q_1+a_1q_2}{lk^p_{\phi_1}}\right)m\tilde{a}_y=\eta_2 m\tilde{a}_y\end{aligned} \tag{6.9}$$

or, equivalently

$$\begin{aligned}\Delta Z_1 &\simeq \frac{1}{t_1}\left[\frac{k_{\phi_1}}{k_\phi}(h-q)+\frac{a_2q_1}{l}+\frac{k_{\phi_1}k_{\phi_2}}{k_\phi l}\left(\frac{a_1q_2}{k^p_{\phi_2}}-\frac{a_2q_1}{k^p_{\phi_1}}\right)\right]m\tilde{a}_y=\eta_1 m\tilde{a}_y\\ \Delta Z_2 &\simeq \frac{1}{t_2}\left[\frac{k_{\phi_2}}{k_\phi}(h-q)+\frac{a_1q_2}{l}+\frac{k_{\phi_1}k_{\phi_2}}{k_\phi l}\left(\frac{a_2q_1}{k^p_{\phi_1}}-\frac{a_1q_2}{k^p_{\phi_2}}\right)\right]m\tilde{a}_y=\eta_2 m\tilde{a}_y\end{aligned} \tag{6.10}$$

where $l = a_1 + a_2$ is the wheelbase, $q = (a_2q_1 + a_1q_2)/l$, and

$$k_\phi = k_{\phi_1} + k_{\phi_2} = \frac{k^s_{\phi_1}k^p_{\phi_1}}{k^s_{\phi_1}+k^p_{\phi_1}} + \frac{k^s_{\phi_2}k^p_{\phi_2}}{k^s_{\phi_2}+k^p_{\phi_2}} \tag{3.145'}$$

is the global roll stiffness.

The two quantities η_1 and η_2, and hence the ratio $\Delta Z_1/\Delta Z_2 = \eta_1/\eta_2$, depend in a peculiar way on the track widths t_i, on the roll stiffnesses of the suspensions $k^s_{\phi_i}$, on the roll stiffnesses of the tires $k^p_{\phi_i}$, on the heights q_i of the no-roll centers Q_i,[3] on the longitudinal position (a_1, a_2) and height h of the center of gravity G (Fig. 6.3). The roll stiffnesses are defined in Sect. 3.10.6, and in particular in (3.145). The no-roll centers are defined in Sect. 3.10.9.

If the tires are supposed to be perfectly rigid, that is $k^p_{\phi_i} \to \infty$ and $k^s_{\phi_i} = k_{\phi_i}$, the expressions of the lateral load transfers (6.10) become much simpler

[3] We call no-roll center what is commonly called roll center.

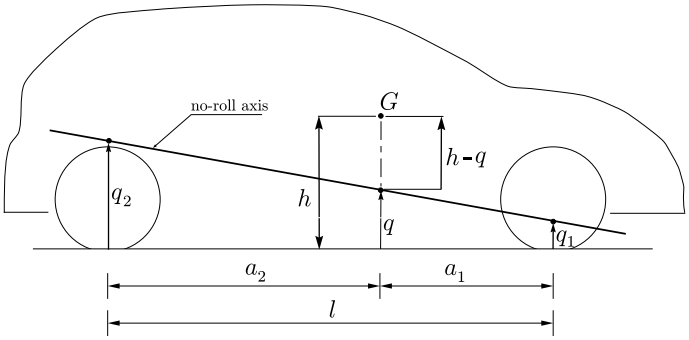

Fig. 6.3 Geometric parameters that affect lateral load transfers

$$\begin{aligned}\Delta Z_1 &\simeq \frac{1}{t_1}\left[\frac{k_{\phi_1}(h-q)}{k_\phi}+\frac{a_2 q_1}{l}\right] m\tilde{a}_y = \eta_1 m\tilde{a}_y \\ \Delta Z_2 &\simeq \frac{1}{t_2}\left[\frac{k_{\phi_2}(h-q)}{k_\phi}+\frac{a_1 q_2}{l}\right] m\tilde{a}_y = \eta_2 m\tilde{a}_y\end{aligned} \tag{6.11}$$

as in (3.155).

Taking (6.8) into account we also obtain that

$$\Delta Z_1 = \eta_1 \frac{l}{a_2} Y_1 \qquad \text{and} \qquad \Delta Z_2 = \eta_2 \frac{l}{a_1} Y_2 \tag{6.12}$$

The ratio

$$\frac{\Delta Z_1}{\Delta Z_2} = \frac{\eta_1}{\eta_2} \tag{6.13}$$

is of paramount importance since it strongly affects the handling behavior. This aspect will be thoroughly discussed in Sect. 6.5.3.

The total vertical loads (3.106) on each tire can be further simplified because the longitudinal load transfer ΔZ is negligible. Moreover, cars with an open differential are not so sporty to have significant aerodynamic vertical loads. Therefore, combining (3.106) and (6.9), we obtain

$$\begin{aligned}Z_{11} = F_{z_{11}} &= \frac{Z_1^0}{2} - \Delta Z_1(\tilde{a}_y) = \frac{mga_2}{2l} - \eta_1 m\tilde{a}_y \\ Z_{12} = F_{z_{12}} &= \frac{Z_1^0}{2} + \Delta Z_1(\tilde{a}_y) = \frac{mga_2}{2l} + \eta_1 m\tilde{a}_y \\ Z_{21} = F_{z_{21}} &= \frac{Z_2^0}{2} - \Delta Z_2(\tilde{a}_y) = \frac{mga_1}{2l} - \eta_2 m\tilde{a}_y \\ Z_{22} = F_{z_{22}} &= \frac{Z_2^0}{2} + \Delta Z_2(\tilde{a}_y) = \frac{mga_1}{2l} + \eta_2 m\tilde{a}_y\end{aligned} \tag{6.14}$$

which shows that the variations of vertical loads are (linear) functions of the lateral acceleration $\tilde{a}_y = ur$.

6.2.4 Roll Angles

Also the (steady-state) roll angles due to suspension deflections (3.144) depend upon Y_1 and Y_2, and hence can be set as functions of the lateral acceleration only[4]

$$\begin{aligned}\phi_1^s &= \frac{1}{k_{\phi_1}^s}\frac{k_{\phi_1}k_{\phi_2}}{k_\phi}\left[\frac{h-q}{k_{\phi_2}} - \frac{a_2 q_1}{l k_{\phi_1}^p} + \frac{a_1 q_2}{l k_{\phi_2}^p}\right] m\tilde{a}_y = \rho_1^s m\tilde{a}_y \\ \phi_2^s &= \frac{1}{k_{\phi_2}^s}\frac{k_{\phi_1}k_{\phi_2}}{k_\phi}\left[\frac{h-q}{k_{\phi_1}} - \frac{a_1 q_2}{l k_{\phi_2}^p} + \frac{a_2 q_1}{l k_{\phi_1}^p}\right] m\tilde{a}_y = \rho_2^s m\tilde{a}_y\end{aligned} \tag{6.15}$$

The same applies to roll angles ϕ_i^p due to tire deformations. According to (3.141) and (6.9) we obtain

$$\begin{aligned}\phi_1^p &= \frac{\Delta Z_1 t_1}{k_{\phi_1}^p} = \frac{\eta_1 t_1}{k_{\phi_1}^p} m\tilde{a}_y = \rho_1^p m\tilde{a}_y \\ \phi_2^p &= \frac{\Delta Z_2 t_2}{k_{\phi_2}^p} = \frac{\eta_2 t_2}{k_{\phi_2}^p} m\tilde{a}_y = \rho_2^p m\tilde{a}_y\end{aligned} \tag{6.16}$$

If the tires are supposed to be rigid, we have $\rho_1^p = \rho_2^p = 0$, and $\rho_1^s = \rho_2^s = (h - q)/k_\phi$.

The roll angles (Fig. 6.4) are important because they affect camber angles and steer angles of the wheels, as shown hereafter.

6.2.5 Camber Angle Variations

Let, $\gamma_{i2}^0 = -\gamma_{i1}^0 = \gamma_i^0$ be the camber angles under static conditions (Fig. 6.5), and let $\Delta\gamma_{i1} = \Delta\gamma_{i2} = \Delta\gamma_i$ be the camber variations due to vehicle roll motion (Fig. 6.6). The camber angles of the two wheels of the same axle are thus given by

$$\gamma_{i1} = -\gamma_i^0 + \Delta\gamma_i \qquad \gamma_{i2} = \gamma_i^0 + \Delta\gamma_i \tag{6.17}$$

where the camber variation $\Delta\gamma_i$, according to (3.110), (6.15) and (6.16), depends on the roll angles, and hence on the lateral acceleration $\tilde{a}_y$

[4] In this model the roll inertial effects are totally disregarded.

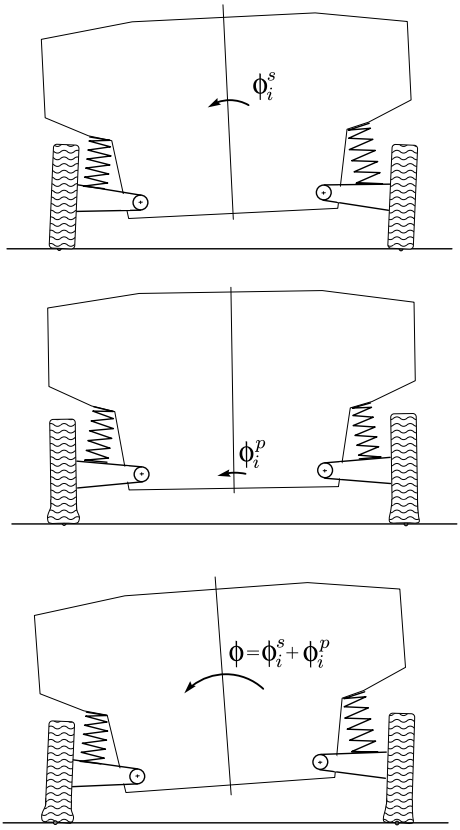

Fig. 6.4 Roll angle ϕ_i^s due to suspension deflections only, roll angle ϕ_i^p due to tire deformations only, and total vehicle roll angle ϕ (front view)

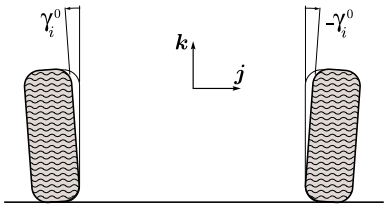

Fig. 6.5 Positive static camber γ_i^0 (front view)

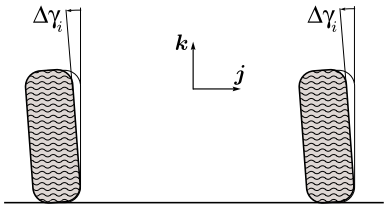

Fig. 6.6 Positive camber variations $\Delta\gamma_i$ due to roll motion (front view)

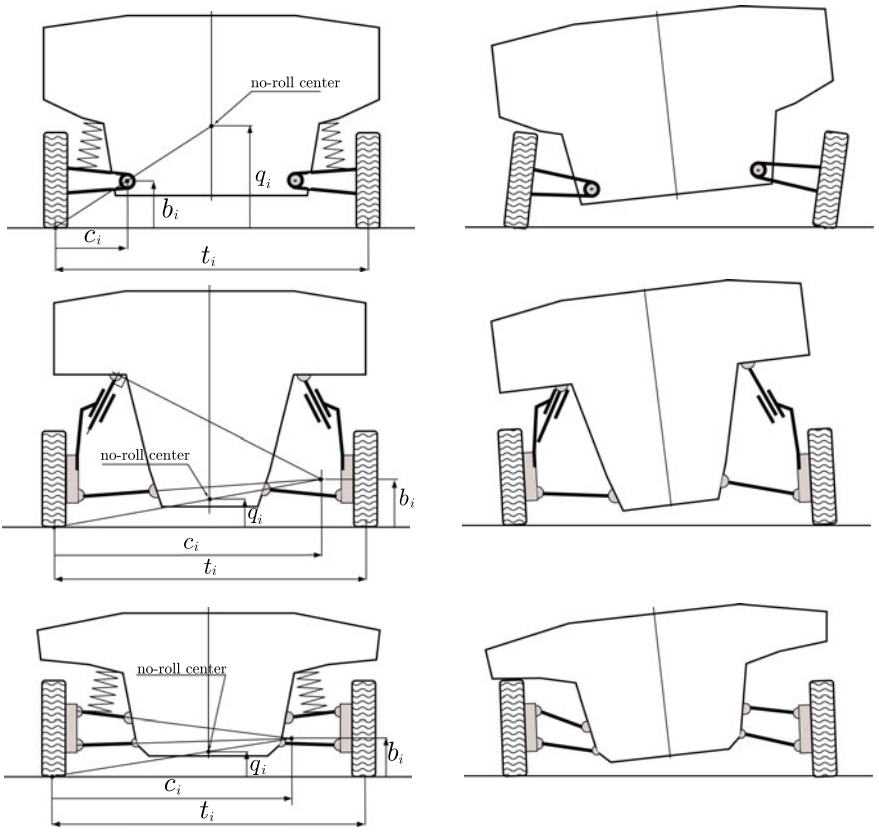

Fig. 6.7 Front view of three different suspensions (right), and their camber variations (left) due to the same positive vehicle roll angle ϕ_i^s (tire roll angle ϕ_i^p not considered)

$$\Delta\gamma_i \simeq \left[-\left(\frac{t_i/2 - c_i}{c_i} \right) \rho_i^s + \rho_i^p \right] m\tilde{a}_y = \chi_i m\tilde{a}_y \tag{6.18}$$

since the term $\pm z_i^s / c_i$ is usually negligible.

Three suspensions with the same t_i, but with different values of c_i, are shown in Fig. 6.7. We see that, as expected, the same amount of vehicle roll angle ϕ_i^s yields different camber variations (tire roll angle ϕ_i^p not considered).

6.2.6 *Steer Angles*

According to (3.198) and taking into account (6.15), we obtain the following (approximate, but very good) expressions for the steering angles of the two wheels of the

same axle

$$\begin{aligned}\delta_{i1} &= -\delta_i^0 + \tau_i \delta_v + \varepsilon_i \frac{t_i}{2l}(\tau_i \delta_v)^2 + \Upsilon_i \rho_i^s m\tilde{a}_y = \delta_{i1}(\delta_v, \tilde{a}_y) \\ \delta_{i2} &= \delta_i^0 + \tau_i \delta_v - \varepsilon_i \frac{t_i}{2l}(\tau_i \delta_v)^2 + \Upsilon_i \rho_i^s m\tilde{a}_y = \delta_{i2}(\delta_v, \tilde{a}_y)\end{aligned} \tag{6.19}$$

which are, obviously, functions of the steering wheel rotation δ_v imposed by the driver and, possibly, of the lateral acceleration $\tilde{a}_y = ur$.

In (6.19), as discussed in Sect. 3.4, δ_i^0 is the static toe angle, τ_i is the first-order gear ratio of the whole steering system, ε_i is the Ackermann coefficient for dynamic toe, Υ_i is the roll steer coefficient and $\rho_i^s m\tilde{a}_y$ is the suspension roll angle ϕ_i^s. If the tires are supposed to be rigid, we have $\rho_1^s = \rho_2^s = (h-q)/k_\phi$. The analysis is considerably simpler if $\Upsilon_i = 0$, that is if there is no roll steer. Most cars have $\tau_2 = 0$, that is no direct steering of the rear wheels.

6.2.7 Tire Slips

As already stated in Sect. 6.1.2, in the model under investigation all wheels are almost under longitudinal pure rolling conditions, that is $\sigma_{x_{ij}} \simeq 0$. Therefore, according to (3.59)

$$\begin{aligned}\omega_{11} r_1 &= (u - rt_1/2)\cos(\delta_{11}) + (v + ra_1)\sin(\delta_{11}) \\ \omega_{12} r_1 &= (u + rt_1/2)\cos(\delta_{12}) + (v + ra_1)\sin(\delta_{12}) \\ \omega_{21} r_2 &= (u - rt_2/2)\cos(\delta_{21}) + (v - ra_2)\sin(\delta_{21}) \\ \omega_{22} r_2 &= (u + rt_2/2)\cos(\delta_{22}) + (v - ra_2)\sin(\delta_{22})\end{aligned} \tag{6.20}$$

where ω_{ij} is the angular velocity of the corresponding rim and r_i is the wheel rolling radius, as defined in (2.38).

Under these assumed operating conditions, the tire *lateral* slips (3.60) become

$$\begin{aligned}\sigma_{y_{11}} &= \frac{(v + ra_1)\cos(\delta_{11}) - (u - rt_1/2)\sin(\delta_{11})}{(u - rt_1/2)\cos(\delta_{11}) + (v + ra_1)\sin(\delta_{11})} \\ \sigma_{y_{12}} &= \frac{(v + ra_1)\cos(\delta_{12}) - (u + rt_1/2)\sin(\delta_{12})}{(u + rt_1/2)\cos(\delta_{12}) + (v + ra_1)\sin(\delta_{12})} \\ \sigma_{y_{21}} &= \frac{(v - ra_2)\cos(\delta_{21}) - (u - rt_2/2)\sin(\delta_{21})}{(u - rt_2/2)\cos(\delta_{21}) + (v - ra_2)\sin(\delta_{21})} \\ \sigma_{y_{22}} &= \frac{(v - ra_2)\cos(\delta_{22}) - (u + rt_2/2)\sin(\delta_{22})}{(u + rt_2/2)\cos(\delta_{22}) + (v - ra_2)\sin(\delta_{22})}\end{aligned} \tag{6.21}$$

where $\delta_{ij} = \delta_{ij}(\delta_v, ur)$ as in (6.19).

Therefore, more compactly

$$\sigma_{y_{ij}} = \sigma_{y_{ij}}\big(v, r; u, \delta_{ij}(\delta_v, ur)\big) \tag{6.22}$$

It will turn useful to have these very same slips expressed in terms of $\beta = v/u$ and $\rho = r/u$

$$\begin{aligned}
\sigma_{y_{11}} &= \frac{(\beta + \rho a_1)\cos(\delta_{11}) - (1 - \rho t_1/2)\sin(\delta_{11})}{(1 - \rho t_1/2)\cos(\delta_{11}) + (\beta + \rho a_1)\sin(\delta_{11})} \\
\sigma_{y_{12}} &= \frac{(\beta + \rho a_1)\cos(\delta_{12}) - (1 + \rho t_1/2)\sin(\delta_{12})}{(1 + \rho t_1/2)\cos(\delta_{12}) + (\beta + \rho a_1)\sin(\delta_{12})} \\
\sigma_{y_{21}} &= \frac{(\beta - \rho a_2)\cos(\delta_{21}) - (1 - \rho t_2/2)\sin(\delta_{21})}{(1 - \rho t_2/2)\cos(\delta_{21}) + (\beta - \rho a_2)\sin(\delta_{21})} \\
\sigma_{y_{22}} &= \frac{(\beta - \rho a_2)\cos(\delta_{22}) - (1 + \rho t_2/2)\sin(\delta_{22})}{(1 + \rho t_2/2)\cos(\delta_{22}) + (\beta - \rho a_2)\sin(\delta_{22})}
\end{aligned} \tag{6.23}$$

and, more compactly

$$\sigma_{y_{ij}} = \sigma_{y_{ij}}\big(\beta, \rho; \delta_{ij}(\delta_v, ur)\big) \tag{6.24}$$

We see that the "main" dependence on u has disappeared.

6.2.8 *Simplified Tire Slips*

Equation (6.21) can be simplified without impairing their accuracy too much. More precisely, taking into account that $u \gg |v|$, $u \gg |rt_i|$, $|\delta_{ij}| \ll 1$, and $\omega_{ij} r_i \simeq u$, we obtain (cf. (3.55))

$$\begin{aligned}
\sigma_{y_{11}} &\simeq \frac{v + ra_1}{u} - \delta_{11} = \beta + \rho a_1 - \delta_{11} \\
\sigma_{y_{12}} &\simeq \frac{v + ra_1}{u} - \delta_{12} = \beta + \rho a_1 - \delta_{12} \\
\sigma_{y_{21}} &\simeq \frac{v - ra_2}{u} - \delta_{21} = \beta - \rho a_2 - \delta_{21} \\
\sigma_{y_{22}} &\simeq \frac{v - ra_2}{u} - \delta_{22} = \beta - \rho a_2 - \delta_{22}
\end{aligned} \tag{6.25}$$

or, more explicitly, according to (6.19)

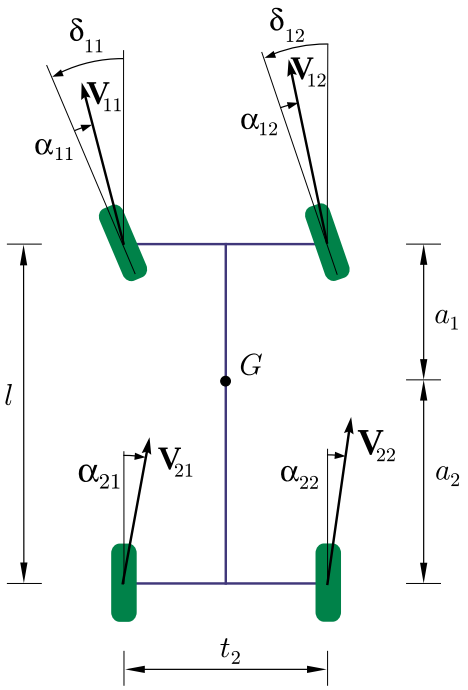

Fig. 6.8 Actual slip angles α_{ij} in the double track model

$$
\begin{aligned}
\sigma_{y_{11}} &\simeq \frac{v + ra_1}{u} - \left(\tau_1\delta_v - \delta_1^0 + \varepsilon_1\frac{t_1}{2l}(\tau_1\delta_v)^2 + \Upsilon_1\rho_1^s mur\right) \simeq -\alpha_{11} \\
\sigma_{y_{12}} &\simeq \frac{v + ra_1}{u} - \left(\tau_1\delta_v + \delta_1^0 - \varepsilon_1\frac{t_1}{2l}(\tau_1\delta_v)^2 + \Upsilon_1\rho_1^s mur\right) \simeq -\alpha_{12} \\
\sigma_{y_{21}} &\simeq \frac{v - ra_2}{u} - \left(\tau_2\delta_v - \delta_2^0 + \varepsilon_2\frac{t_2}{2l}(\tau_2\delta_v)^2 + \Upsilon_2\rho_2^s mur\right) \simeq -\alpha_{21} \\
\sigma_{y_{22}} &\simeq \frac{v - ra_2}{u} - \left(\tau_2\delta_v + \delta_2^0 - \varepsilon_2\frac{t_2}{2l}(\tau_2\delta_v)^2 + \Upsilon_2\rho_2^s mur\right) \simeq -\alpha_{22}
\end{aligned}
\tag{6.26}
$$

where α_{ij} are the *actual* tire slip angles (Fig. 6.8), already defined in (3.55) and (3.58). Most cars have $\tau_2 = 0$, that is no direct steering of the rear wheels.

Again, more compactly

$$
\sigma_{y_{ij}} = \sigma_{y_{ij}}\big(v, r; u, \delta_{ij}(\delta_v, ur)\big) \simeq -\alpha_{ij} \tag{6.27}
$$

almost like in (6.22).

Equations (6.21) and (6.26) show how the lateral tire slips σ_{ij} are related to the global vehicle motion, to the kinematic steer angles, to the toe-in/out angles, and to the roll steer angle. None of these contributions can be neglected, in general.

6.2.9 Tire Lateral Forces

The lateral force exerted by each tire on the vehicle depends on many quantities, as shown in the second equation in (2.85). For sure, there is a strong dependence on the vertical loads Z_{ij} and on the lateral slips $\sigma_{y_{ij}}$, while, in this vehicle model, the longitudinal slips $\sigma_{x_{ij}}$ are negligible. The camber angles γ_{ij} need to be considered as well, since they are quite influential, even if small. According to (3.200), the spin slips φ_{ij} are directly related to γ_{ij}. Therefore, a suitable model for the lateral force of each wheel with tire is (Fig. 6.1)

$$F_{y_{ij}} = F_{y_{ij}}\big(Z_{ij},\ \gamma_{ij},\ \sigma_{y_{ij}}\big) \tag{6.28}$$

Of course, extensive tire testing is required to make these functions available.

Needless to say, many other parameters affect the tire performance: road surface, temperature, inflation pressure, etc.

The lateral force Y_i for each axle of the vehicle is obtained by adding the lateral forces of the left wheel and of the right wheel (cf. (3.82) and (6.3), with $F_{x_{ij}} \simeq 0$)

$$\begin{aligned} Y_1 &= F_{y_{11}} \cos(\delta_{11}) + F_{y_{12}} \cos(\delta_{12}) \\ Y_2 &= F_{y_{21}} + F_{y_{22}} \\ \Delta X_1 &= [F_{y_{11}} \sin(\delta_{11}) - F_{y_{12}} \sin(\delta_{12})]/2 \end{aligned} \tag{6.29}$$

In general, the two wheels of the same axle undergo different vertical loads, different camber angles, and different lateral slips. Therefore, the two lateral forces are very different, as shown, e.g., in Fig. 3.26 and also in Fig 6.12. Equations (6.14) and (6.18), when inserted into (6.28), allow to take all these aspects into account. Therefore (Fig. 6.1)

$$\begin{aligned} Y_1 &= F_{y_{11}}\Big(Z_{11}(ur),\ \gamma_{11}(ur),\ \sigma_{y_{11}}\Big)\cos\big(\delta_{11}(\delta_v, ur)\big) \\ &\quad + F_{y_{12}}\Big(Z_{12}(ur),\ \gamma_{12}(ur),\ \sigma_{y_{12}}\Big)\cos\big(\delta_{12}(\delta_v, ur)\big) \\ &= F_{y_1}(\sigma_{y_{11}}, \sigma_{y_{12}}, \delta_v, ur), \\ Y_2 &= F_{y_{21}}\Big(Z_{21}(ur),\ \gamma_{21}(ur),\ \sigma_{y_{21}}\Big) + F_{y_{22}}\Big(Z_{22}(ur),\ \gamma_{22}(ur),\ \sigma_{y_{22}}\Big) \\ &= F_{y_2}(\sigma_{y_{21}}, \sigma_{y_{22}}, ur), \\ \Delta X_1 &= F_{y_{11}}\Big(Z_{11}(ur),\ \gamma_{11}(ur),\ \sigma_{y_{11}}\Big)\sin\big(\delta_{11}(\delta_v, ur)\big) \\ &\quad - F_{y_{12}}\Big(Z_{12}(ur),\ \gamma_{12}(ur),\ \sigma_{y_{12}}\Big)\sin\big(\delta_{12}(\delta_v, ur)\big) \\ &= \Delta X_1(\sigma_{y_{11}}, \sigma_{y_{12}}, \delta_v, ur) \end{aligned} \tag{6.30}$$

It should be clearly understood that the functions in (6.30) are assumed to be *known* algebraic functions.

A general comment on this vehicle model is in order here: some quantities depend (linearly) only on the lateral acceleration $\tilde{a}_y = ur$. However, it must be remarked that this peculiarity needs an open differential, no aerodynamic forces, almost constant forward speed.

6.3 Double Track Model

6.3.1 Governing Equations of the Double Track Model

Summing up, the vehicle model for studying the handling of road cars is governed by the following three sets of equations:

- two *equilibrium* equations (lateral and yaw), as in (6.4)

$$\begin{aligned} m(\dot{v} + ur) &= Y_1 + Y_2 = Y \\ J_z \dot{r} &= Y_1 a_1 - Y_2 a_2 + \Delta X_1 t_1 = N \end{aligned} \tag{6.31}$$

- three *constitutive* equations, as in (6.30), which are affected by several set-up parameters and by the vertical loads

$$\begin{aligned} Y_1 &= F_{y_1}(\sigma_{y_{11}}, \sigma_{y_{12}}, \delta_v, ur) \\ Y_2 &= F_{y_2}(\sigma_{y_{21}}, \sigma_{y_{22}}, ur) \\ \Delta X_1 &= \Delta X_1(\sigma_{y_{11}}, \sigma_{y_{12}}, \delta_v, ur) \end{aligned} \tag{6.32}$$

- four *congruence* equations (tire lateral slips), as in (6.21), which take care, among other things, of the Ackermann coefficient

$$\begin{aligned} \sigma_{y_{11}} &= \sigma_{y_{11}}(v, r; u, \delta_{11}(\delta_v, ur)) \\ \sigma_{y_{12}} &= \sigma_{y_{12}}(v, r; u, \delta_{12}(\delta_v, ur)) \\ \sigma_{y_{21}} &= \sigma_{y_{21}}(v, r; u, \delta_{21}(\delta_v, ur)) \\ \sigma_{y_{22}} &= \sigma_{y_{22}}(v, r; u, \delta_{22}(\delta_v, ur)) \end{aligned} \tag{6.33}$$

We have simply $\delta_{ij} = \delta_{ij}(\delta_v)$ if there is no roll steer.

This vehicle model for road vehicle handling is fairly general, and it is usually called *double track model*.

6.3.2 Dynamical Equations of the Double Track Model

The dynamical equations for road vehicle handling are now promptly obtained. As a final step, it suffices to insert (6.32) and (6.33) into (6.31)

$$\begin{aligned} m(\dot{v} + ur) &= Y(v, r; u, \delta_v) \\ J_z \dot{r} &= N(v, r; u, \delta_v) \end{aligned} \tag{6.34}$$

This is a dynamical system with two state variables, namely, but not necessarily, $v(t)$ and $r(t)$, as discussed in Sect. 6.3.3. The driver controls the steering wheel angle $\delta_v(t)$ and the forward speed u.

The double track model can be used to simulate and investigate the vehicle handling behavior under steady-state or transient conditions (i.e., nonconstant $\delta_v(t)$).

Unfortunately, the *double track model* is not as popular as the *single track model* (often and mistakenly also named "bicycle model"). The effort required to build a computer program and to run simulations with the double track model is comparable to the effort required by the less accurate single track model (introduced and discussed in Sect. 6.5).

6.3.3 Alternative State Variables (β and ρ)

The use of $v(t)$ and $r(t)$ as state variables is not mandatory, and other options can be envisaged. Other state variables may provide a better insight into vehicle handling, if properly handled.

The state variables $\beta(t)$ and $\rho(t)$ have been already introduced in (3.16) and (3.17). They are repeated here for ease of reading

$$\beta = \frac{v}{u} = -\frac{S}{R} \tag{3.16'}$$

and

$$\rho = \frac{r}{u} = \frac{1}{R} \tag{3.17'}$$

They are just v and r normalized with respect to u.

The corresponding three sets of equations of the double track model become:

- equilibrium equations (cf. (3.23), (3.27) and (6.31))

$$\begin{aligned} m(\dot{\beta}u + \beta\dot{u} + u^2\rho) &= Y = Y_1 + Y_2 \\ J_z(\dot{\rho}u + \rho\dot{u}) &= N = Y_1 a_1 - Y_2 a_2 + \Delta X_1 t_1 \end{aligned} \tag{6.35}$$

- constitutive equations (as in (6.32), with $\tilde{a}_y = ur = u^2\rho$)

$$\begin{aligned} Y_1 &= F_{y_1}(\sigma_{y_{11}}, \sigma_{y_{12}}, \delta_v, u^2\rho) \\ Y_2 &= F_{y_2}(\sigma_{y_{21}}, \sigma_{y_{22}}, u^2\rho) \\ \Delta X_1 &= \Delta X_1(\sigma_{y_{11}}, \sigma_{y_{12}}, \delta_v, u^2\rho) \end{aligned} \tag{6.36}$$

- congruence equations (cf. (6.33), with $\tilde{a}_y = ur = u^2\rho$)

$$\begin{aligned} \sigma_{y_{11}} &= \sigma_{y_{11}}(\beta, \rho; \delta_{11}(\delta_v, u^2\rho)) \\ \sigma_{y_{12}} &= \sigma_{y_{12}}(\beta, \rho; \delta_{12}(\delta_v, u^2\rho)) \\ \sigma_{y_{21}} &= \sigma_{y_{21}}(\beta, \rho; \delta_{21}(\delta_v, u^2\rho)) \\ \sigma_{y_{22}} &= \sigma_{y_{22}}(\beta, \rho; \delta_{22}(\delta_v, u^2\rho)) \end{aligned} \tag{6.37}$$

Therefore, in this case, the two dynamical equations (6.34) of the double track model become

$$\begin{aligned} m(\dot{\beta}u + \beta\dot{u} + u^2\rho) &= Y(\beta, \rho; \delta_v, u^2\rho) \\ J_z(\dot{\rho}u + \rho\dot{u}) &= N(\beta, \rho; \delta_v, u^2\rho) \end{aligned} \tag{6.38}$$

where $|\dot{u}| \simeq 0$ and can be discarded. The dependence of Y and N on the lateral acceleration $u^2\rho$, and hence on the forward speed u, disappears if there is no roll steer. This is the main advantage in using β and ρ as state variables in the double track model.

Quite remarkably, we will see in (6.75) that in the single track model there is no dependence of Y and N on u when β and ρ are used as state variables, even if roll steer is taken into account.

6.4 Vehicle in Steady-State Conditions

An essential step in understanding the behavior of a dynamical system, and therefore of a motor vehicle, is the determination of the steady-state (equilibrium) configurations (v_p, r_p). In physical terms, a vehicle is in steady-state conditions when, with fixed position δ_v of the steering wheel and at constant forward speed u, it goes around with *circular trajectories* of all of its points.

After having set $\dot{\delta}_v = 0$ and $\dot{u} = 0$, the mathematical conditions for the system being in steady state is to have $\dot{v} = 0$ and $\dot{r} = 0$ in (6.34). Accordingly, the *lateral acceleration* drops the $\dot{v}$ term and becomes at steady state

$$\tilde{a}_y = ur = u^2\rho = \frac{u^2}{R} \tag{6.39}$$

This equation was already introduced in (3.28).

Finding the equilibrium points (v_p, r_p), that is how the vehicle moves under given and constant δ_v and u, amounts to solving the system of two *algebraic* equations

$$\begin{aligned} mur &= Y(v, r; u, \delta_v) \\ 0 &= N(v, r; u, \delta_v) \end{aligned} \tag{6.40}$$

or, equivalently and more formally

$$\begin{aligned} 0 &= Y(v, r; u, \delta_v) - mur = f_v(v, r; u, \delta_v) \\ 0 &= N(v, r; u, \delta_v) = f_r(v, r; u, \delta_v) \end{aligned} \tag{6.41}$$

to get (v_p, r_p) such that

$$f_v(v_p, r_p; u, \delta_v) = 0 \qquad \text{and} \qquad f_r(v_p, r_p; u, \delta_v) = 0 \tag{6.42}$$

Because of the nonlinearity of the axle characteristics, the number of possible solutions (v_p, r_p), for given (δ_v, u), is not known a priori. Typically, if more than one solution exists, at most only one is stable.

Equation (6.42) define implicitly the two *maps*

$$v_p = \hat{v}_p(\delta_v, u) \qquad \text{and} \qquad r_p = \hat{r}_p(\delta_v, u) \tag{6.43}$$

that is, the totality of steady-state (equilibrium) conditions as functions of the forward speed u and of the steering wheel angle δ_v. Given and kept constant the forward speed u and the steering wheel angle δ_v, after a while (a few seconds at most) the vehicle reaches the corresponding steady-state condition, characterized by a constant lateral speed v_p and a constant yaw rate r_p.

For a more "geometric", and hence more intuitive, analysis of the handling of vehicles, it is convenient to employ $\beta = v/u$ and $\rho = r/u$ instead of v and r, as done in Sect. 6.3.3. Therefore, (6.43) can be replaced by

$$\beta_p = \hat{\beta}_p(\delta_v, u) \qquad \text{and} \qquad \rho_p = \hat{\rho}_p(\delta_v, u) \tag{6.44}$$

The steady-state handling behavior is completely characterized by these *handling maps* of β and ρ, both as functions of two variables, namely, but not necessarily, u and δ_v

$$(\delta_v, u) \implies (\beta_p, \rho_p) \tag{6.45}$$

Indeed, it is common practice to employ $(\delta_v, \tilde{a}_y)$, instead of (δ_v, u), as parameters to characterize a steady-state condition. This is possible because

$$\tilde{a}_y = ur_p(\delta_v, u) \quad \text{which can be solved to get} \quad u = u(\delta_v, \tilde{a}_y) \tag{6.46}$$

Therefore, (6.43) becomes

$$v_p = v_p(\delta_v, \tilde{a}_y) \qquad \text{and} \qquad r_p = r_p(\delta_v, \tilde{a}_y) \tag{6.47}$$

and, accordingly, (6.44) becomes

$$\beta_p = \beta_p(\delta_v, \tilde{a}_y) \qquad \text{and} \qquad \rho_p = \rho_p(\delta_v, \tilde{a}_y) \tag{6.48}$$

At first it may look a bit odd to employ $(\delta_v, \tilde{a}_y)$ instead of (δ_v, u), but it is not, since it happens that in most road cars some steady-state quantities are functions of $\tilde{a}_y$ only. This is quite a remarkable fact, but it should not be taken as a general rule.[5]

Equation (6.44) or (6.48) provide a fairly general point of view that leads to a new global approach that we present here and that we call Map of Achievable Performance (MAP).

These MAPs can be obtained experimentally or through simulations. Therefore, they are not limited to mathematical models. Actually, as will be discussed in the next chapter, they exist also for race cars, including Formula cars with very high aerodynamic downforces.

A detailed description of the MAP approach is provided in Chap. 8, although some information can be found also in Sect. 6.8 (see also Sect. 6.7). Now we prefer to address more classical topics, like the single track model and the handling diagram.

6.5 Single Track Model

The goal of this Section is to present a comprehensive analysis of the single track model [2–4, 6, 10, 14, 16], thus showing also its limitations. In many courses or books on vehicle dynamics (e.g., [6, p. 199]) the single track model (Fig. 6.9) is proposed without explaining in detail why, despite its awful appearance, it can provide in some cases useful insights into vehicle handling, particularly for educational purposes. Vehicle engineers should be well aware of the steps taken to simplify the model, and hence realize that in some cases the single track model may miss some crucial phenomena, and the double track model should be used instead.

6.5.1 From Double to Single

To go from the double track to the single track model we need to further simplify (6.26). Beside $u \gg |rt_i|$, that is $|R| \gg t_i$, we need the following additional assumption: *the Ackermann coefficients have to be set equal to zero*, that is

$$\varepsilon_1 = \varepsilon_2 = 0 \tag{6.49}$$

[5] For instance, vehicles equipped with a locked differential and/or with relevant aerodynamic downforces always need (at least) two parameters.

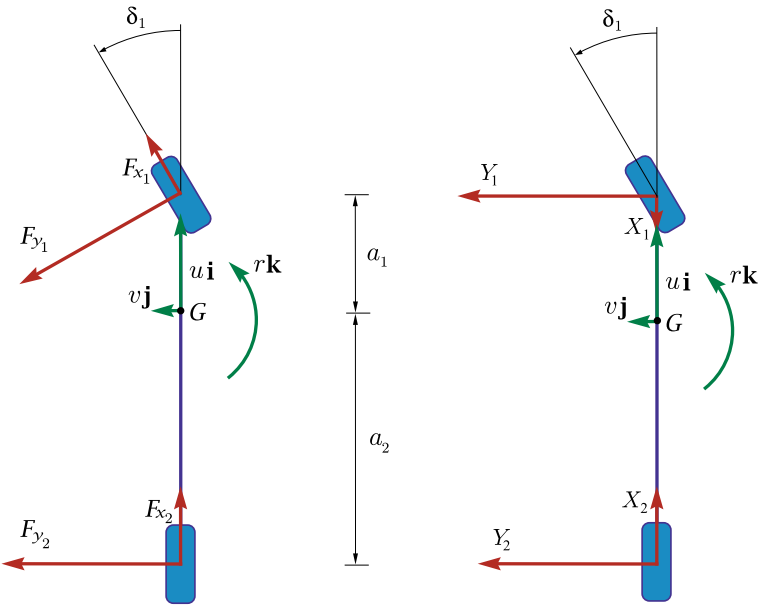

Fig. 6.9 Equivalent schematic representations of the single track model (with $\delta_2 = 0$)

which is consistent with *small steering angles*. Indeed the Ackermann correction is a second order contribution in (6.26) and, important as it can be, it cannot be included in the single track model.

Therefore, we can define the steer angle δ_1 of the front *axle* and the steer angle δ_2 of the rear *axle* (Fig. 6.9)

$$\begin{aligned} \delta_1 &= \tau_1 \delta_v = (1 + \kappa)\delta \\ \delta_2 &= \chi \tau_1 \delta_v = \kappa \delta \end{aligned} \tag{6.50}$$

where

$$\delta = \delta_1 - \delta_2 = (1 - \chi)\tau_1 \delta_v = \tau \delta_v \tag{6.51}$$

is called *net steer angle* of the wheels of the vehicle.

In this single track model there is a one-to-one relationship between δ and δ_v, that is we have a *rigid* steering system.[6] Usually, $\kappa = 0$ and hence δ is just the steering angle δ_1 of the front axle. However, $\kappa \neq 0$ leaves room for rear steering δ_2 as well.

This (not necessarily true) hypothesis (6.49) on the Ackermann coefficients, if combined with the simplified expressions (6.26), leads to the following (first-order) expressions for the lateral tire slips

[6] A vehicle model with *compliant* steering system is developed in Sect. 6.16.

$$\begin{aligned}
\sigma_{y_{11}} &\simeq \left(\frac{v + ra_1}{u} - \delta_v \tau_1\right) + \delta_1^0 - \Upsilon_1 \rho_1^s m \tilde{a}_y \\
\sigma_{y_{12}} &\simeq \left(\frac{v + ra_1}{u} - \delta_v \tau_1\right) - \delta_1^0 - \Upsilon_1 \rho_1^s m \tilde{a}_y \\
\sigma_{y_{21}} &\simeq \left(\frac{v - ra_2}{u} - \delta_v \tau_2\right) + \delta_2^0 - \Upsilon_2 \rho_2^s m \tilde{a}_y \\
\sigma_{y_{22}} &\simeq \left(\frac{v - ra_2}{u} - \delta_v \tau_2\right) - \delta_2^0 - \Upsilon_2 \rho_2^s m \tilde{a}_y
\end{aligned} \tag{6.52}$$

It is important to note that we can still take into account the toe-in/toe-out terms δ_i^0, and also, possibly, the roll steer contributions.

It is now possible to define (cf. (3.55)) what can be called the *apparent* slip angles α_1 and α_2 of the front and rear *axles*, respectively

$$\begin{aligned}
\alpha_1 &= \delta_v \tau_1 - \frac{v + ra_1}{u} = \alpha_1(v, r; u, \delta_v) = \alpha_1(\beta, \rho; \delta_v) \\
\alpha_2 &= \delta_v \tau_2 - \frac{v - ra_2}{u} = \alpha_2(v, r; u, \delta_v) = \alpha_2(\beta, \rho; \delta_v)
\end{aligned} \tag{6.53}$$

Combining (6.52) and (6.53), we obtain that both front lateral slips $\sigma_{y_{1i}}$ are *known* functions of only *two* variables, namely α_1 and $\tilde{a}_y$. Similarly, both rear lateral slips $\sigma_{y_{2i}}$ are *known* functions of the two variables α_2 and $\tilde{a}_y$

$$\begin{aligned}
\sigma_{y_{11}} &\simeq -\alpha_1 + \delta_1^0 - \Upsilon_1 \rho_1^s m \tilde{a}_y = \sigma_{y_{11}}(\alpha_1, \tilde{a}_y) \\
\sigma_{y_{12}} &\simeq -\alpha_1 - \delta_1^0 - \Upsilon_1 \rho_1^s m \tilde{a}_y = \sigma_{y_{12}}(\alpha_1, \tilde{a}_y) \\
\sigma_{y_{21}} &\simeq -\alpha_2 + \delta_2^0 - \Upsilon_2 \rho_2^s m \tilde{a}_y = \sigma_{y_{21}}(\alpha_2, \tilde{a}_y) \\
\sigma_{y_{22}} &\simeq -\alpha_2 - \delta_2^0 - \Upsilon_2 \rho_2^s m \tilde{a}_y = \sigma_{y_{22}}(\alpha_2, \tilde{a}_y)
\end{aligned} \tag{6.54}$$

This is the peculiar feature of the single track model (cf. (6.27)). It is the fundamental brick for the next step.

But before doing that, it is worth noting in (6.54) the crucial difference between the *actual* slip angles α_{ij} of each wheel, which were defined in (3.58) and in (6.26), and the *apparent* slip angles α_i of each axle, defined in (6.53). To avoid confusion, it would have been probably better not to use so similar names and symbols. The apparent slip angles α_i only exist in the single track model (Fig. 6.20), not in the real vehicle.

Also observe that the two wheels of the same axle undergo, in this model, the same apparent slip angle, but not necessarily the same lateral slip. The key point for the model to be single track is that the difference between left and right lateral slips must be a function of $\tilde{a}_y$, as we are going to show shortly.

It is very common in traditional vehicle dynamics not to take into account toe-in/toe-out and roll steering, thus obtaining

$$\begin{aligned} \sigma_{y_{11}} &\simeq \sigma_{y_{12}} \simeq -\alpha_1 \\ \sigma_{y_{21}} &\simeq \sigma_{y_{22}} \simeq -\alpha_2 \end{aligned} \tag{6.55}$$

6.5.2 *"Forcing" the Lateral Forces*

Owing to the just obtained (6.54), the first two equations in (6.30) become

$$\begin{aligned} Y_1 &= F_{y_{11}}\Big(Z_{11}(\tilde{a}_y), \gamma_{11}(\tilde{a}_y), \sigma_{y_{11}}(\alpha_1, \tilde{a}_y)\Big) + F_{y_{12}}\Big(Z_{12}(\tilde{a}_y), \gamma_{12}(\tilde{a}_y), \sigma_{y_{12}}(\alpha_1, \tilde{a}_y)\Big) \\ &= F_{y_{11}}(\alpha_1, \tilde{a}_y) + F_{y_{12}}(\alpha_1, \tilde{a}_y) \\ &= F_{y_1}(\alpha_1, \tilde{a}_y); \\ Y_2 &= F_{y_{21}}\Big(Z_{21}(\tilde{a}_y), \gamma_{21}(\tilde{a}_y), \sigma_{y_{21}}(\alpha_2, \tilde{a}_y)\Big) + F_{y_{22}}\Big(Z_{22}(\tilde{a}_y), \gamma_{22}(\tilde{a}_y), \sigma_{y_{22}}(\alpha_2, \tilde{a}_y)\Big) \\ &= F_{y_{21}}(\alpha_2, \tilde{a}_y) + F_{y_{22}}(\alpha_2, \tilde{a}_y) \\ &= F_{y_2}(\alpha_2, \tilde{a}_y), \end{aligned} \tag{6.56}$$

while the third equation in (6.30) is set to zero because of the assumed very small steer angles

$$\Delta X_1 = 0 \tag{6.57}$$

It is really crucial for a vehicle engineer to understand and keep in mind the differences between (6.30) and (6.56).

As already obtained in (6.8) at the beginning of this Chapter, we have that the lateral forces are basically linear functions of $\tilde{a}_y$ (open differential)

$$Y_1 \simeq \frac{ma_2}{l}\tilde{a}_y \qquad \text{and} \qquad Y_2 \simeq \frac{ma_1}{l}\tilde{a}_y \tag{6.58}$$

Therefore, $F_{y_1}(\alpha_1, \tilde{a}_y)$ and $F_{y_2}(\alpha_2, \tilde{a}_y)$ must be such that

$$F_{y_1}(\alpha_1, \tilde{a}_y) = \frac{ma_2}{l}\tilde{a}_y \qquad \text{and} \qquad F_{y_2}(\alpha_2, \tilde{a}_y) = \frac{ma_1}{l}\tilde{a}_y \tag{6.59}$$

These equations can be solved with respect to the lateral acceleration, thus obtaining[7]

$$\tilde{a}_y = g_1(\alpha_1) \qquad \text{and} \qquad \tilde{a}_y = g_2(\alpha_2) \tag{6.60}$$

The final, crucial, step is inserting (i.e.,"forcing") this result back into (6.58), thus obtaining the *axle characteristics* of the single track model

$$\begin{aligned} Y_1(\alpha_1) &= F_{y_1}\big(\alpha_1, g_1(\alpha_1)\big) \\ Y_2(\alpha_2) &= F_{y_2}\big(\alpha_2, g_2(\alpha_2)\big) \end{aligned} \tag{6.61}$$

[7] This step would not be possible with F_{y_i} as in (6.30).

that is, two functions, one per axle, that give the axle lateral force as a function of *only* the corresponding *apparent* slip angle, that is of *only one variable*.

In other words, each axle behaves pretty much as an equivalent single wheel with tire. However, it should not be forgotten that the axle characteristics are also affected by many other set-up parameters, like camber angles, roll steer, toe-in/toe-out, etc., as discussed in detail in Sect. 6.5.3.

Forcing the lateral forces to be as in (6.61) is an approximation when the vehicle is in transient conditions. Moreover, to go from (6.30) to (6.56) we made assumptions (6.49) about the steer kinematics (parallel steering) and small steer angles.

The double track model provides more accurate results when running simulations. On the other hand, the single track model is a useful tool for educational purposes and for investigating steady-state conditions. It is less accurate, but more intuitive.

Equation (6.60) implies that in the single track model there is a link between α_1 and α_2

$$g_1(\alpha_1) = \tilde{a}_y = g_2(\alpha_2) \tag{6.62}$$

and that this link is not affected by u or δ_v. In a real vehicle this is not necessarily true. Vehicle engineers should be aware that the single track model is somehow an inconsistent model, albeit very appealing.

6.5.3 Axle Characteristics

By *axle characteristics* we mean two algebraic functions (one per axle) of the form

$$Y_i = F_{y_i} = Y_i(\alpha_i) \tag{6.63}$$

which provide the total lateral force as a function of the apparent slip angle only, with the effects, e.g., of the lateral load transfers already accounted for. They were obtained in (6.61), but the topic is so relevant to deserve an in-depth discussion.

6.5.3.1 The Basics

The basic procedure to obtain the axle characteristics is described here. The goal is to provide an intuitive and physical approach to the construction of the axle characteristics in the single track model. "Basic" means that only the effects of the lateral load transfers ΔZ_i are taken into account. Of course, lateral load transfers cannot be avoided. They must necessarily be included in the analysis.

The first step is to test the tire under symmetric vertical loads with respect to the reference value $Z_i^0/2$, as shown in Fig. 6.10. "Symmetric" means that tests have to be always carried out in pairs, that is with $F_z = Z_i^0/2 \pm \Delta Z_i$. In Fig. 6.10 two such pairs are shown.

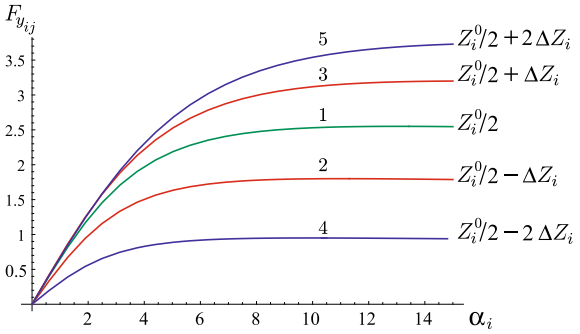

Fig. 6.10 Tire tested under symmetric vertical loads with respect to the static load $Z_0/2$

The second step is to add the two tire curves obtained with symmetric vertical loads, as shown in Fig. 6.11(top), thus getting a sort of axle curve. To legitimate this second step (6.53) is crucial, that is that the two wheels of the same axle undergo the same apparent slip angle α_i. As expected, the higher the lateral load transfer ΔZ_i, the lower the corresponding axle curve.

The third step is to draw a straight line according to (6.12), to linearly relate the lateral load transfer ΔZ_i to the axle lateral force F_{y_i}.

The fourth and final step is to pick the *unique point* on each axle curve that corresponds to a real operating (steady-state) condition for the vehicle, as shown in Fig. 6.11(top). As a matter of fact, each axle curve was obtained testing the tire with given and constant $\pm\Delta Z_i$, but this amount of lateral load transfer requires a definite value of the lateral force F_{y_i} in the vehicle, and hence a definite value of α_i.

The sought *axle characteristic* $Y_i(\alpha_i)$ is just the curve connecting all these points, as schematically shown in Fig. 6.11.

Changing the value of η_i in (6.12) results in a different straight line and hence in different axle characteristics, as shown in Fig. 6.11(bottom). The axle curves are not affected by η_i, but the points corresponding to real operating conditions are.

6.5.3.2 The Extras

Now we should be ready to address the construction of the axle characteristics with greater generality.

According to (6.30), (6.54), (6.56) and (6.58), the general framework for a given vehicle is that:

1. there is a one-to-one correspondence between the lateral acceleration $\tilde{a}_y$ and the following quantities:
   - lateral load transfers ΔZ_i, see (6.9);
   - camber angles γ_{ij}, see (6.17) and (6.18);
   - roll steer angles $\Upsilon_i \phi_i^s$, see (6.19);

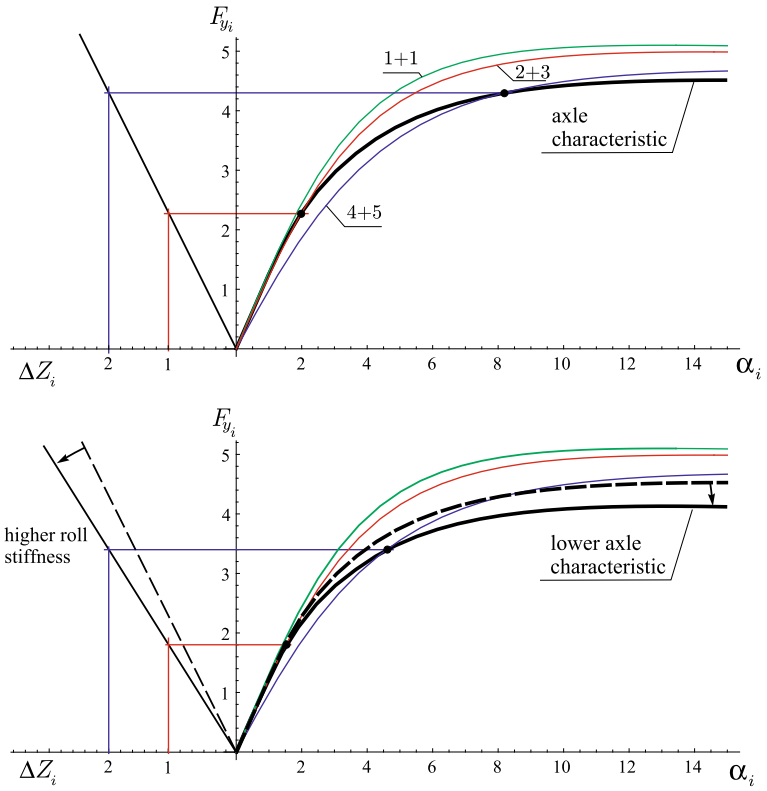

Fig. 6.11 Basic graphic construction of the axle characteristic and influence of changing the roll stiffness

2. both left and right tire lateral forces are known functions of the lateral acceleration $\tilde{a}_y$ and of the *same apparent slip angle* α_i, see (6.56);
3. each axle lateral force $F_{y_i}(\alpha_i, \tilde{a}_y)$ is the sum of the left and right tire lateral forces, see (6.56);
4. each axle lateral force Y_i is determined solely by the lateral acceleration $\tilde{a}_y$, see (6.58).

Therefore, for any given value of $\tilde{a}_y$, we can obtain the corresponding load transfers, camber angles and roll steer angles and, consequently, we can plot (measure) the lateral forces $F_{y_{i1}}(\alpha_i, \tilde{a}_y)$ and $F_{y_{i2}}(\alpha_i, \tilde{a}_y)$ of each wheel as functions of α_i *only*, that is using $\tilde{a}_y$ as a parameter

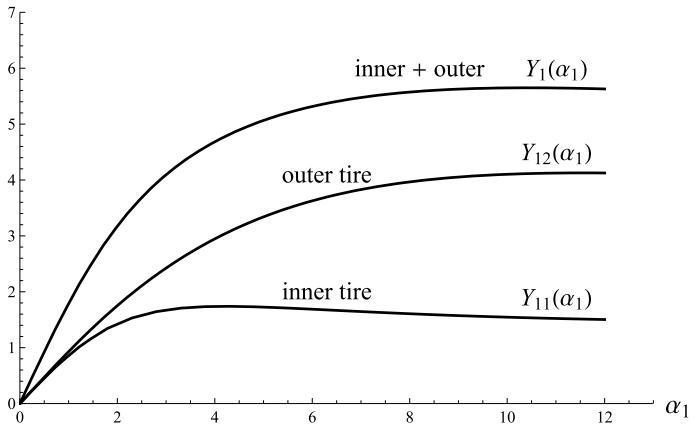

Fig. 6.12 Example of lateral forces exerted by the inner and outer tires of the same axle, in a vehicle that can be modeled as single track

$$\begin{aligned} Y_{11}(\alpha_1) &= F_{y_{11}}\big(\alpha_1, g_1(\alpha_1)\big) \\ Y_{12}(\alpha_1) &= F_{y_{12}}\big(\alpha_1, g_1(\alpha_1)\big) \\ Y_{21}(\alpha_2) &= F_{y_{21}}\big(\alpha_2, g_2(\alpha_2)\big) \\ Y_{22}(\alpha_2) &= F_{y_{22}}\big(\alpha_2, g_2(\alpha_2)\big) \end{aligned} \tag{6.64}$$

Typical curves for the inner and the outer tires of the same axle are shown in Fig. 6.12. As expected, the outer tire provides the larger lateral force. Also interesting is to observe that the maximum lateral forces are not attained for the same apparent slip angle.

The two *axle characteristics* are then given by

$$\begin{aligned} Y_1(\alpha_1) &= Y_{11}(\alpha_1) + Y_{12}(\alpha_1) \\ Y_2(\alpha_2) &= Y_{21}(\alpha_2) + Y_{22}(\alpha_2) \end{aligned} \tag{6.65}$$

Of course, any calculation of this type assumes the availability of tire data.

To know how to affect the vehicle handling behavior, it is necessary to understand the effect of changing some set-up parameters on the axle characteristics. This extremely relevant topic is discussed hereafter, taking into account the effects of changing the:

1. roll stiffnesses;
2. static camber angles;
3. toe-in/toe-out;
4. roll steer;
5. roll camber.

All plots in this section are for a car making a left turn ($\tilde{a}_y > 0$). In all plots in this section, the apparent slip angles are in degrees and the lateral forces are in kN. All curves with the same kind of dashing were obtained with the same lateral acceleration of the vehicle.

6.5.3.3 Roll Stiffness

In addition to Figs. 6.10 and 6.11, two basic examples are shown in Fig. 6.13. They are basic in the sense that it is assumed that the parameter $\tilde{a}_y$ affects only the load transfer ΔZ_i. More precisely, it is assumed that $\gamma_{ij} = \delta_i^0 = \Upsilon_i = 0$.

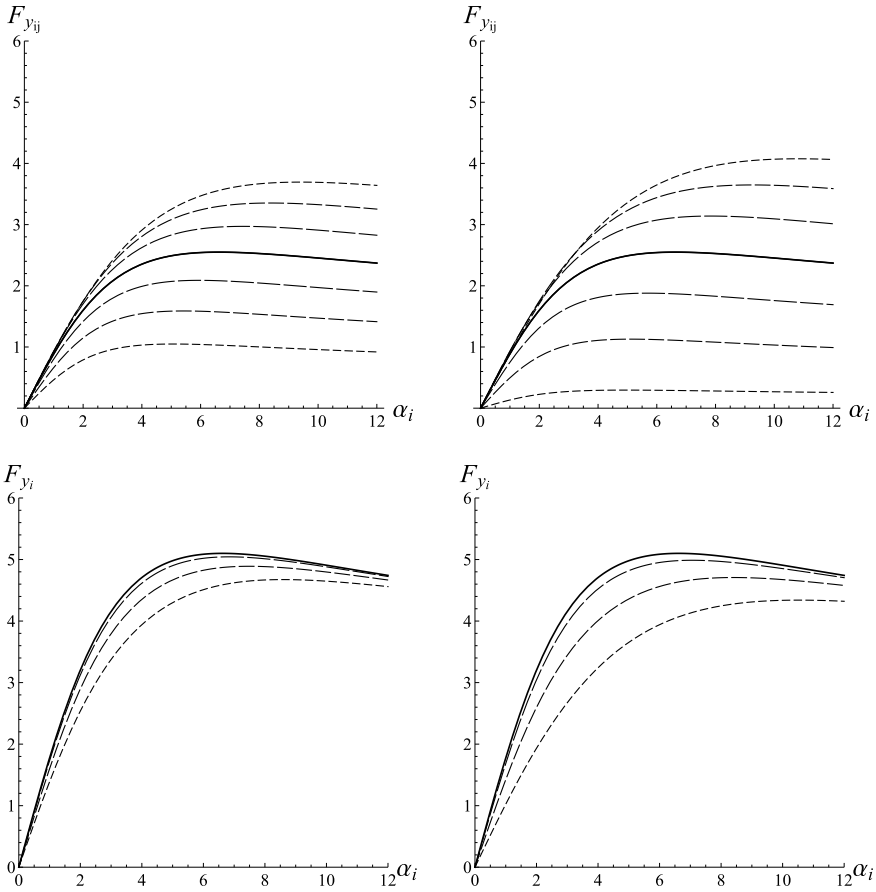

Fig. 6.13 Plots of $F_{y_{i1}}(\alpha_i, \tilde{a}_y)$ and $F_{y_{i2}}(\alpha_i, \tilde{a}_y)$ (top) and of their sum $F_{y_i}(\alpha_i, \tilde{a}_y)$ (bottom), for four values of $\tilde{a}_y \geq 0$ (solid line: $\tilde{a}_y = 0$) and two different set-ups: stiffer in the second case (right)

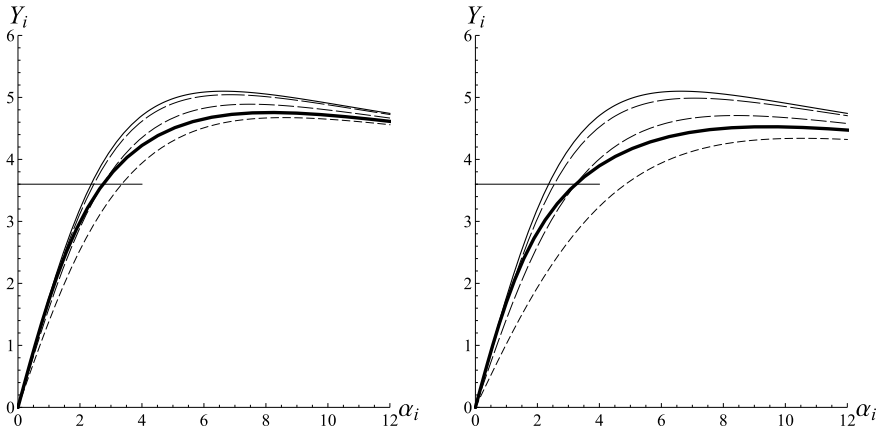

Fig. 6.14 Axle characteristics (thick solid line) for the two cases of Fig. 6.13

The two cases in Fig. 6.13 have different values of η_i, and hence different load transfers for the same lateral acceleration (higher load transfers in the second case, probably due to higher roll stiffness).

A very relevant fact in vehicle dynamics, as stated in Sects. 2.11.2 and 2.13, is that the lateral force exerted by a single tire grows *less than proportionally* with respect to the vertical load. This is clearly shown in Fig. 6.13 (top), and confirmed in Fig. 6.13 (bottom), where the higher the lateral acceleration and hence the load transfer, the lower the resulting curve of $F_{y_i}(\alpha_i, \tilde{a}_y)$.

Once the functions F_{y_i} have been obtained as in Fig. 6.13 (bottom), there is only one final step to obtain the axle characteristic. Indeed, only one point of each curve $F_{y_i}(\alpha_i, \tilde{a}_y)$ is actually a working point for the vehicle. The reason, as already discussed, is that there is a one-to-one correspondence between $\tilde{a}_y$ and F_{y_i}. Mathematically, it amounts to solving equations (6.59), that is

$$F_{y_i}(\alpha_i, \tilde{a}_y) = \frac{m\tilde{a}_y(l - a_i)}{l} \tag{6.66}$$

as done in Fig. 6.14. The *axle characteristics* $Y_i(\alpha_i)$ (thick solid line) picks up just one point of each dashed curve. The higher η_i in (6.9) or (6.11), the lower the axle characteristic, as shown in Fig. 6.14.

6.5.3.4 Static Camber

The definition of static camber is given in Fig. 6.5. The effects of negative and positive static camber angles, i.e. $\gamma_{ij}^0 \neq 0$, are shown in Fig. 6.15, left and right, respectively. If the top of the wheel is farther out than the bottom (that is, away from the axle), it is called positive static camber. If the bottom of the wheel is farther out than the top,

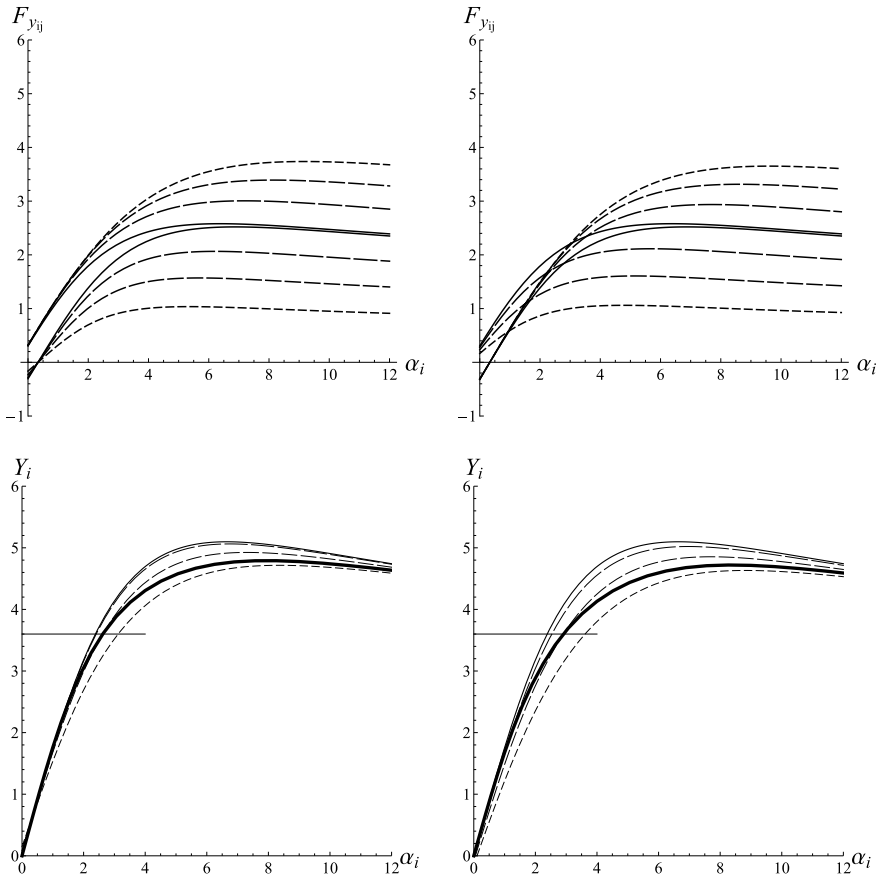

Fig. 6.15 As in Fig. 6.13 (left), but with *negative camber* (left) or *positive camber* (right). Also shown are the resulting axle characteristics, as in Fig. 6.14

it is called negative camber. We see that there are lateral forces on each wheel even when the car is going straight (solid line).

6.5.3.5 Toe-In, Toe-Out

The definition of toe-in/toe-out is given in Fig. 3.14. The effects of toe-in ($\delta_i^0 > 0$) and toe-out ($\delta_i^0 < 0$), are shown in Fig. 6.16, left and right, respectively. We see that also in this case there are lateral forces on the wheels, when the car is going straight (solid line). Indeed, toe-in and positive camber, or toe-out and negative camber, can be combined to reduce these lateral forces.

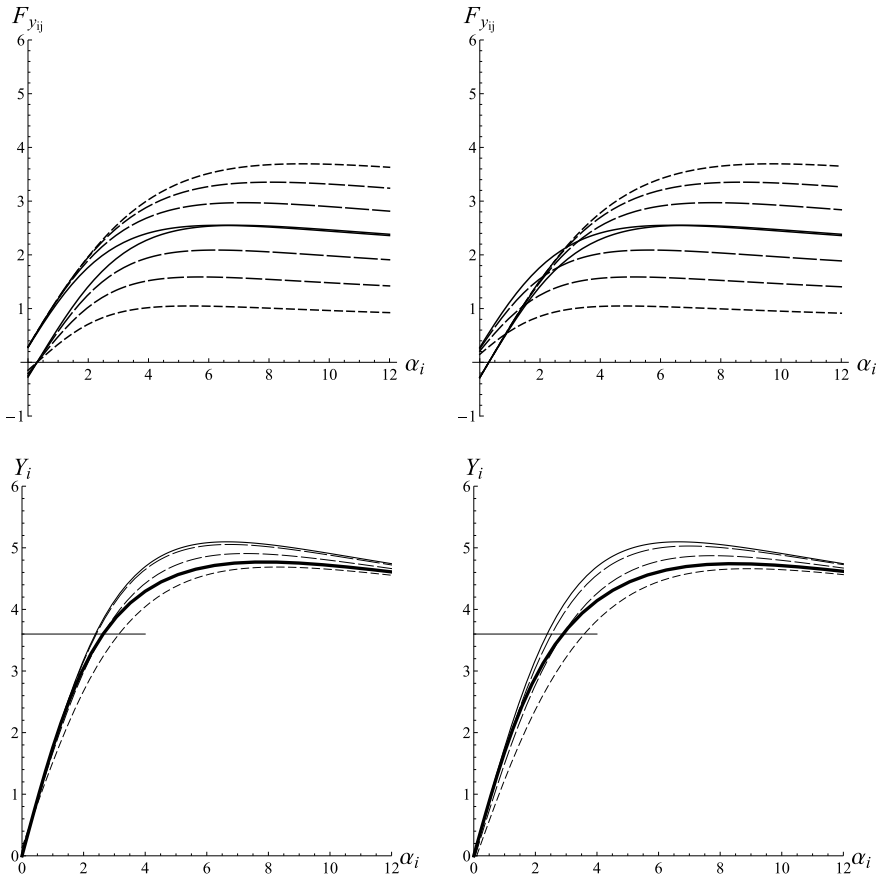

Fig. 6.16 As in Fig. 6.13 (left), but with *toe-in* (left) or *toe-out* (right). Also shown are the resulting axle characteristics, as in Fig. 6.14

6.5.3.6 Roll Steer

Also interesting is the case of roll steer, i.e. $\Upsilon_i \neq 0$, shown in Fig. 6.17. While all other effects considered so far are symmetric with respect to the vehicle axis, and hence the contributions of the two wheels cancel each other at low lateral acceleration, the roll steer is anti-symmetric, and hence it affects the axle characteristic even at low lateral accelerations.

6.5.3.7 Roll Camber

As shown in Fig. 6.18, the effects of roll camber $\Delta\gamma_i$ are anti-symmetric, pretty much like roll steer. Positive camber variations due to roll motion are shown in Fig. 6.6.

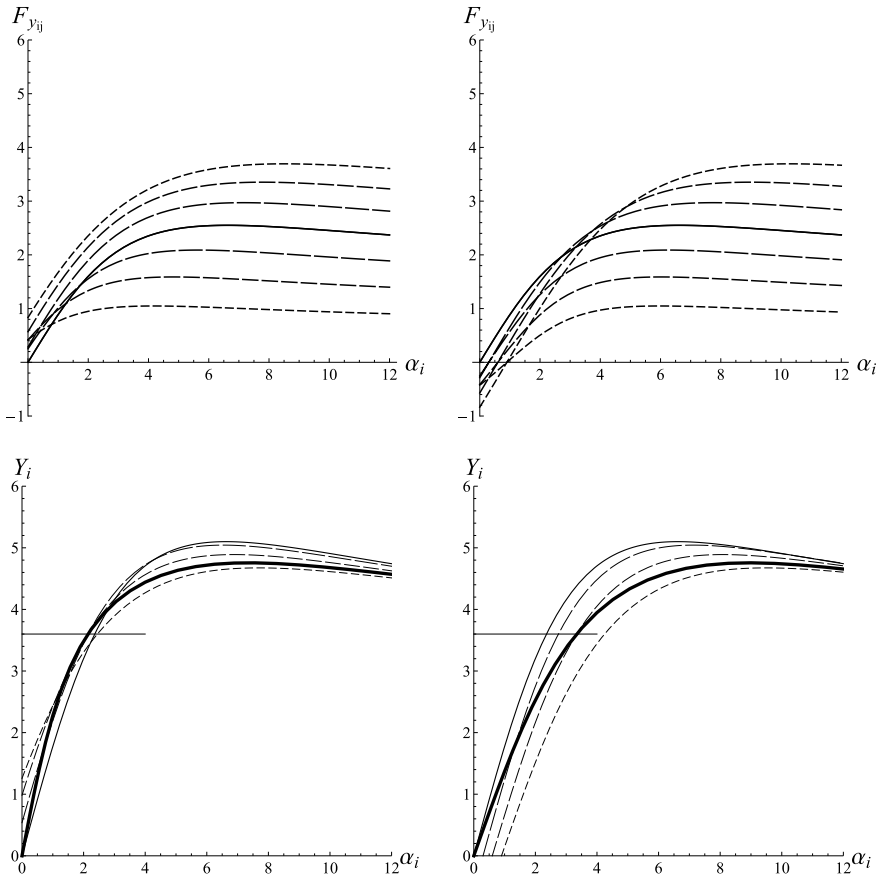

Fig. 6.17 As in Fig. 6.13 (left), but with *positive roll steer* (left) or *negative roll steer* (right). Also shown are the resulting axle characteristics, as in Fig. 6.14

Also useful may be Fig. 6.7, which shows how the suspension architecture strongly affects roll camber.

6.5.3.8 General Case

Of course, in general all these effects may very well coexist in a real car. In Fig. 6.19, the curve in the middle is the axle characteristic of Fig. 6.14 (left), the top curve was obtained including all parameters of the left-hand cases of Figs. 6.15–6.17, that is negative camber, toe-in and positive roll steer, whereas the lower curve was obtained including the parameters of all right-hand cases in the same figures (positive camber, toe-out, negative roll steer). The curves differ in the initial slope (slip stiffness) and also in the maximum value. Both aspects have a big influence on vehicle handling.

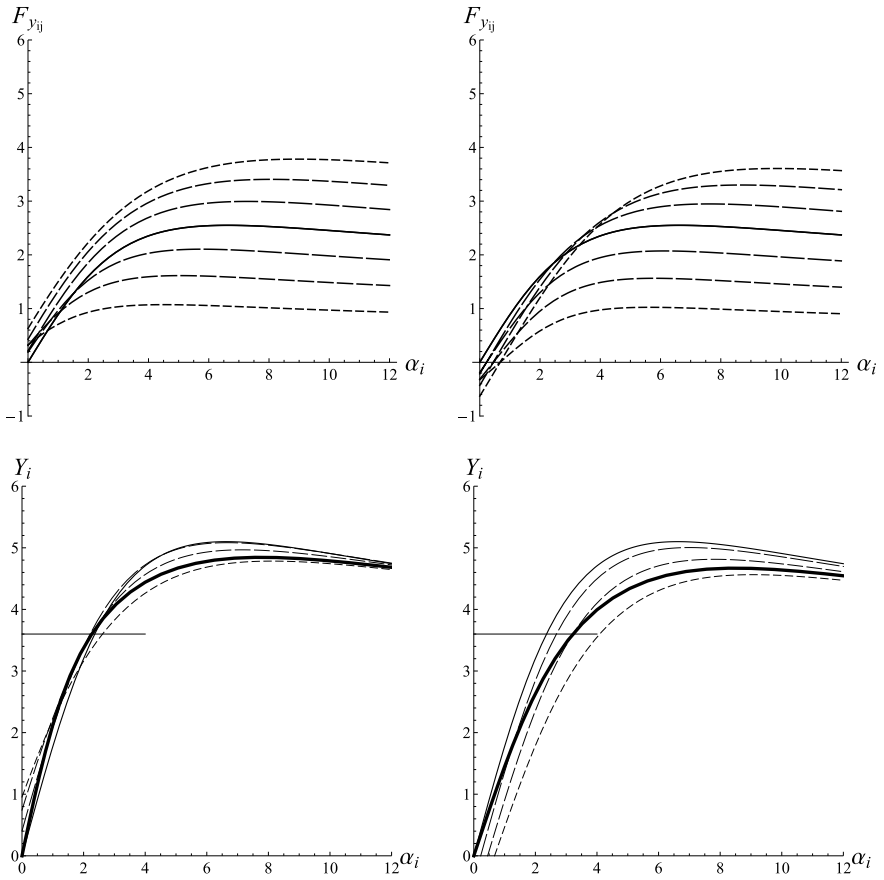

Fig. 6.18 As in Fig. 6.13 (left), but with *negative roll camber* $\Delta\gamma_i$ (left) or *positive roll camber* $\Delta\gamma_i$ (right). Also shown are the resulting axle characteristics, as in Fig. 6.14

The axle characteristics are what most characterize vehicle dynamics, indeed. We remark that the axle characteristics, under an apparent simplicity, contain a lot of information about the vehicle features and set-up (see also [10, Chap. 6]).

6.5.4 Governing Equations of the Single Track Model

Summing up, the single track model is governed by the following three sets of fairly simple equations:

- two *equilibrium* equations (lateral and yaw), as in (6.4)

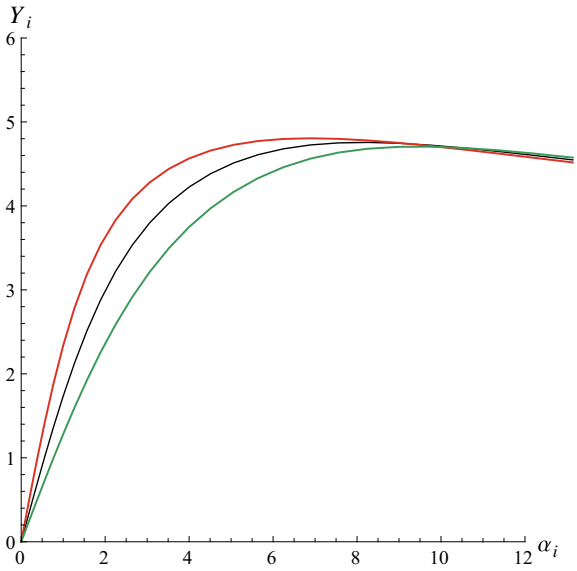

Fig. 6.19 Comparison of axle characteristics obtained with very different set-ups

$$\begin{aligned} m(\dot{v} + ur) &= Y = Y_1 + Y_2 \\ J_z \dot{r} &= N = Y_1 a_1 - Y_2 a_2 \end{aligned} \tag{6.67}$$

- two *congruence* equations (apparent slip angles), as in (6.53)

$$\begin{aligned} \alpha_1 &= \delta_v \tau_1 - \frac{v + r a_1}{u} \\ \alpha_2 &= \delta_v \tau_2 - \frac{v - r a_2}{u} \end{aligned} \tag{6.68}$$

- two *constitutive* equations (axle characteristics, which include the effects of several set-up parameters), as in (6.61)

$$\begin{aligned} Y_1 &= Y_1(\alpha_1) \\ Y_2 &= Y_2(\alpha_2) \end{aligned} \tag{6.69}$$

A comparison with the governing equations of the double track model (Sect. 6.3.1) shows that here:

- the term $\Delta X_1 t_1$ has disappeared from the equilibrium equations;
- there are two, instead of four, congruence equations;
- the constitutive equations are (apparently) simpler.

A pictorial version of the single track model is shown in Fig. 6.20, where $\delta_1 = \delta_v \tau_1$ and $\delta_2 = \delta_v \tau_2$. Indeed, the equations governing such dynamical system are precisely (6.67)–(6.69). Therefore, the system of Fig. 6.20 can be used as a *shortcut* to obtain

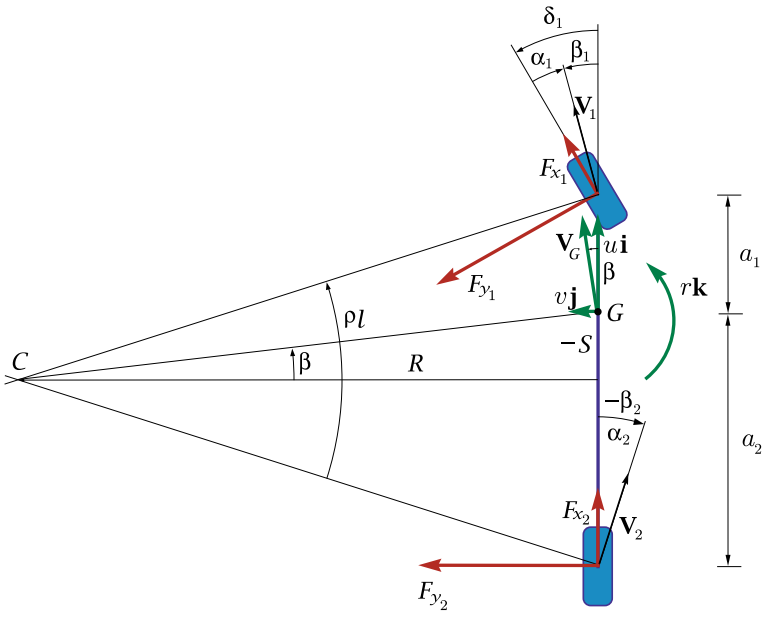

Fig. 6.20 Single track model

the simplified equations of a vehicle. However, the vehicle model still has four wheels, lateral load transfers, camber and camber variations, roll steer, as shown in Sect. 6.5.3 on axle characteristics.

The main feature of this model is that the two wheels of the same axle undergo the same *apparent* slip angle α_i, and hence can be replaced by a sort of equivalent wheel, like in Fig. 6.20. However, that does not imply that the real slip angles of the two wheels of the same axle are the same. Neither are the camber angles, the roll steer angles, the vertical loads. Therefore, the single track model is not really single track! It retains many of the features of the double track model.

In other words, it is not necessary to assume that the center of mass of the vehicle is at road level [9, p. 170], neither that the lateral forces of the left and right tires to be equal to each other [1, p. 53]. Actually, both assumptions would be strikingly false in any car.

Assuming the total mass to be concentrated at G, as if the vehicle were like a point mass, is another unrealistic, and unnecessary, assumption [15, p. 223].

6.5.5 *Dynamical Equations of the Single Track Model*

Among the governing equations, only the two equilibrium equations are differential equations, and both are first-order. The other four algebraic equations must be inserted

into the equilibrium equations to ultimately obtain the two *dynamical equations* of the *single track model*

$$\begin{aligned} m(\dot{v}+ur) &= Y_1\left(\delta_v\tau_1 - \frac{v+ra_1}{u}\right) + Y_2\left(\delta_v\tau_2 - \frac{v-ra_2}{u}\right) \\ J_z\dot{r} &= a_1Y_1\left(\delta_v\tau_1 - \frac{v+ra_1}{u}\right) - a_2Y_2\left(\delta_v\tau_2 - \frac{v-ra_2}{u}\right) \end{aligned} \tag{6.70}$$

or, more compactly

$$\begin{aligned} m(\dot{v}+ur) &= Y(v,r;u,\delta_v) \\ J_z\dot{r} &= N(v,r;u,\delta_v) \end{aligned} \tag{6.71}$$

Therefore, the single track model is a dynamical system with two state variables, namely, but not necessarily, $v(t)$ and $r(t)$, as discussed in Sect. 6.5.6. The driver controls the steering wheel angle $\delta_v(t)$ and the forward speed u.

6.5.6 Alternative State Variables (β and ρ)

As already done in Sect. 6.3.3, instead of $v(t)$ and $r(t)$, we can use $\beta(t) = v/u$ and $\rho(t) = r/u$ to describe the handling of a vehicle.

The corresponding governing equations of the single track model become:

- equilibrium equations (cf. (6.67))

$$\begin{aligned} m(\dot{\beta}u + \beta\dot{u} + u^2\rho) &= Y = Y_1 + Y_2 \\ J_z(\dot{\rho}u + \rho\dot{u}) &= N = Y_1a_1 - Y_2a_2 \end{aligned} \tag{6.72}$$

- congruence equations (cf. (6.68))

$$\begin{aligned} \alpha_1 &= \delta_v\tau_1 - \beta - \rho a_1 \\ \alpha_2 &= \delta_v\tau_2 - \beta + \rho a_2 \end{aligned} \tag{6.73}$$

- constitutive equations (cf. (6.69))

$$\begin{aligned} Y_1 &= Y_1(\alpha_1) \\ Y_2 &= Y_2(\alpha_2) \end{aligned} \tag{6.74}$$

Combining these three sets of equations, we obtain the dynamical equations, that is the counterpart of (6.70)

$$\begin{aligned} m(\dot{\beta}u + \beta\dot{u} + u^2\rho) &= Y(\beta,\rho;\delta_v) \\ J_z(\dot{\rho}u + \rho\dot{u}) &= N(\beta,\rho;\delta_v) \end{aligned} \tag{6.75}$$

where $|\dot{u}| \simeq 0$.

It is worth noting that, differently from (6.38) of the double track model, the axle lateral forces Y_1 and Y_2, and hence also the total lateral force Y and the yaw moment N, do *not* depend explicitly on the forward speed u, even if roll steer is taken into account.[8]

Moreover, the expressions of Y and N in (6.75) are even simpler than those in (6.71).

6.5.7 Inverse Congruence Equations

The state variables v and r appear in both congruence equations (6.68). However, it is possible to invert these equations to obtain two other equivalent equations, with $\rho = r/u$ appearing only in the first equation and $\beta = v/u$ only in the second equation

$$\begin{aligned} \rho &= \frac{r}{u} = \frac{\delta_1 - \delta_2}{l} - \frac{\alpha_1 - \alpha_2}{l} \\ \beta &= \frac{v}{u} = \frac{\delta_1 a_2 + \delta_2 a_1}{l} - \frac{\alpha_1 a_2 + \alpha_2 a_1}{l} \end{aligned} \tag{6.76}$$

where the more compact notation $\delta_1 = \delta_v \tau_1$ and $\delta_2 = \delta_v \tau_2$ has been used.

It is important to realize that all these inverse congruence equations are not limited to steady-state conditions, although they are mostly used for the evaluation of some steady-state features.

Another very common way to rewrite the first equation in (6.76) is as follows

$$\alpha_1 - \alpha_2 = (\delta_1 - \delta_2) - \frac{l}{R} = \delta - \frac{l}{R} \tag{6.77}$$

where $R = u/r$. Should $\alpha_1 = \alpha_2 = 0$ (very low speed), then $\delta = l/R$, which is often called Ackermann angle (not to be confused with Ackermann steering geometry, discussed in Sect. 3.4).

6.5.8 β_1 and β_2 as State Variables

Another useful set of state variables may be the vehicle slip angles at each axle midpoint (Fig. 6.20)

$$\begin{aligned} \beta_1 &= \beta + \rho a_1 = \delta_1 - \alpha_1 = (1 + \kappa)\tau\delta_v - \alpha_1 \\ \beta_2 &= \beta - \rho a_2 = \delta_2 - \alpha_2 = \kappa\tau\delta_v - \alpha_2 \end{aligned} \tag{6.78}$$

[8] All the effects of the lateral acceleration $\tilde{a}_y = ur = u^2\rho$ on Y and N are already included in the axle characteristics.

The inverse equations are

$$\begin{aligned} \rho &= \frac{\beta_1 - \beta_2}{l} \\ \beta &= \frac{\beta_1 a_2 + \beta_2 a_1}{l} \end{aligned} \tag{6.79}$$

The corresponding governing equations of the single track model become:

- equilibrium equations

$$\begin{aligned} \dot{\beta}_1 u + \beta_1 \dot{u} + (\beta_1 - \beta_2)\frac{u^2}{l} &= \frac{Y}{m} + \frac{N}{J_z} a_1 \\ \dot{\beta}_2 u + \beta_2 \dot{u} + (\beta_1 - \beta_2)\frac{u^2}{l} &= \frac{Y}{m} - \frac{N}{J_z} a_2 \end{aligned} \tag{6.80}$$

- congruence equations

$$\begin{aligned} \alpha_1 &= \delta_v \tau_1 - \beta_1 = \delta_1 - \beta_1 \\ \alpha_2 &= \delta_v \tau_2 - \beta_2 = \delta_2 - \beta_2 \end{aligned} \tag{6.81}$$

- constitutive equations (from the axle characteristics)

$$\begin{aligned} Y_1 &= Y_1(\alpha_1) \\ Y_2 &= Y_2(\alpha_2) \end{aligned} \tag{6.82}$$

The two first-order differential equations (6.70) or (6.75), governing the dynamical system, become

$$\begin{aligned} \dot{\beta}_1 u + \beta_1 \dot{u} + (\beta_1 - \beta_2)\frac{u^2}{l} &= \frac{J_z + m a_1^2}{m J_z} Y_1(\delta_v \tau_1 - \beta_1) + \frac{J_z - m a_1 a_2}{m J_z} Y_2(\delta_v \tau_2 - \beta_2) \\ \dot{\beta}_2 u + \beta_2 \dot{u} + (\beta_1 - \beta_2)\frac{u^2}{l} &= \frac{J_z + m a_2^2}{m J_z} Y_2(\delta_v \tau_2 - \beta_2) + \frac{J_z - m a_1 a_2}{m J_z} Y_1(\delta_v \tau_1 - \beta_1) \end{aligned} \tag{6.83}$$

where, again, the terms on the r.h.s. do not depend on u.

These equations highlight an interesting feature. The terms $(J_z - m a_1 a_2)$, which appear in both equations, are often very small in road cars, and could even be purposely set equal to zero. Therefore, the coupling between the two equations is fairly weak.

We observe that (6.77) becomes

$$\alpha_1 - \alpha_2 = (\delta_1 - \delta_2) - (\beta_1 - \beta_2) \tag{6.84}$$

and we also have

$$\alpha_1 a_2 + \alpha_2 a_1 = (\delta_1 a_2 + \delta_2 a_1) - (\beta_1 a_2 + \beta_2 a_1) \tag{6.85}$$

6.5.9 Driving Force

At the beginning of this chapter, and precisely in (6.1), we made the assumption of small longitudinal forces. But small does not mean zero. Indeed, a small amount of power is necessary even for keeping a vehicle in steady-state conditions. To make this statement quantitative, let us consider a rear-wheel-drive single track model (Fig. 6.20, with $F_{x_1} = 0$). The power balance

$$(F_{x_2} - F_{y_1}\delta_1)u + F_{y_1}(v_p + r_p a_1) + F_{y_2}(v_p - r_p a_2) - \left(\frac{1}{2}\rho S C_x u^2\right) u = 0 \quad (6.86)$$

provides the following driving force F_{x_2}

$$\begin{aligned} F_{x_2} &= F_{y_1}\left(\delta_1 - \frac{v_p + r_p a_1}{u}\right) + F_{y_2}\left(-\frac{v_p - r_p a_2}{u}\right) + \frac{1}{2}\rho S C_x u^2 \\ &= F_{y_1}\alpha_1 + F_{y_2}\alpha_2 + \frac{1}{2}\rho S C_x u^2 \end{aligned} \quad (6.87)$$

This force has to counteract the aerodynamic drag (obvious) and also the drag due to tire slips (maybe not so obvious at first).

That tire slips induce drag can be better appreciated from Fig. 6.21 (where, for simplicity, the aerodynamic drag is not considered). Points C and A do not coincide because of the slip angles α_1 and α_2. Therefore, a longitudinal driving force F_{x_2} is required to achieve the dynamic equilibrium (cf. [10, p. 67]).

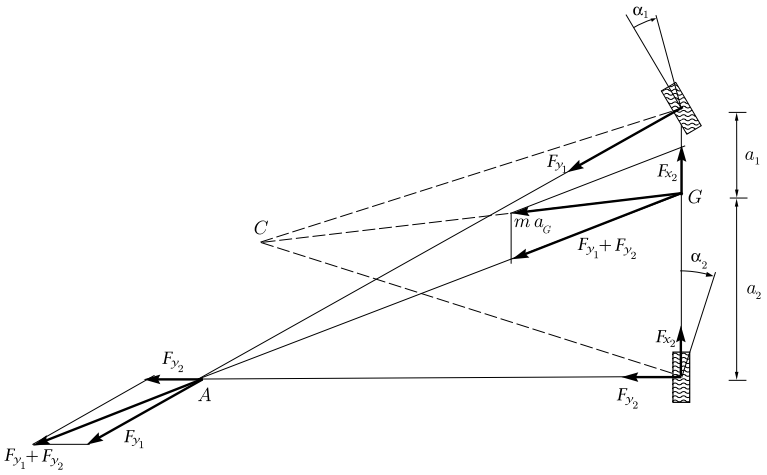

Fig. 6.21 Graphical evaluation of the driving force F_{x_2} at steady state

Of course, Fig. 6.21 is just a scheme. In real cases, slip angles are smaller. Therefore, the distances of points C and A from the vehicle are much greater, and F_{x_2} becomes much smaller, as assumed in (6.1).

6.5.10 The Role of the Steady-State Lateral Acceleration

As already stated in Sect. 6.4, it is common practice to employ $(\delta_v, \tilde{a}_y)$, instead of (δ_v, u), as parameters to characterize a steady-state condition. In the single track model some steady-state quantities are functions of $\tilde{a}_y$ only.

The reason for such a fortunate coincidence in the case under examination is promptly explained. Just look at the equilibrium equations at steady state, with the inclusion of the axle characteristics, that is for the single track model

$$\begin{aligned} m\tilde{a}_y &= Y_1(\alpha_1) + Y_2(\alpha_2) \\ 0 &= Y_1(\alpha_1)a_1 - Y_2(\alpha_2)a_2 \end{aligned} \tag{6.88}$$

They yield this result (already obtained in (6.8) and (6.58))

$$\frac{Y_1(\alpha_1)l}{ma_2} = \tilde{a}_y \qquad \text{and} \qquad \frac{Y_2(\alpha_2)l}{ma_1} = \tilde{a}_y \tag{6.89}$$

which can be more conveniently rewritten as

$$\frac{Y_1(\alpha_1)l}{mga_2} = \frac{Y_1(\alpha_1)}{Z_1^0} = \frac{\tilde{a}_y}{g} \qquad \text{and} \qquad \frac{Y_2(\alpha_2)l}{mga_1} = \frac{Y_2(\alpha_2)}{Z_2^0} = \frac{\tilde{a}_y}{g} \tag{6.90}$$

where Z_1^0 and Z_2^0 are the static vertical loads on each axle.

Therefore, if we take the monotone part of each axle characteristic, there is a one-to-one correspondence between $\tilde{a}_y$ and the apparent slip angles at steady state (Fig. 6.24)

$$\alpha_1 = \alpha_1(\tilde{a}_y) \qquad \text{and} \qquad \alpha_2 = \alpha_2(\tilde{a}_y) \tag{6.91}$$

This is the key fact for using $\tilde{a}_y$. Both apparent slip angles only "feel" the lateral acceleration, no matter if the vehicle has small u and large δ_v or, vice versa, large u and small δ_v. In other words, the radius of the circular trajectory of the vehicle does not matter at all. Only $\tilde{a}_y$ matters to the lateral forces and hence to the apparent slip angles. Actually, this very same property has been already used to build the axle characteristics equations (6.91) are just the inverse functions of (6.60).

We remark that (6.91) must not be taken as a general rule, but rather as a fortunate coincidence (it applies only to vehicles with two axles, open differential, no wings and parallel steering).

Another very important result comes directly from (6.90)

$$\frac{Y_1(\alpha_1)}{Z_1^0} = \frac{Y_2(\alpha_2)}{Z_2^0} = \frac{\tilde{a}_y}{g} \tag{6.92}$$

that is, at steady state, the lateral forces are always proportional to the corresponding static vertical loads. Therefore, the *normalized axle characteristics*

$$\hat{Y}_1(\alpha_1) = \frac{Y_1(\alpha_1)}{Z_1^0} \quad \text{and} \quad \hat{Y}_2(\alpha_2) = \frac{Y_2(\alpha_2)}{Z_2^0} \tag{6.93}$$

are what really matters in the vehicle dynamics of the single track model. The normalized axle characteristics are non-dimensional. Their maximum value is equal to the grip available in the lateral direction and is, therefore, a very relevant piece of information.

6.5.11 Slopes of the Axle Characteristics

It turns out that vehicle handling is pretty much affected by the slopes (derivatives) of the axle characteristics

$$\Phi_1 = \frac{\mathrm{d}Y_1}{\mathrm{d}\alpha_1} \quad \text{and} \quad \Phi_2 = \frac{\mathrm{d}Y_2}{\mathrm{d}\alpha_2} \tag{6.94}$$

Obviously, $\Phi_i > 0$ in the monotone increasing part of the axle characteristics.

According to (6.91), in the single track model we have that the slopes Φ_i of the axle characteristics are functions of the lateral acceleration only

$$\begin{aligned} \Phi_1 &= \Phi_1(\alpha_1) = \Phi_1(\alpha_1(\tilde{a}_y)) = \Phi_1(\tilde{a}_y) \\ \Phi_2 &= \Phi_2(\alpha_2) = \Phi_2(\alpha_2(\tilde{a}_y)) = \Phi_2(\tilde{a}_y) \end{aligned} \tag{6.95}$$

From (6.89)

$$\frac{\mathrm{d}\tilde{a}_y}{\mathrm{d}\alpha_1} = \frac{l\Phi_1}{ma_2} \quad \text{and} \quad \frac{\mathrm{d}\tilde{a}_y}{\mathrm{d}\alpha_2} = \frac{l\Phi_2}{ma_1} \tag{6.96}$$

and hence

$$\frac{\mathrm{d}\alpha_1}{\mathrm{d}\tilde{a}_y} = \frac{ma_2}{l\Phi_1} \quad \text{and} \quad \frac{\mathrm{d}\alpha_2}{\mathrm{d}\tilde{a}_y} = \frac{ma_1}{l\Phi_2} \tag{6.97}$$

6.6 Double Track, or Single Track?

Equation (6.34) for the double track model and Eq. (6.71) for the single track model are quite similar. Then, what are the substantial differences between these two models?

One relevant difference is that in the single track model Y and N are functions of $(\beta, \rho; \delta_v)$, whereas in the double track model Y and N are, in general, functions of $(\beta, \rho; u, \delta_v)$, as shown in (6.75) and (6.38), respectively. Other differences are:

- parallel steering;
- small steer angles; $u \gg |rt_i|$.

All these assumptions lead to the truly fundamental difference: in the single track model *the axle lateral forces Y_1 and Y_2 can be given as known functions of only one variable*. They are the celebrated axle characteristics.

However, the effort for building a numerical model and running simulations is pretty much the same. Of course the double track model is more general. It does not require the assumption of parallel steering. Moreover, it can deal with cases in which $u \gg |rt_i|$ does not hold.

The single track model is less realistic, but simpler, and hence more predictable for a human being. Almost all the complexity boils down to the axle characteristics. As already mentioned, the single track model can provide in many cases useful insights into vehicle handling, particularly for educational purposes.

6.7 Steady-State Maps

We have already stated that the two functions (6.48) define *all* steady-state conditions of the double track model. However, the topic is so relevant to deserve additional attention and discussion.

From (6.47), (6.50), (6.76) and (6.91) we have, at *steady state*, the following maps

$$\begin{aligned} \rho_p &= \rho_p(\delta_v, \tilde{a}_y) = \frac{r_p}{u} = \frac{\tau \delta_v}{l} - \frac{\alpha_1(\tilde{a}_y) - \alpha_2(\tilde{a}_y)}{l} \\ \beta_p &= \beta_p(\delta_v, \tilde{a}_y) = \frac{v_p}{u} = \left(\frac{(1+\kappa)a_2 + \kappa a_1}{l} \right) \tau \delta_v - \frac{\alpha_1(\tilde{a}_y)a_2 + \alpha_2(\tilde{a}_y)a_1}{l} \end{aligned} \tag{6.98}$$

A vehicle has unique functions $\rho_p(\delta_v, \tilde{a}_y)$ and $\beta_p(\delta_v, \tilde{a}_y)$. As will be shown, they tell us a lot about the global vehicle steady-state behavior. In other words, these two maps fully characterize *any* steady-state condition of the vehicle.

The two functions $\rho_p(\delta_v, \tilde{a}_y)$ and $\beta_p(\delta_v, \tilde{a}_y)$ can also be obtained experimentally, once a prototype vehicle is available, by performing some rather simple tests on a flat proving ground. With the vehicle driven at almost constant speed u and a slowly increasing steering wheel angle δ_v, it suffices to measure the following quantities: r_p, v_p, u, $\tilde{a}_y$ and δ_v. It is worth noting that none of these quantities does require to know whether the vehicle has two axles or more, or how long the wheelbase is. In other words, they are all *well defined in any vehicle, including race cars*.

Of course, the r.h.s. part of (6.98) is strictly linked to the single track model, and it is useful to the vehicle engineer to understand how to modify the vehicle behavior.

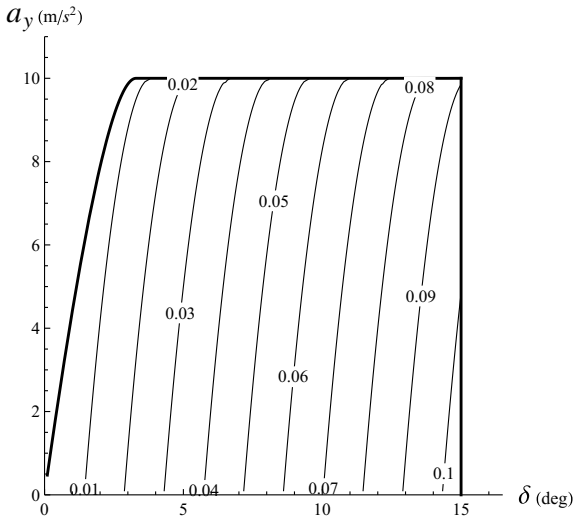

Fig. 6.22 Curves at constant ρ (1/m) in the plane $(\delta, \tilde{a}_y)$, for an understeer vehicle

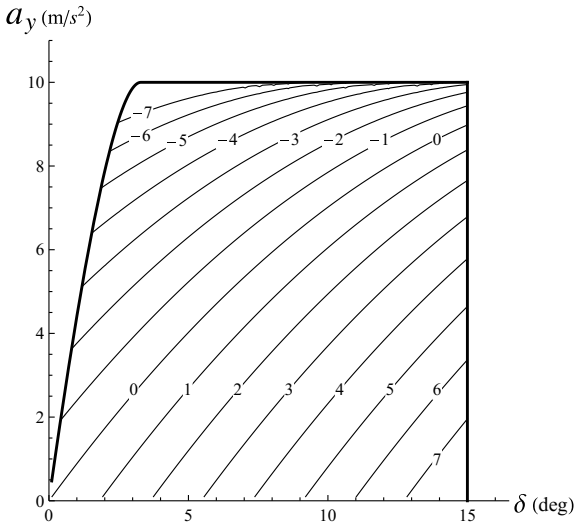

Fig. 6.23 Curves at constant β (deg) in the plane $(\delta, \tilde{a}_y)$, for an understeer vehicle

A key feature, confirmed by tests on real road cars (with open differential and no wings), is that the δ_v-dependence and the $\tilde{a}_y$-dependence are clearly *separated*.[9]

As shown in Figs. 6.22 and 6.23, both maps in (6.98) are (in the single track model) *linear* with respect to the steering wheel angle δ_v, whereas they are *nonlinear* with respect to the steady-state lateral acceleration $\tilde{a}_y$. The linear parts are totally under control, in the sense that both of them are simple functions of the steer gear ratios

[9] We remark that this is no longer true in vehicles with limited-slip differential and/or aerodynamic vertical loads.

and of a_1 and a_2. The nonlinear parts are more challenging, coming directly from the interplay of the axle characteristics.

Figures 6.22 and 6.23, where $\delta = \tau\delta_v$, anticipate the Map of Achievable Performance (MAP) approach, presented in Sect. 6.8.

6.7.1 Steady-State Gradients

It is informative, and hence quite useful, to define and compute/measure the *gradients* of the two maps $\beta_p(\delta_v, \tilde{a}_y)$ and $\rho_p(\delta_v, \tilde{a}_y)$, defined in (6.98)

$$\begin{aligned} \text{grad } \rho_p &= \left(\frac{\partial \rho_p}{\partial \tilde{a}_y}, \frac{\partial \rho_p}{\partial \delta_v}\right) = (\rho_y, \rho_\delta) \\ \text{grad } \beta_p &= \left(\frac{\partial \beta_p}{\partial \tilde{a}_y}, \frac{\partial \beta_p}{\partial \delta_v}\right) = (\beta_y, \beta_\delta) \end{aligned} \tag{6.99}$$

As well known, gradients are vectors orthogonal to the level curves.

For the single track model, the explicit expressions of the components of the gradients grad ρ_p and grad β_p are as follows

$$\begin{aligned} \rho_y &= -\frac{m}{l^2}\left(\frac{\Phi_2 a_2 - \Phi_1 a_1}{\Phi_1 \Phi_2}\right) & \rho_\delta &= \frac{\tau}{l} \\ \beta_y &= -\frac{m}{l^2}\left(\frac{\Phi_1 a_1^2 + \Phi_2 a_2^2}{\Phi_1 \Phi_2}\right) & \beta_\delta &= \tau\left(\frac{(1+\kappa)a_2 + \kappa a_1}{l}\right) \end{aligned} \tag{6.100}$$

where, to compute β_y and ρ_y, we took into account (6.97).

It is worth noting that, for a given single track model of a vehicle, the two gradient components β_δ and ρ_δ are *constant*, whereas the other two gradient components β_y and ρ_y are functions of $\tilde{a}_y$ *only*.

As will be discussed shortly, only one out of four gradient components is usually employed in classical vehicle dynamics,[10] thus missing a lot of information. But this is not the only case in which classical vehicle dynamics turns out to be far from systematic and rigorous. This lack of generality of classical vehicle dynamics is the motivation for some of the next sections.

[10] It is the well known understeer gradient K, defined in (6.116). Unfortunately, it is not a good parameter and should be replaced by the gradient components (6.99), as demonstrated in Sect. 6.14.1.

6.7.2 Alternative Steady-State Gradients

Although not commonly done, we evaluate the gradients of the front and rear slip angles $\beta_1(\delta_v, \tilde{a}_y)$ and $\beta_2(\delta_v, \tilde{a}_y)$, which were defined in (6.78)

$$\begin{aligned} \beta_{1y} &= -\frac{ma_2}{l\Phi_1} & \beta_{1\delta} &= (1+\kappa)\tau \\ \beta_{2y} &= -\frac{ma_1}{l\Phi_2} & \beta_{2\delta} &= \kappa\tau \end{aligned} \tag{6.101}$$

A fairly obvious result, but that can turn out to be useful in some cases.

6.7.3 Understeer and Oversteer

For further developments, it is convenient to rewrite (6.98) in a more compact form

$$\begin{aligned} \rho_p &= \rho_p(\delta_v, \tilde{a}_y) = \left(\frac{\tau_1 - \tau_2}{l}\right)\delta_v - f_\rho(\tilde{a}_y) \\ \beta_p &= \beta_p(\delta_v, \tilde{a}_y) = \left(\frac{\tau_1 a_2 + \tau_2 a_1}{l}\right)\delta_v - f_\beta(\tilde{a}_y) \end{aligned} \tag{6.102}$$

where, in the single track model

$$\begin{aligned} f_\rho(\tilde{a}_y) &= \frac{\alpha_1(\tilde{a}_y) - \alpha_2(\tilde{a}_y)}{l} \\ f_\beta(\tilde{a}_y) &= \frac{\alpha_1(\tilde{a}_y)a_2 + \alpha_2(\tilde{a}_y)a_1}{l} \end{aligned} \tag{6.103}$$

The two functions $f_\rho(\tilde{a}_y)$ and $f_\beta(\tilde{a}_y)$ are nonlinear functions, peculiar to a given road vehicle. They are called *slip functions* here.

Let us discuss this topic by means of a few examples.

First, let us consider the normalized axle characteristics (6.93) (multiplied by g) shown in Fig. 6.24(left). In this example, it has been assumed that both axles have the same lateral grip equal to 1. Moreover, to keep, for the moment, the analysis as simple as possible, we also assume that $\hat{Y}_1(x) = \hat{Y}_2(kx)$, with $k > 0$. When inverted, they provide the apparent slip angles $\alpha_1(\tilde{a}_y)$ and $\alpha_2(\tilde{a}_y)$ shown in Fig. 6.24(right). Assuming a wheelbase $l = 2.5\,\text{m}$, $a_1 = 1.125\,\text{m}$, and $a_2 = 1.375\,\text{m}$, we get from (6.103) the two slip functions f_ρ and f_β of Fig. 6.25.

In all Figures, angles are in degree, accelerations in m/s^2, and a_y should be read as $\tilde{a}_y$.

A vehicle with a monotone increasing slip function $f_\rho(\tilde{a}_y)$, as in Fig. 6.25, is said to be an *understeer* vehicle. A more precise definition is given in (6.106).

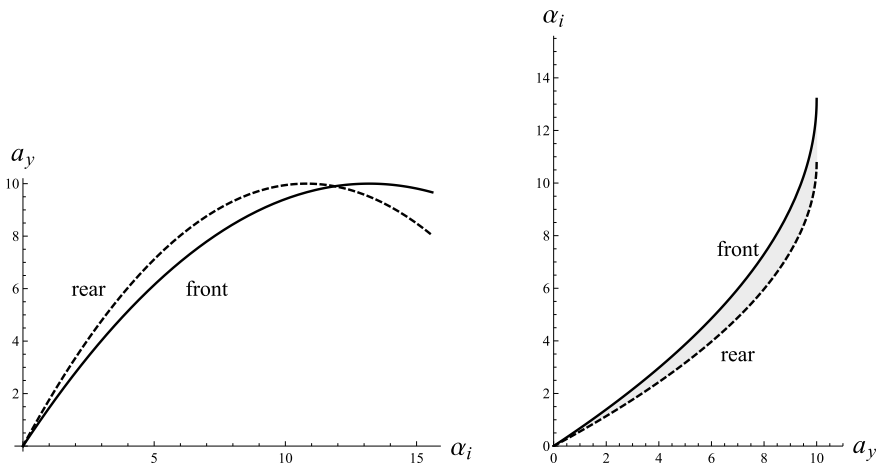

Fig. 6.24 Normalized axle characteristics (multiplied by g) of an *understeer* vehicle (left) and corresponding apparent slip angles (right)

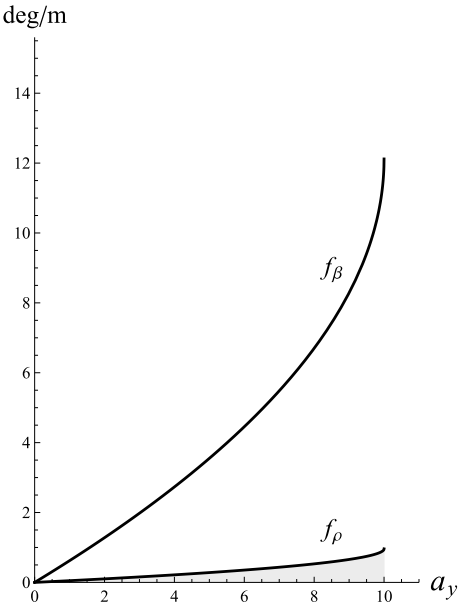

Fig. 6.25 Slip functions of an *understeer* vehicle

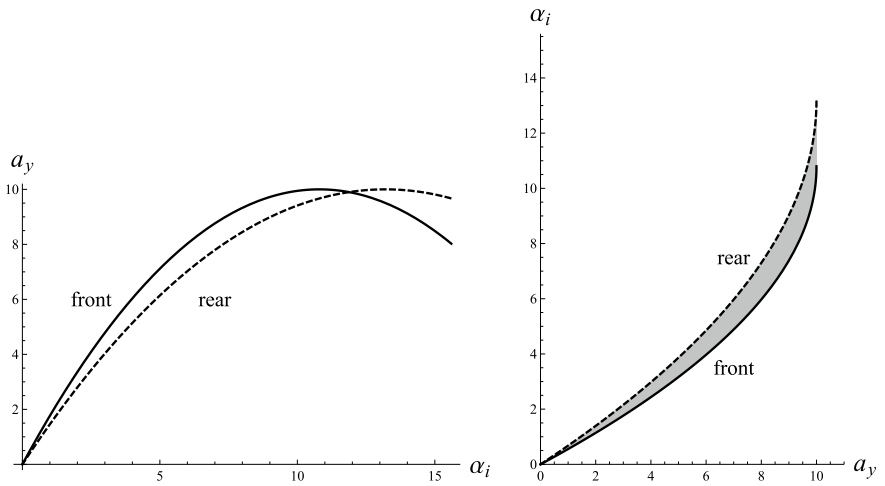

Fig. 6.26 Normalized axle characteristics (multiplied by g) of an *oversteer* vehicle (left) and corresponding apparent slip angles (right)

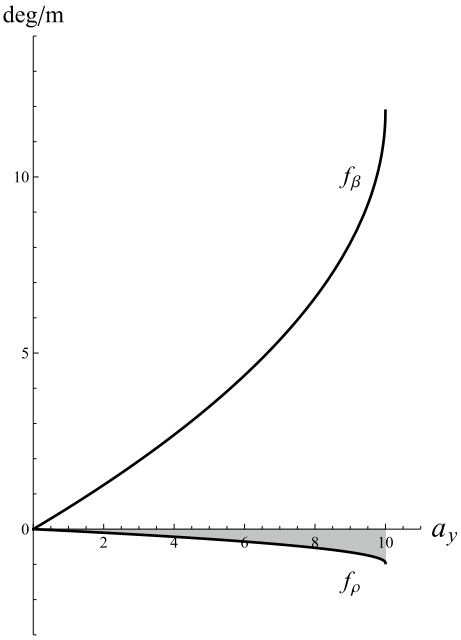

Fig. 6.27 Slip functions of an *oversteer* vehicle

As a second example, let us consider the normalized axle characteristics (multiplied by g) shown in Fig. 6.26(left). They are like in Fig. 6.24, but interchanged. When inverted, they provide the two functions $\alpha_1(\tilde{a}_y)$ and $\alpha_2(\tilde{a}_y)$ shown in Fig. 6.26(right). In this case the two slip functions f_ρ and f_β are as in Fig. 6.27.

A vehicle with a monotone decreasing function $f_\rho(\tilde{a}_y)$, as in Fig. 6.27, is said to be an *oversteer* vehicle. A more precise definition is given in (6.108).

6.7.4 Handling Diagram

Usually, only the function $f_\rho(\tilde{a}_y)$ is considered in classical vehicle dynamics, while $f_\beta(\tilde{a}_y)$ is neglected.

Since, at steady state, $\rho_p = \tilde{a}_y/u^2 = 1/R$, the first equation in (6.102) becomes

$$\frac{\tilde{a}_y}{u^2} = \left(\frac{\tau_1 - \tau_2}{l}\right)\delta_v - f_\rho(\tilde{a}_y) \tag{6.104}$$

which, for given u and δ_v, is an equation for the unknown $\tilde{a}_y = \tilde{a}_y(\delta_v, u)$. See also (6.46).

However, it is customary [11–13] to rewrite (6.104) as a system of two equations

$$\begin{cases} y = \left(\dfrac{\tau_1 - \tau_2}{l}\right)\delta_v - \dfrac{\tilde{a}_y}{u^2} \\ y = f_\rho(\tilde{a}_y) = \dfrac{\alpha_1(\tilde{a}_y) - \alpha_2(\tilde{a}_y)}{l} \end{cases} \tag{6.105}$$

Solving this system amounts to obtaining the values of $(\tilde{a}_y, f_\rho)$ attained under the imposed operating conditions (δ_v, u). Geometrically, that can be seen as the intersection between a *straight line* (i.e., the first equation in (6.105)) and the so-called *handling curve* $y = f_\rho(\tilde{a}_y)$ (i.e., the second equation in (6.105)).

Together, the handling curve and the straight lines form the celebrated *handling diagram* [11–13]. Examples are shown in Figs. 6.28 and 6.29 (where a_y is indeed $\tilde{a}_y$ and y is in deg/m).

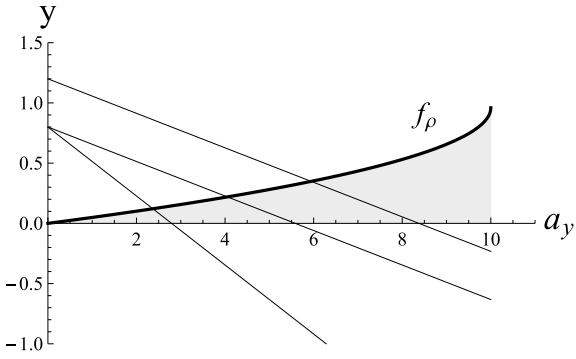

Fig. 6.28 Handling diagram of an understeer vehicle (y in deg/m)

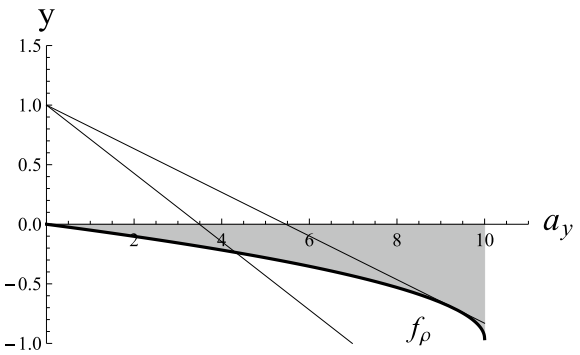

Fig. 6.29 Handling diagram of an oversteer vehicle (y in deg/m)

The handling curve $y = f_\rho(\tilde{a}_y)$ is peculiar to each vehicle (in the single track model it depends on the normalized axle characteristics only). Therefore, for a given road vehicle it has to be drawn once and for all.

On the other hand, the straight line depends on the selected operating conditions (δ_v, u). For instance, in Fig. 6.28 the two intersecting lines correspond to two operating conditions with the same value of δ_v, while the two parallel lines share the same value of u.

Perhaps, the best way to understand the handling diagram (Figs. 6.28 and 6.29) is by assuming that the steering wheel angle δ_v is kept constant, while the forward speed u is (slowly) increased.

In Fig. 6.28, an increasing u, with constant δ_v, results also in an increasing y. Therefore, from (6.109) with constant δ_v (and hence constant δ), the higher the forward speed u, the larger the radius R of the trajectory of the vehicle. This is called *understeer behavior*. More precisely, we have understeer whenever

$$\frac{\mathrm{d}f_\rho}{\mathrm{d}\tilde{a}_y} > 0 \tag{6.106}$$

where, in the single track model

$$\frac{\mathrm{d}f_\rho}{\mathrm{d}\tilde{a}_y} = \frac{m}{l^2}\left(\frac{\Phi_2 a_2 - \Phi_1 a_1}{\Phi_1 \Phi_2}\right) \tag{6.107}$$

On the contrary, if the handling curve is, e.g., like in Fig. 6.29, the higher the forward speed u, with constant δ_v, the smaller the radius R. This is called *oversteer behavior*. More precisely, we have oversteer whenever

$$\frac{\mathrm{d}f_\rho}{\mathrm{d}\tilde{a}_y} < 0 \tag{6.108}$$

Actually, when the straight line becomes tangent to the handling curve, as shown in Fig. 6.29, the vehicle becomes unstable. It means that the vehicle has reached the

critical speed associated to that value of δ_v. The concept of critical speed will be discussed in Sect. 6.13 in a more general framework.

Another, most classical, way to recast the system (6.105) is

$$\delta - \frac{l}{R} = \alpha_1(\tilde{a}_y) - \alpha_2(\tilde{a}_y) = f_\rho(\tilde{a}_y) l \tag{6.109}$$

where

$$\delta = (\tau_1 - \tau_2)\ \delta_v \tag{6.110}$$

is the *net steer angle*, already defined in (6.51).

Vehicles with aerodynamic devices and/or limited-slip differential do not exhibit a handling curve [11, p. 172], but a *handling surface* instead [5]. More precisely, (6.109) still holds true, but with $f_\rho(\tilde{a}_y, 1/R)$. This topic is addressed in Sect. 7.5.

Classical vehicle dynamics stops about here. In the next section a fresh, more comprehensive, global approach is developed. It brings new insights into the global steady-state behavior of real vehicles, along with some new hints about the transient behavior.

6.8 Map of Achievable Performance (MAP)

The handling diagram, although noteworthy, does not provide a complete picture of the handling behavior. Just consider that the use of $\tilde{a}_y$ as input variable, that is one variable instead of two, hides some features of the vehicle handling behavior.

Here we suggest a completely new approach, a *global* one. That is, an approach that unveils, *at a glance*, the overall steady-state features of the vehicle under investigation, thus making it easier to distinguish between a "good" vehicle and a "not-so-good" one.

As already stated in (6.44), the steady-state handling behavior is completely described by the handling maps

$$\begin{aligned} \rho_p &= \hat{\rho}_p(\delta_v, u) = \left(\frac{\tau_1 - \tau_2}{l}\right) \delta_v - \frac{\alpha_1(\delta_v, u) - \alpha_2(\delta_v, u)}{l} \\ \beta_p &= \hat{\beta}_p(\delta_v, u) = \left(\frac{\tau_1 a_2 + \tau_2 a_1}{l}\right) \delta_v - \frac{\alpha_1(\delta_v, u) a_2 + \alpha_2(\delta_v, u) a_1}{l} \end{aligned} \tag{6.111}$$

where the last terms are peculiar to the single track model.

In the single track model, it is convenient to define the *net steer angle* δ, as already done in (6.51) and in (6.110)

$$\begin{aligned} (1 + \kappa)\delta = \delta_1 &= \tau_1 \delta_v \\ \kappa \delta = \delta_2 &= \tau_2 \delta_v \end{aligned} \tag{6.112}$$

Usually, $\kappa = 0$ and hence $\delta = \delta_1$ is just the steering angle of the front wheel. However, $\kappa \neq 0$ leaves room for direct rear steering as well. In general,

$$\delta = \delta_1 - \delta_2 = (\tau_1 - \tau_2)\delta_v \tag{6.113}$$

With this notation, the *handling maps* (6.111) become

$$\begin{aligned} \rho &= \rho(\delta, u) = \frac{\delta}{l} - \frac{\alpha_1(\delta, u) - \alpha_2(\delta, u)}{l} \\ \beta &= \beta(\delta, u) = \left(\frac{(1+\kappa)a_2 + \kappa a_1}{l}\right)\delta - \frac{\alpha_1(\delta, u)a_2 + \alpha_2(\delta, u)a_1}{l} \end{aligned} \tag{6.114}$$

where, for the sake of compactness, we dropped the subscript p. These two maps fully characterize the steady-state behavior of the vehicle. This is a fairly general point of view that leads to a global approach that we call Map of Achievable Performance (MAP).

Actually, under the acronym MAP we will present several types of possible graphical representations of the handling maps, each one on the corresponding *achievable region*. This is another key concept.

Figures in this section are for road cars with the following features: mass $m = 2000\,\text{kg}$, wheelbase $l = 2.5\,\text{m}$, $a_1 = 1.125\,\text{m}$, $a_2 = 1.375\,\text{m}$, grip coefficient $\mu = 1$, maximum speed $u_{\max} = 40\,\text{m/s}$, maximum steer angle of the front wheels $\delta_{\max} = 15°$. The understeer version has normalized axle characteristics as in Fig. 6.24. The oversteer version has normalized axle characteristics as in Fig. 6.26. In all figures, angles are in degree, accelerations in m/s^2, and ρ in m^{-1}.

6.8.1 MAP Fundamentals

The main idea behind the MAP approach is simple: the driver controls (δ, u), the vehicle reacts with (ρ, β). That is

$$(\delta, u) \quad \Longrightarrow \quad (\rho, \beta) \tag{6.115}$$

The input values (δ, u) that a given vehicle can really *achieve* are subject to three limitations:

- maximum steer angle $\delta_{\max}$;
- maximum speed $u_{\max}$, or critical speed u_{cr}, if $u_{\text{cr}} < u_{\max}$;
- maximum lateral acceleration (grip limited).

This is shown in Fig. 6.30 (left). Each achievable point (δ, u) results in the vehicle performing with precise values (ρ, β). Therefore, the *achievable input region* of Fig. 6.30 (left) is mapped onto the *achievable output region* shown in Fig. 6.30 (right).

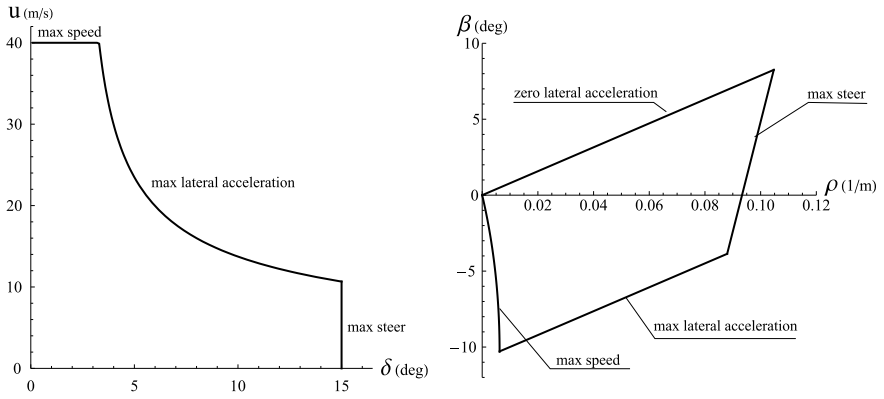

Fig. 6.30 Achievable *input* region (left) and achievable *output* region (right) for an understeer vehicle

Quite interesting are the MAPs (Maps of Achievable Performance) that can be drawn inside these achievable regions. For instance, curves at constant $\tilde{a}_y$ are drawn on both regions in Fig. 6.31. In an understeer vehicle without significant aerodynamic vertical loads, the grip-limited bound is just the curve at constant $\tilde{a}_y = \mu g$.

While the yaw rate r_p has typically the same sign as δ, the same does not apply to the lateral speed v_p. As shown in Fig. 6.32, in a left turn the vehicle slip angle $\beta = v_p/u$ can either be positive or negative. As a rule of thumb, at low forward speed the vehicle goes around "nose-out" ($\beta > 0$), whereas at high speed the vehicle goes around "nose-in" ($\beta < 0$). This statement can be made *quantitative* by drawing the curves at constant β on the achievable input region, as shown in Fig. 6.33. The almost horizontal line $\beta = 0$ clearly splits the region into a lower part with $\beta > 0$, and an upper part with $\beta < 0$.

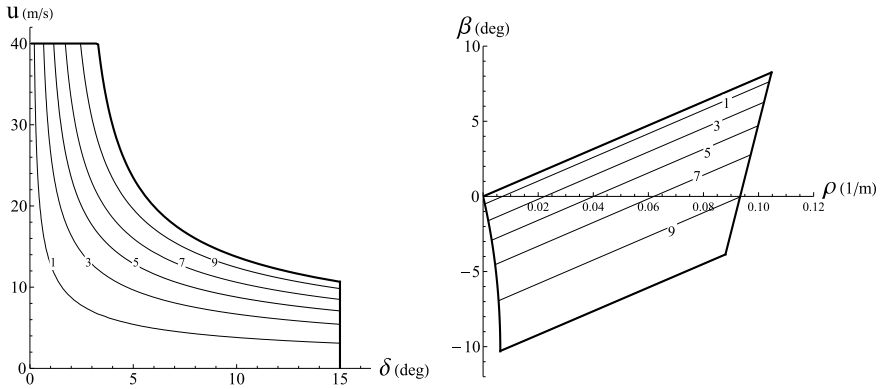

Fig. 6.31 Lines at constant lateral acceleration $\tilde{a}_y$ for an understeer vehicle

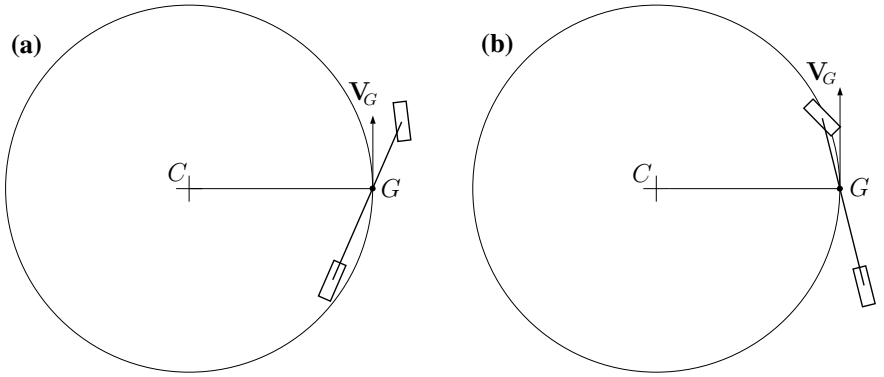

Fig. 6.32 Steady-state behavior: **a** nose-out (low speed), **b** nose-in (high speed)

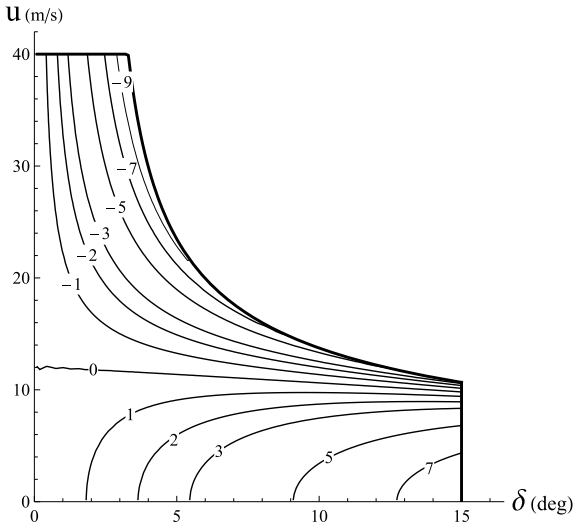

Fig. 6.33 u-δ MAP with curves at constant vehicle slip angle β for an understeer vehicle

Drawing curves at constant curvature ρ also highlights the overall understeer/oversteer behavior of a vehicle. For instance, it is quite obvious that the pattern of Fig. 6.34 is typical of an understeer vehicle: the faster you go, the more you have to steer to keep ρ constant. Moreover, it is worth comparing Fig. 6.22, which is the contour plot of $\rho(\delta, \tilde{a}_y)$, and Fig. 6.34, which is the contour plot of $\rho(\delta, u)$. For instance, the first MAP is linear with respect to δ, whereas the second one is not. The reason is that the other independent variable is different: linear behavior with respect to δ requires constant lateral acceleration $\tilde{a}_y$, not constant forward speed u.

Curves at constant speed u, and also lines at constant steer angle δ, are shown in Fig. 6.35 for an understeer vehicle. As expected, moving top to bottom along each line at constant steer angle, that is with increasing speed, brings smaller values of the curvature ρ. Also interesting is to observe that at low speed the slip angle β grows

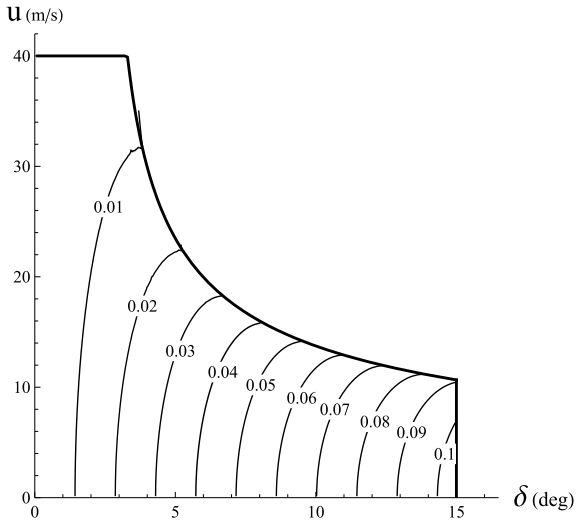

Fig. 6.34 u-δ MAP with curves at constant curvature ρ for an understeer vehicle

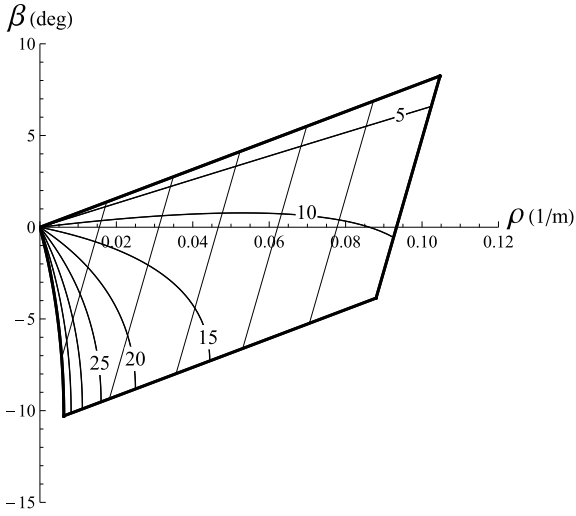

Fig. 6.35 ρ-β MAP with curves at constant u and lines at constant δ for an understeer vehicle

with δ, whereas at high speed it is the other way around. The same phenomena can be observed more clearly in Fig. 6.33.

These MAPs can be obtained experimentally or through simulations. Therefore, they are not limited to the single track model. Actually, as will be discussed in the next chapter, they exist also for race cars, including cars with very high aerodynamic downforces.

The effects of *rear steering* (in addition to front steering, of course) are shown in Fig. 6.36. The picture on the left is for the case of rear wheels turning opposite of the front wheels with $\delta_2 = -0.1\delta_1$, whereas the picture on the right is for rear

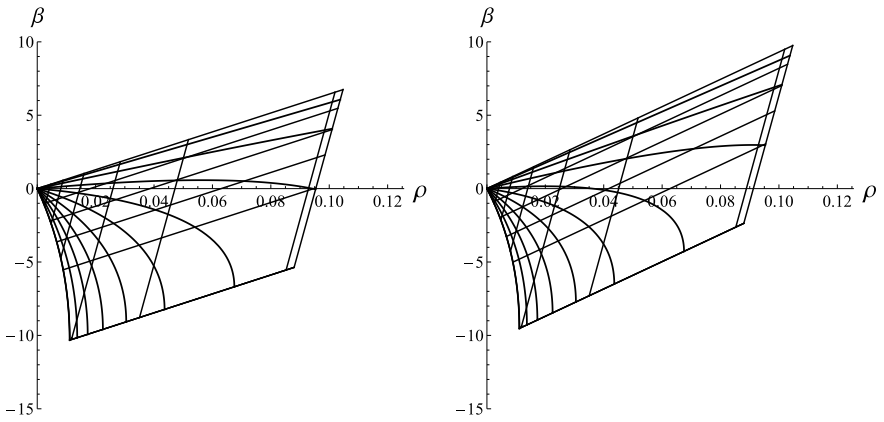

Fig. 6.36 Effects of rear steering on the achievable region: rear wheels turning opposite of the front wheels (left), rear wheels turning like the front wheels (right)

wheels turning like the front wheels, with $\delta_2 = 0.1\delta_1$. The vehicle slip angle β is pretty much affected. Basically, a positive χ moves the achievable region upwards, and vice versa. On the other hand, rear steering does not impinge on the achievable region in the plane (δ, ρ), as will be discussed in Sect. 6.8.2.

Vehicles behave in a better way if β spans a small range. To have a narrower achievable output region in the plane (ρ, β) we have to move down the upper part and move up the lower part. This is indeed the effect of a steering system with rear wheels turning opposite of the front wheels at low speed, and turning like the front wheels at high speed. That is a steering system with, e.g., $\kappa(u) = -\kappa_0 \cos(\pi u/u_{\max})$. The net result can be appreciated by comparing Fig. 6.37 with Fig. 6.35. The MAP approach provides a better insight into rear steering effects than by looking at, e.g., Fig. 6.38.

The achievable region in case of an *oversteer* vehicle is limited by the critical speeds, not by grip. A typical achievable input region, with noteworthy lines, is shown in Fig. 6.39.

The achievable region in the plane (ρ, β) for an *oversteer* vehicle is shown in Fig. 6.40, along with curves at constant speed u and lines at constant steer angle δ. As expected, moving top to bottom along the lines at constant steer angles, that is with increasing speed, entails larger values of the curvature ρ.

Very instructive is the comparison between Figs. 6.35 and 6.40, that is between an understeer and an oversteer vehicle. The two achievable regions have different shapes also because an oversteer vehicle becomes *unstable* for certain combinations of speed and steer angle. These critical combinations form a sort of stability boundary which collects all points where the u-curves and δ-lines are *tangent* to each other, as shown in Fig. 6.40.

On the opposite side, a vehicle with *too much understeer* has an achievable region like in Fig. 6.41 (see also Fig. 6.45 for a more intuitive MAP).

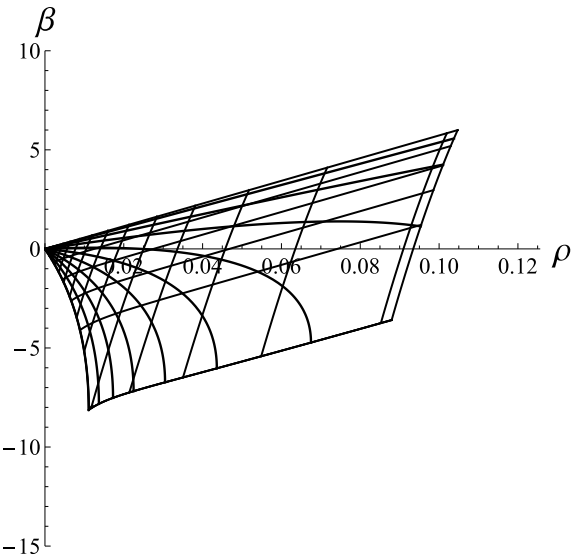

Fig. 6.37 ρ-β MAP for a vehicle with rear wheels turning opposite of the front wheels at low speed and like the front wheels at high speed

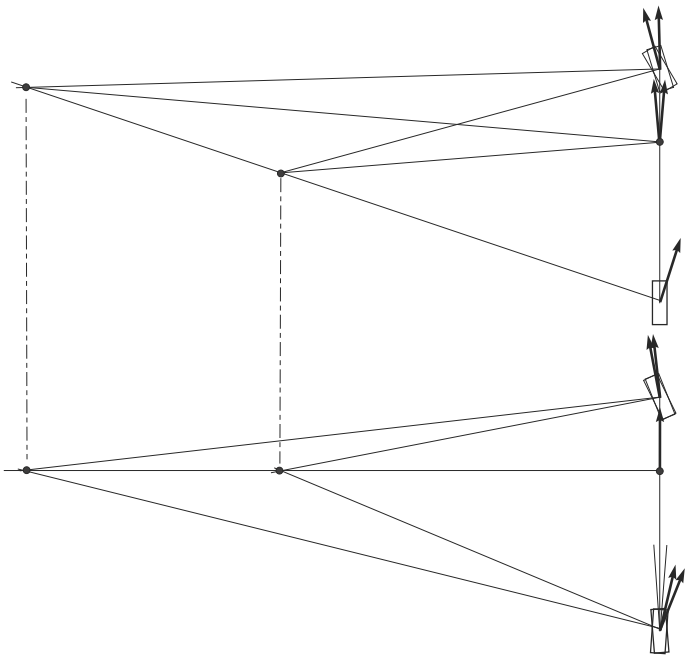

Fig. 6.38 Effect of rear steering on β: front steering only (top); front and rear steering (bottom). All cases have the same $\tilde{a}_y$, and hence the same α_1 and α_2

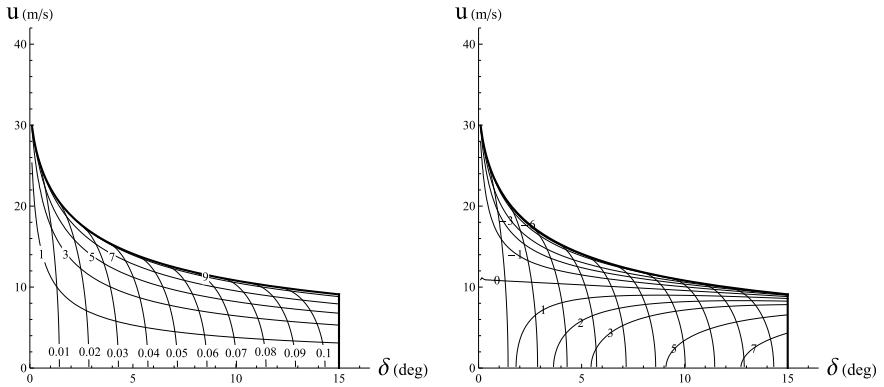

Fig. 6.39 Oversteer vehicle: u-δ MAPs with curves at constant ρ (both), constant $\tilde{a}_y$ (left) and constant β (right)

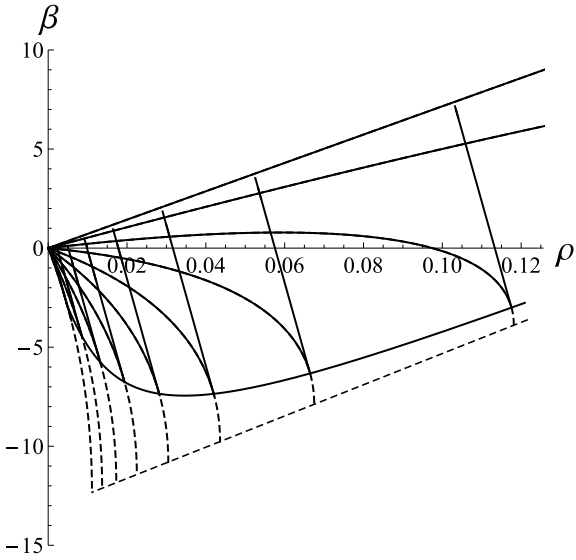

Fig. 6.40 Oversteer vehicle: ρ-β MAP with curves at constant speed u and lines at constant steer angle δ

6.8.2 MAP Curvature ρ Versus Steer Angle δ

A central issue in vehicle dynamics is how a vehicle responds to the driver input commands (namely, the steering wheel angle δ_v and the forward speed u). Well, let us map it. The plane (δ, ρ) suits the purpose in a fairly intuitive and quantitative way.

Let us consider again a vehicle with the front and rear *normalized* axle characteristics (multiplied by g) shown in Fig. 6.24.[11] We recall that it is an understeer

[11] To keep, for the moment, the analysis as simple as possible, we also assume that $\hat{Y}_1(x) = \hat{Y}_2(kx)$, with $k > 0$.

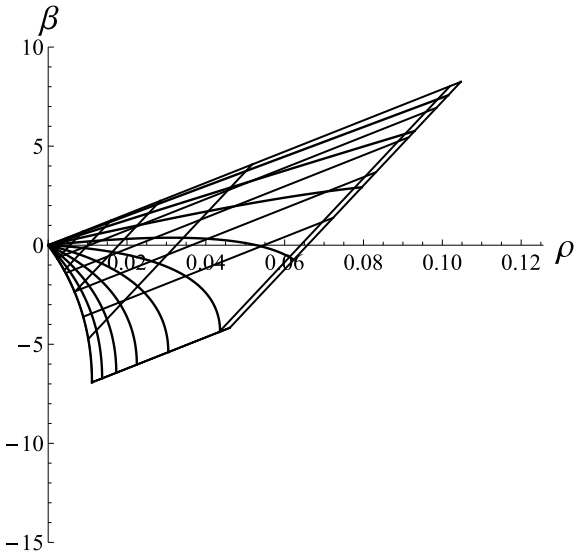

Fig. 6.41 Vehicle with too much understeer: ρ-β MAP with lines at constant u, $\tilde{a}_y$ and δ

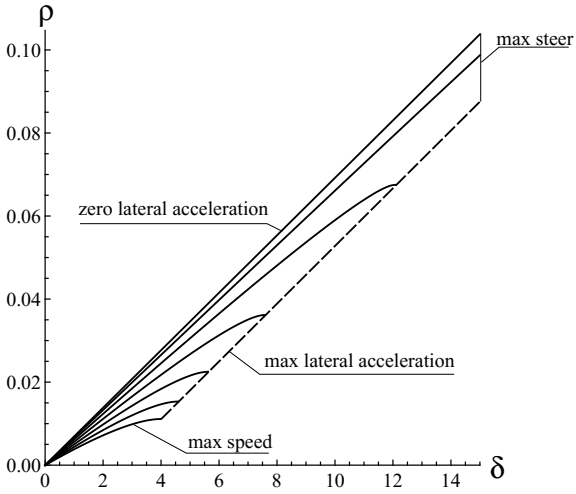

Fig. 6.42 Constant speed lines on the ρ-δ MAP for an understeer vehicle

vehicle and that the corresponding slip functions and handling diagram are shown in Figs. 6.25 and 6.28, respectively.

If we draw the lines at constant speed u in the plane (δ, ρ), we get the plot shown in Fig. 6.42, if $\rho \geq 0$. In the same achievable region, we can draw the lines at constant lateral acceleration $\tilde{a}_y$, as shown in Fig. 6.43. According to (6.98), they are parallel straight lines. In Fig. 6.44, both lines at constant u and constant $\tilde{a}_y$ are drawn on the whole achievable region.

The *achievable region* is bounded by:

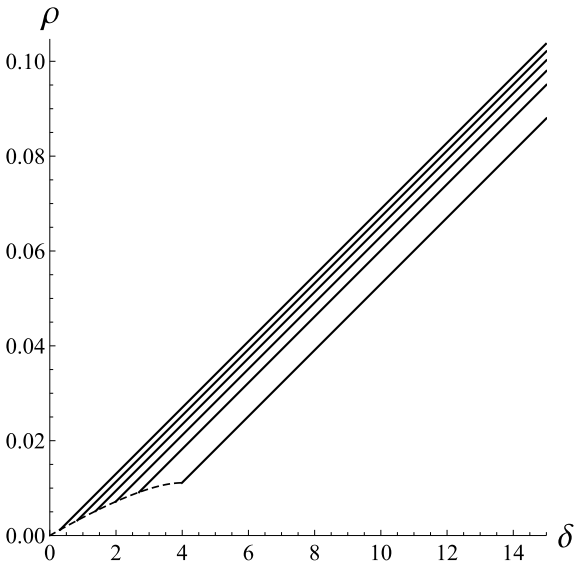

Fig. 6.43 Constant lateral acceleration lines on the ρ-δ MAP for an understeer vehicle

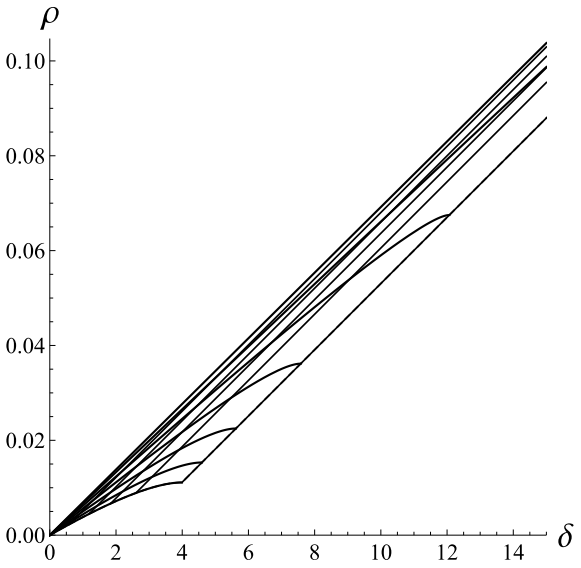

Fig. 6.44 ρ-δ MAP for an understeer vehicle

1. maximum speed (dashed line in Fig. 6.43);
2. maximum lateral acceleration (dashed line in Fig. 6.42);
3. zero lateral acceleration;
4. maximum steer angle.

We see that the driver must act on both u and δ to control the vehicle, that is to drive it on a curve with curvature ρ and lateral acceleration $\tilde{a}_y$. But, the key feature is that it can be done fairly easily because the lines at constant speed are "well shaped", that is quite far apart from each other and neither too flat, nor too steep (Fig. 6.42).

In Fig. 6.44, all lines at constant speed intersect all lines at constant lateral acceleration. This is typical of all vehicles without significant aerodynamic vertical loads. This is another piece of information that is provided by this kind of maps on the achievable region.

An example of a not-so-nice achievable region is shown in Fig. 6.45. A vehicle with a map like in Fig. 6.45 shows too much understeer: the lines at high speed are too flat, showing that the driver can increase δ without getting a significant increase in ρ. Not a desirable behavior.

Another example of undesirable behavior, but for opposite reasons, is shown in Fig. 6.46. This is a vehicle with too little understeer. It has a very narrow achievable region, which means that the driver has a very heavy task in controlling the vehicle: the lines at zero and maximum lateral acceleration are very close together.

An oversteer vehicle (whose corresponding slip functions and handling diagram are shown in Figs. 6.27 and 6.29, respectively) has an achievable region as in Fig. 6.47. The lines at constant $\tilde{a}_y$, shown in Fig. 6.47, are quite far apart like in Fig. 6.43, but

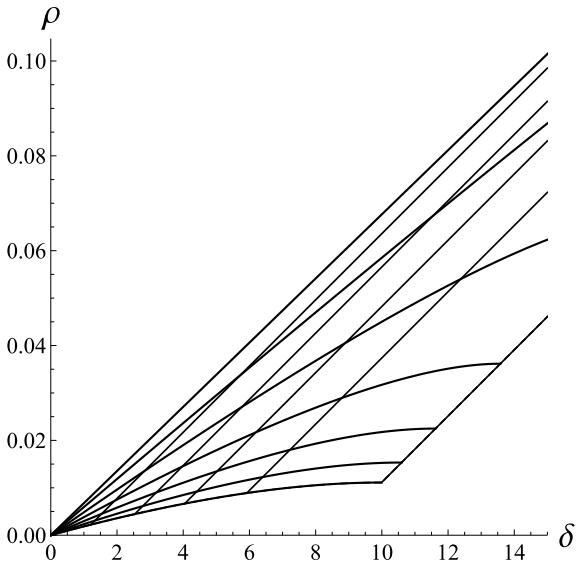

Fig. 6.45 ρ-δ MAP for a vehicle with too much understeer

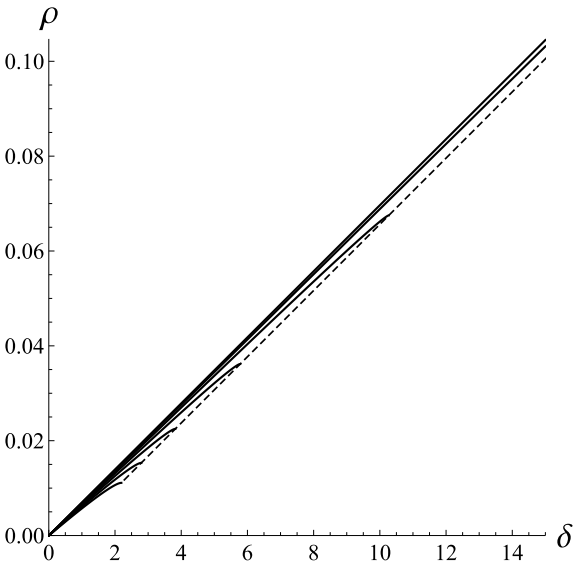

Fig. 6.46 Constant lateral acceleration lines on the ρ-δ MAP for a vehicle with too little understeer

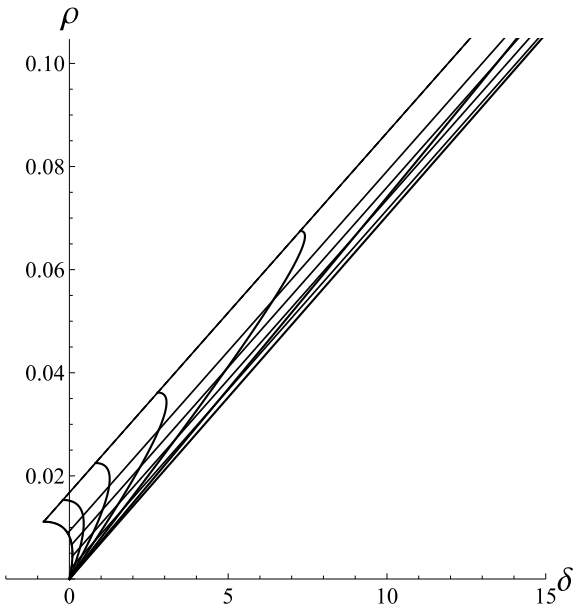

Fig. 6.47 Apparent achievable region on the ρ-δ MAP for an oversteer vehicle

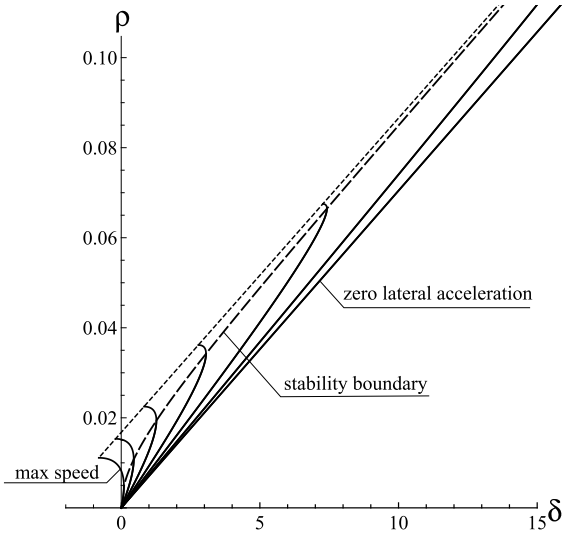

Fig. 6.48 Constant speed lines and truly achievable region on the ρ-δ MAP for an oversteer vehicle

the lines at constant speed u are very badly shaped. At high speed they are too steep, meaning that a small variation of δ drastically changes ρ and $\tilde{a}_y$.

Moreover, the vehicle becomes unstable when the u-lines have vertical slope. Accordingly, the truly achievable region becomes smaller, as shown in Fig. 6.48, where the truly achievable region is bounded by the stability boundary (long-dashed line).

All these examples show how the map *curvature* vs *steer angle* provides a very clear and global picture of the vehicle handling behavior. It makes clear why a well tuned vehicle must be moderately understeer. Too much or too little understeer are not desirable because the vehicle becomes much more difficult to drive (for opposite reasons).

The difference between understeer and oversteer is laid bare (Figs. 6.44 and 6.47). Both have far apart $\tilde{a}_y$-lines, but covering achievable regions on opposite sides. In fact, the u-lines are totally different.

The more one observes these handling MAPs on the corresponding achievable regions, the more the global handling behavior becomes clear.

6.8.3 Other Possible MAPs

So far we have discussed the fundamental MAPs (δ, u) and (ρ, β), and also the fairly intuitive, and very useful, MAP (ρ, δ).

Of course, several other MAPs are possible. For instance, in Fig. 6.49, curves at constant δ are drawn in the planes (ρ, u) and (β, u) for an understeer vehicle. The same kind of MAPs, but for an oversteer vehicle, are shown in Fig. 6.50. The onset of

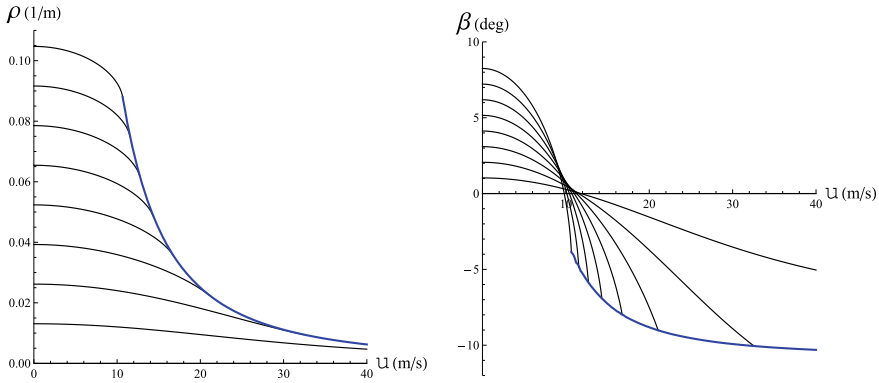

Fig. 6.49 Constant steer curves for an understeer vehicle

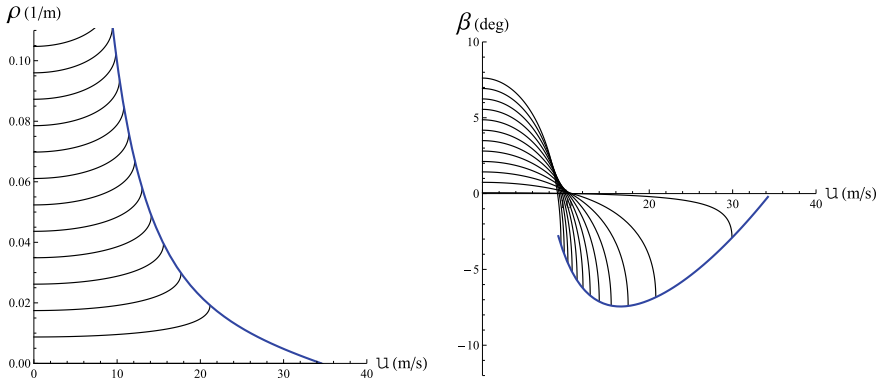

Fig. 6.50 Constant steer curves for an oversteer vehicle

instability is clearly indicated, e.g., by the vertical tangent of the curves at constant δ in the plane (β, u).

Moreover, the MAP $(\delta, \tilde{a}_y)$ was introduced in Sect. 6.7 and is extensively employed in Sect. 6.10.

6.9 Weak Concepts in Classical Vehicle Dynamics

Some "fundamental" concepts in vehicle dynamics are indeed very weak if addressed with open mind. They are either not well defined, particularly when we look at real vehicles, or they are commonly defined in an unsatisfactory way. This is a serious practical drawback that can lead to wrong results and conclusions.

6.9.1 The Understeer Gradient

According to the SAE J266 Standard, *Steady-State Directional Control Test Procedures For Passenger Cars and Light Trucks*

> understeer/oversteer gradient K is defined as the difference between steer angle gradient and Ackermann steer angle gradient.

This definition of K is equivalent to the following formula

$$K = \frac{\mathrm{d}}{\mathrm{d}\tilde{a}_y}\left(\delta - \frac{l}{R}\right) = l\frac{\mathrm{d}f_\rho(\tilde{a}_y)}{\mathrm{d}\tilde{a}_y} \tag{6.116}$$

which comes directly from (6.109). See also (6.107).

Therefore, to compute/measure K we need both the *net steer angle* δ and the *Ackermann steer angle* l/R. Unfortunately, none of them is clearly defined in a real vehicle. In fact, they are well defined only in the single track model, as it is done, e.g., in Figure A1 in the SAE J266 Standard.

In a real vehicle, the two front wheels have typically different steer angles (Fig. 6.51). Therefore, the net steer angle δ is not precisely defined.

The Ackermann steer angle l/R also gets in trouble whenever a vehicle has three or more axles, as the wheelbase l is no longer a clear concept (Fig. 6.51). One may object that almost all cars have two axles. Nonetheless, we cannot ground a theory on such a weak concept.

The understeer gradient K has been an important performance metric in analyzing the handling behavior of vehicles. Unfortunately, it should not have been. It will be demonstrated in Sect. 6.14.1 that it is not a good parameter to measure the handling behavior of a vehicle. Nor even of a single track model.

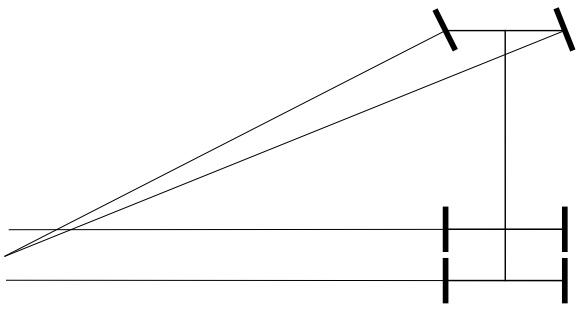

Fig. 6.51 Case not covered by the classical theory

6.9.2 *Popular Definitions of Understeer/Oversteer*

Perhaps, the most astonishing case of use of unclear concepts is the popular way to "define" understeer and oversteer:

> Oversteer is what occurs when a car steers by more than the amount commanded by the driver. Conversely, understeer is what occurs when a car steers less than the amount commanded by the driver.
>
> Understeer: a tendency of an automobile to turn less sharply than the driver intends (or would expect).
>
> The term understeer means that you have to give your car more steering input than the corner should require to get it to go around.

What is the "amount commanded by the driver"? What is the scientific, quantitative meaning of what "the driver intends"? What does "than the corner should require" mean?

6.10 Double Track Model in Transient Conditions

Steady-state analysis cannot be the whole story. Indeed, a vehicle is quite often in transient conditions, that is with time-varying quantities (forces, speeds, yaw rate, etc.). Addressing the transient behavior is, of course, more difficult than "simply" analyzing the steady state. More precisely, the steady-state conditions (also called trim conditions) are just the equilibrium points from which a transient behavior can start or can end.

The general way to study the transient behavior of any dynamical system is through in-time simulations. However, this approach has some drawbacks. Even after a large number of simulations it is quite hard to predict beforehand what the outcome of the next simulation will be.

One way to simplify the analysis of a non-linear dynamical system is to consider only small perturbations (oscillations) about steady-state (trim) conditions. This idea leads to the approach based on *stability derivatives* and *control derivatives* (as they are called in aerospace engineering [10, p. 151]).

The nonlinear equations of motion of the *double track* model of the vehicle are (cf. (6.38))

$$\begin{aligned} m(u\dot{\beta} + \dot{u}\beta + u^2\rho) &= Y(\beta, \rho; u, \delta_v) \\ J_z(u\dot{\rho} + \dot{u}\rho) &= N(\beta, \rho; u, \delta_v) \end{aligned} \tag{6.117}$$

We prefer to use (ρ, β) as state variables, instead of (v, r), because they provide a more "geometric" description of the vehicle motion. Since $\beta = v/u$ and $\rho = r/u$, it is pretty much like having normalized with respect to the forward speed u.

6.10.1 Equilibrium Points

At steady state we have, by definition, $\dot{v} = \dot{r} = 0$, that is $\dot{\beta} = \dot{\rho} = 0$. The driver has direct control on u and δ_v, which are kept constant and whose trim values are named u_a and δ_{va}. The subscript a is introduced here to distinguish clearly between the generic and the trim values (i.e., *a*ssigned values).

The equations of motion (6.117) become

$$\begin{aligned} m u_a^2 \rho &= Y(\beta, \rho; u_a, \delta_{va}) \\ 0 &= N(\beta, \rho; u_a, \delta_{va}) \end{aligned} \tag{6.118}$$

which can be solved to get the steady-state maps (exactly as in (6.44) or (6.111))

$$\begin{aligned} \beta_p &= \hat{\beta}_p(u_a, \delta_{va}) = \frac{v_p(u_a, \delta_{va})}{u_a} \\ \rho_p &= \hat{\rho}_p(u_a, \delta_{va}) = \frac{r_p(u_a, \delta_{va})}{u_a} \end{aligned} \tag{6.119}$$

These maps have been thoroughly discussed in Sect. 6.8, where the new concept of MAP (Map of Achievable Performance) was introduced.

Actually, when applying the MAP approach to the vehicle transient behavior it is more convenient to do like in (6.98), that is to use $\tilde{a}_y = u_a r_p(u_a, \delta_{va})$, which provides $u_a = u_a(\delta_{va}, \tilde{a}_y)$ and hence

$$\begin{aligned} \beta_p &= \beta_p(\delta_{va}, \tilde{a}_y) = \hat{\beta}_p(u_a(\delta_{va}, \tilde{a}_y), \delta_{va}) \\ \rho_p &= \rho_p(\delta_{va}, \tilde{a}_y) = \hat{\rho}_p(u_a(\delta_{va}, \tilde{a}_y), \delta_{va}) \end{aligned} \tag{6.120}$$

An example of achievable region in $(\delta, \tilde{a}_y)$ is shown in Fig. 6.52 for an understeer vehicle, along with lines at constant β (left) and constant ρ (right). In a real vehicle, these maps can be obtained by means of classical steady-state tests. Therefore, they do not require departing from the traditional way of vehicle testing.

6.10.2 Free Oscillations (No Driver Action)

The basic idea is to linearize around an equilibrium point to obtain information in its neighborhood about the dynamical behavior. It is a standard approach for almost any kind of nonlinear dynamical systems.

Assuming that the driver takes no action (i.e., both $u = u_a$ and $\delta_v = \delta_{va}$ are constant in time), the first-order Taylor series expansion of the equations of motion (6.117) around the equilibrium point (6.119) are as follows

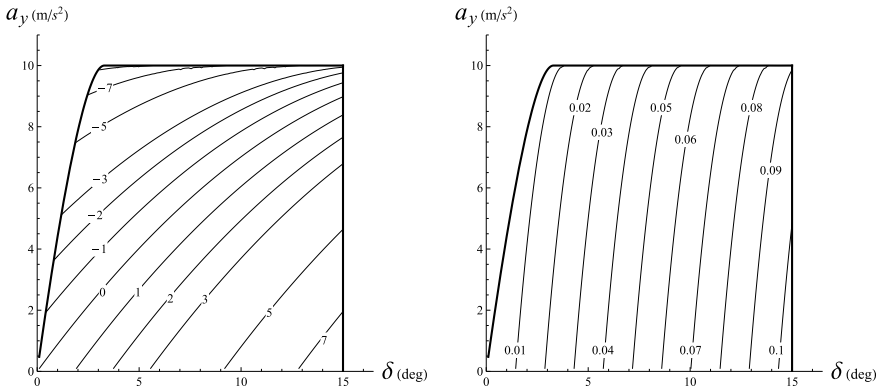

Fig. 6.52 MAPs in the plane $(\delta, \tilde{a}_y)$ with curves at constant β (left) and constant ρ (right) for an understeer vehicle

$$\begin{aligned} m(u_a\dot{\beta} + u_a^2\rho) &= Y_0 + Y_\beta(\beta - \beta_p) + Y_\rho(\rho - \rho_p) \\ J_z u_a \dot{\rho} &= N_0 + N_\beta(\beta - \beta_p) + N_\rho(\rho - \rho_p) \end{aligned} \tag{6.121}$$

where

$$Y_0 = Y(\beta_p, \rho_p; u_a, \delta_{va}) = mu_a^2\rho_p, \qquad N_0 = N(\beta_p, \rho_p; u_a, \delta_{va}) = 0 \tag{6.122}$$

The *stability derivatives* Y_β, Y_ρ, N_β and N_ρ are simply the partial derivatives

$$Y_\beta = \frac{\partial Y}{\partial \beta}, \qquad Y_\rho = \frac{\partial Y}{\partial \rho}, \qquad N_\beta = \frac{\partial N}{\partial \beta}, \qquad N_\rho = \frac{\partial N}{\partial \rho}, \tag{6.123}$$

all evaluated at the equilibrium (trim) conditions $(\beta_p, \rho_p; u_a, \delta_{va})$. Like Y and N, each stability derivative depends on the whole set of chosen coordinates. When evaluated at an equilibrium point, they depend ultimately on the two input coordinates.

In the single track model

$$Y_\rho = N_\beta \tag{6.124}$$

and hence there are only three independent stability derivatives. See Sect. 6.14 for more details.

It is convenient to introduce the *shifted coordinates*

$$\beta_t(t) = \beta(t) - \beta_p \qquad \text{and} \qquad \rho_t(t) = \rho(t) - \rho_p \tag{6.125}$$

into the linearized system of Eq. (6.121), thus getting

$$\begin{aligned} mu_a\dot{\beta}_t &= Y_\beta\beta_t + (Y_\rho - mu_a^2)\rho_t \\ J_z u_a \dot{\rho}_t &= N_\beta\beta_t + N_\rho\rho_t \end{aligned} \tag{6.126}$$

where $\dot{\beta} = \dot{\beta}_t$ and $\dot{\rho} = \dot{\rho}_t$. The shifted coordinates are just the distance of the current values from the selected trim values.

The same system of two first-order linear differential equations with constant coefficients can be rewritten in matrix notation as

$$\begin{bmatrix} \dot{\beta}_t \\ \dot{\rho}_t \end{bmatrix} = \begin{bmatrix} \frac{Y_\beta}{mu_a} & \frac{Y_\rho - mu_a^2}{mu_a} \\ \frac{N_\beta}{J_z u_a} & \frac{N_\rho}{J_z u_a} \end{bmatrix} \begin{bmatrix} \beta_t \\ \rho_t \end{bmatrix} = \mathbf{A} \begin{bmatrix} \beta_t \\ \rho_t \end{bmatrix} \tag{6.127}$$

where the matrix $\mathbf{A}$ is not time dependent.

As a possible further analytical step, we can reformulate the problem as *two identical* second order linear differential equations, with constant coefficients, one in $\rho_t(t)$ and the other in $\beta_t(t)$ (see Sect. 6.18.6 for details)

$$\begin{aligned} &\ddot{\rho}_t + \dot{\rho}_t \left(\frac{-mN_\rho - J_z Y_\beta}{J_z mu_a} \right) + \rho_t \left(\frac{Y_\beta N_\rho - (Y_\rho - mu_a^2) N_\beta}{J_z mu_a^2} \right) \\ &= \ddot{\rho}_t - \mathrm{tr}(\mathbf{A})\dot{\rho}_t + \det(\mathbf{A})\rho_t \\ &= \ddot{\rho}_t + 2\zeta\omega_n \dot{\rho}_t + \omega_n^2 \rho_t = 0 \\ &= \ddot{\beta}_t + 2\zeta\omega_n \dot{\beta}_t + \omega_n^2 \beta_t = 0 \end{aligned} \tag{6.128}$$

The solutions of (6.127) depend on two initial conditions, i.e. $\beta_t(0)$ and $\rho_t(0)$. From the system of Eq. (6.126) we get $\dot{\beta}(0)$ and $\dot{\rho}(0)$, which are the two additional initial conditions needed in (6.128). Therefore, the two state variables have identical dynamic behavior (i.e., same ζ and ω_n) and are not independent from each other.

The matrix $\mathbf{A}$ in (6.127) has two eigenvalues

$$\lambda_j = -\zeta\omega_n \pm \omega_n \sqrt{\zeta^2 - 1}, \quad j = 1, 2 \tag{6.129}$$

with

$$\begin{aligned} 2\zeta\omega_n &= -\mathrm{tr}(\mathbf{A}) = -\frac{mN_\rho + J_z Y_\beta}{J_z mu_a} = -(\lambda_1 + \lambda_2) \\ \omega_n^2 &= \det(\mathbf{A}) = \frac{Y_\beta N_\rho - (Y_\rho - mu_a^2) N_\beta}{J_z mu_a^2} = \lambda_1 \lambda_2 \end{aligned} \tag{6.130}$$

From (6.130) we can also obtain the damping ratio

$$\zeta = -\frac{mN_\rho + J_z Y_\beta}{2\sqrt{J_z m}\sqrt{Y_\beta N_\rho - (Y_\rho - mu_a^2) N_\beta}} \tag{6.131}$$

If $\zeta < 1$, the two eigenvalues are complex conjugate

$$\lambda_j = -\zeta\omega_n \pm \mathrm{i}\omega_n \sqrt{1 - \zeta^2} = -\zeta\omega_n \pm \mathrm{i}\omega_s \tag{6.132}$$

and the system has a damped oscillation with natural angular frequency

$$\omega_s = \omega_n \sqrt{1 - \zeta^2} \tag{6.133}$$

It is kind of interesting to observe that all these relevant dynamic parameters ζ, ω_n and ω_s depend on the following four quantities

$$Y_\beta N_\rho - (Y_\rho - m u_a^2) N_\beta \qquad m N_\rho + J_z Y_\beta \qquad J_z m \qquad u_a \tag{6.134}$$

Of course, the eigenvalues depend on (u_a, δ_{va}), as shown in Figs. 6.53 and 6.54 for (the single track model of) an understeer vehicle. In these figures, the real part (gray lines) and the imaginary parts (black lines) are plotted as functions of the forward speed u_a. In Fig. 6.53 the car is going straight, that is with $\delta = 0$. In Fig. 6.54 the car has a net steer angle $\delta = 5°$ (defined in (6.50)). In both cases, the eigenvalues are complex conjugate for speeds higher than about 4m/s.

Interestingly enough, when the car goes straight (Fig. 6.53), the real part $-\zeta\omega_n$ and the imaginary part ω_s are almost constant for $u_a > 25\,\mathrm{m/s}$, that is for about

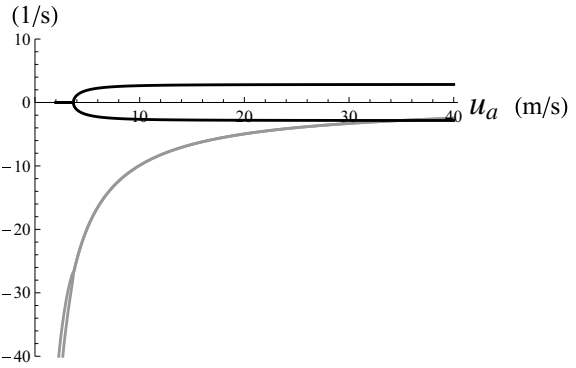

Fig. 6.53 Real and imaginary parts of the two eigenvalues (6.132), for $\delta = 0$

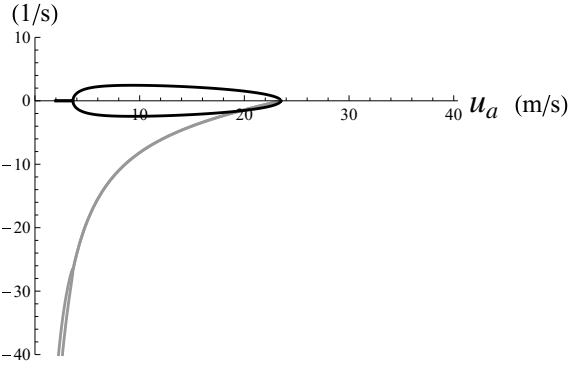

Fig. 6.54 Real and imaginary parts of the two eigenvalues (6.132), for $\delta = 5°$

$u_a > 90\,\mathrm{km/h}$. Indeed, it is at $u_a \simeq 100\,\mathrm{km/h}$ that car makers typically perform the steering harmonic sweep test, in which the steer input is a harmonic function but with a slowly increasing frequency.

As expected, Fig. 6.54 is almost like Fig. 6.53 for low speeds, say $u_a < 10\,\mathrm{m/s}$. For higher speeds, the two figures are very different. The maximum speed is limited by grip when a vehicle is making a turn.

6.10.3 MAP for Transient Behavior

A clearer picture of the global dynamical features of the vehicle is provided by the MAP approach (6.120) when applied to the damping ratio $\zeta(\delta, \tilde{a}_y)$ and to the damped natural frequency $\omega_s(\delta, \tilde{a}_y)$, as in Fig. 6.55. It immediately arises that the closer the vehicle is to the grip limit (maximum lateral acceleration), the lower both ζ and ω_s. Therefore, the dynamical behavior of the vehicle changes significantly. Perhaps, an expert driver may take advantage of these phenomena to "feel" how close the vehicle is to the grip limit.

Summing up, we have seen that the dynamical features of the vehicle in the neighborhood of an equilibrium point depend on *four stability derivatives* (6.123), besides m, J_z and u_a. The characterization of the vehicle requires knowledge of these stability derivatives.

In the single track model, $Y_\rho = N_\beta$, and hence there are only three independent stability derivatives. See Sect. 6.14 for more details.

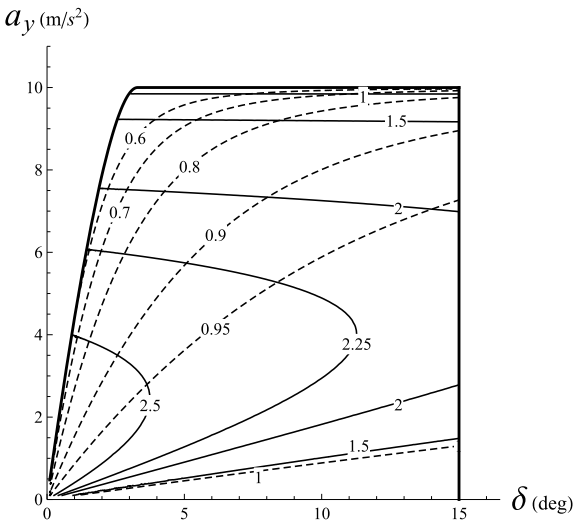

Fig. 6.55 MAP in the plane $(\delta, \tilde{a}_y)$ with curves at constant damping ratio ζ (dashed lines) and constant damped natural angular frequency ω_s (solid lines)

6.10.4 Stability of the Equilibrium

An equilibrium point can be either stable or unstable. The typical way to assess whether there is stability or not is by looking at the eigenvalues (6.129). As well known

$$\text{stability} \iff \text{Re}(\lambda_1) < 0 \quad \text{and} \quad \text{Re}(\lambda_2) < 0 \tag{6.135}$$

that is, both eigenvalues must have a negative real part. A convenient way to check this condition without computing the two eigenvalues is

$$\text{stability} \iff \big(\lambda_1 + \lambda_2 = \text{tr}(\mathbf{A})\big) < 0 \quad \text{and} \quad \big(\lambda_1\lambda_2 = \det(\mathbf{A})\big) > 0 \tag{6.136}$$

Typically, vehicles may become unstable because one of the two real eigenvalues becomes positive.

6.10.5 Forced Oscillations (Driver Action)

Linearized systems can also be used to study the effect of small driver actions on the forward speed and/or on the steering wheel angle to control the vehicle. More precisely, we have $u = u_a + u_t$ and $\delta_v = \delta_{va} + \delta_{vt}$.

The linearized inertial terms in (6.117) are

$$\begin{aligned} m(u\dot{\beta} + \dot{u}\beta + u^2\rho) &\simeq m(u_a\dot{\beta} + \dot{u}\beta_p + u_a^2\rho_p + u_a^2\rho_t + 2u_a u_t\rho_p) \\ J_z(u\dot{\rho} + \dot{u}\rho) &\simeq J_z(u_a\dot{\rho} + \dot{u}\rho_p) \end{aligned} \tag{6.137}$$

where $mu_a^2\rho_p = Y_0$, according to (6.118).

The linearized system becomes

$$\begin{aligned} m(u_a\dot{\beta}_t + \dot{u}\beta_p + u_a^2\rho_t + 2u_a\rho_p u_t) &= Y_\beta\beta_t + Y_\rho\rho_t + Y_u u_t + Y_\delta\delta_{vt} \\ J_z(u_a\dot{\rho}_t + \dot{u}\rho_p) &= N_\beta\beta_t + N_\rho\rho_t + N_u u_t + N_\delta\delta_{vt} \end{aligned} \tag{6.138}$$

where, in addition to the four stability derivatives (6.123), there are also four *control derivatives*

$$Y_\delta = \frac{\partial Y}{\partial\delta_v}, \qquad Y_u = \frac{\partial Y}{\partial u}, \qquad N_\delta = \frac{\partial N}{\partial\delta_v}, \qquad N_u = \frac{\partial N}{\partial u} \tag{6.139}$$

evaluated, like the others, at the equilibrium point $(\beta_p, \rho_p; u_a, \delta_{va})$. A better way to write (6.138) is

$$\begin{aligned} mu_a\dot{\beta}_t &= Y_\beta\beta_t + (Y_\rho - mu_a^2)\rho_t + (Y_u - 2mu_a\rho_p)u_t + Y_\delta\delta_{vt} - m\beta_p\dot{u}_t \\ J_z u_a\dot{\rho}_t &= N_\beta\beta_t + N_\rho\rho_t + N_u u_t + N_\delta\delta_{vt} - J_z\rho_p\dot{u}_t \end{aligned} \tag{6.140}$$

which generalizes (6.126).

The most intuitive case is the driver acting only on the steering wheel, which is described by the simplified set of equations

$$\begin{aligned} mu_a\dot{\beta}_t &= Y_\beta\beta_t + (Y_\rho - mu_a^2)\rho_t + Y_\delta\delta_{vt} \\ J_z u_a\dot{\rho}_t &= N_\beta\beta_t + N_\rho\rho_t + N_\delta\delta_{vt} \end{aligned} \tag{6.141}$$

since $u_t = \dot{u} = 0$. Moreover, $\dot{u} = 0$ is consistent with the assumptions made at the beginning of this chapter.

In matrix notation, (6.140) become

$$\begin{bmatrix} \dot{\beta}_t \\ \dot{\rho}_t \end{bmatrix} = \mathbf{A}\begin{bmatrix} \beta_t \\ \rho_t \end{bmatrix} + \mathbf{B}\begin{bmatrix} u_t \\ \delta_{vt} \\ \dot{u}_t \end{bmatrix} = \mathbf{A}\begin{bmatrix} \beta_t \\ \rho_t \end{bmatrix} + \mathbf{b} \tag{6.142}$$

or, in an even more compact notation

$$\dot{\mathbf{w}} = \mathbf{A}\mathbf{w} + \mathbf{b} \tag{6.143}$$

where the entries of matrix $\mathbf{A}$ are, exactly as in (6.127)

$$\begin{aligned} a_{11} &= Y_\beta/(mu_a) \qquad a_{12} = (Y_\rho - mu_a^2)/(mu_a) \\ a_{21} &= N_\beta/(J_z u_a) \qquad a_{22} = N_\rho/(J_z u_a) \end{aligned} \tag{6.144}$$

and the components of vector $\mathbf{b}$ are

$$\begin{aligned} b_1 &= \frac{1}{mu_a}[(Y_u - 2mu_a\rho_p)u_t + Y_\delta\delta_{vt} - m\beta_p\dot{u}_t] \\ b_2 &= \frac{1}{J_z u_a}[N_u u_t + N_\delta\delta_{vt} - J_z\rho_p\dot{u}_t] \end{aligned} \tag{6.145}$$

Like in (6.128), we can recast the problem (6.140) as two second-order linear differential equations, only apparently independent from each other

$$\begin{aligned} \ddot{\beta}_t + 2\zeta\omega_n\dot{\beta}_t + \omega_n^2\beta_t &= -a_{22}b_1 + a_{12}b_2 + \dot{b}_1 = F_\beta \\ \ddot{\rho}_t + 2\zeta\omega_n\dot{\rho}_t + \omega_n^2\rho_t &= a_{21}b_1 - a_{11}b_2 + \dot{b}_2 = F_\rho \end{aligned} \tag{6.146}$$

where

$$\begin{aligned} \dot{b}_1 &= \frac{1}{mu_a}[(Y_u - 2mu_a\rho_p)\dot{u}_t + Y_\delta\dot{\delta}_v - m\beta_p\ddot{u}_t] \\ \dot{b}_2 &= \frac{1}{J_z u_a}[N_u\dot{u}_t + N_\delta\dot{\delta}_v - J_z\rho_p\ddot{u}_t] \end{aligned} \tag{6.147}$$

Again, if the driver acts only on the steering wheel, like in (6.141), all these expressions become much simpler. More precisely

$$b_1 = \frac{Y_\delta}{mu_a}\delta_{vt}, \quad b_2 = \frac{N_\delta}{J_z u_a}\delta_{vt}, \quad \dot{b}_1 = \frac{Y_\delta}{mu_a}\dot{\delta}_v, \quad \dot{b}_2 = \frac{N_\delta}{J_z u_a}\dot{\delta}_v \tag{6.148}$$

and hence

$$\begin{aligned} F_\beta &= \left(\frac{-N_\rho Y_\delta + (Y_\rho - mu_a^2)N_\delta}{mJ_z u_a^2}\right)\delta_{vt} + \frac{Y_\delta}{mu_a}\dot{\delta}_v \\ F_\rho &= \left(\frac{N_\beta Y_\delta - Y_\beta N_\delta}{mJ_z u_a^2}\right)\delta_{vt} + \frac{N_\delta}{J_z u_a}\dot{\delta}_v \end{aligned} \tag{6.149}$$

The two differential equations (6.146) have identical values of ζ and ω_n, but different forcing terms F_β and F_ρ. However, in (6.149) we still find the four quantities listed in (6.134).

The fundamental result of this analysis is that the transient dynamics of a vehicle in the neighborhood of an equilibrium point is fully characterized by a *finite number* of normalized stability derivatives and control derivatives:

- stability derivatives Y_β/m, Y_ρ/m, N_β/J_z, and N_ρ/J_z;
- control derivatives Y_u/m, Y_δ/m, N_u/J_z, and N_δ/J_z.

It will be discussed shortly that in most cases $Y_u = N_u = 0$, thus leaving six derivatives. It is worth noting that the equality $Y_\rho = N_\beta$ does not reduce the number of relevant derivatives to five. Indeed, we still have $Y_\rho/m \neq N_\beta/J_z$.

The key point is how to measure (identify) all the stability derivatives and all the control derivatives. Their knowledge would be very relevant practical information. The next section presents indeed a novel method to extract these data from the results of steady-state tests. This approach appears to be simpler and more reliable than direct measurements.

6.11 Relationship Between Steady-State Data and Transient Behavior

Most classical vehicle dynamics deals with steady-state data. Understeer and oversteer are steady-state concepts. Or they are not? This is a crucial question. What does a professional driver mean when he/she complains about his/her car being understeer or oversteer? Does it have anything to do with the classical definition of understeer/oversteer as discussed in Sect. 6.7?

Two aspects should be carefully taken into account. While the concepts of velocity, acceleration, mass, stability etc. arise in any branch of mechanics, why do the concepts of understeer and oversteer only belong to vehicle dynamics? This is rather surprising. Why are vehicles so special dynamical systems that they need concepts conceived uniquely for them?

The other aspect is somehow more practical. Why should steady-state tests tell us anything about the transient behavior of a vehicle? In more technical terms, why should steady-state data be related to stability derivatives? Are they or not? If they are related, what is the relationship?

This section is devoted to the investigation of the link between the universe of steady-state data and the universe of the dynamical, hence transient, behavior of a vehicle. It will be shown that a link does indeed exist, but it is not direct, not to mention obvious.

It is worth noting that this section is not strictly related to the single track model. The theory developed here is applicable to real road vehicles.

6.11.1 Stability Derivatives from Steady-State Gradients

The starting point is a sort of mathematical trick. At steady state, the lateral force Y and the yawing moment N have very simple values

$$Y_0 = m\tilde{a}_y \qquad \text{and} \qquad N_0 = 0 \tag{6.150}$$

Nevertheless, by combining (6.118) and (6.120), they can be given, as functions, the following expressions

$$\begin{aligned} Y_0(\delta_{va}, \tilde{a}_y) &= Y\big(\beta_p(\delta_{va}, \tilde{a}_y),\, \rho_p(\delta_{va}, \tilde{a}_y);\, u_a(\delta_{va}, \tilde{a}_y),\, \delta_{va}\big) = m\tilde{a}_y \\ N_0(\delta_{va}, \tilde{a}_y) &= N\big(\beta_p(\delta_{va}, \tilde{a}_y),\, \rho_p(\delta_{va}, \tilde{a}_y);\, u_a(\delta_{va}, \tilde{a}_y),\, \delta_{va}\big) = 0 \end{aligned} \tag{6.151}$$

Now, the key idea is to take the partial derivatives of the just defined function $Y_0(\delta_{va}, \tilde{a}_y)$, thus obtaining

$$\begin{aligned} \frac{\partial Y_0}{\partial \tilde{a}_y} &= Y_\beta \frac{\partial \beta_p}{\partial \tilde{a}_y} + Y_\rho \frac{\partial \rho_p}{\partial \tilde{a}_y} + Y_u \frac{\partial u_a}{\partial \tilde{a}_y} = m \frac{\partial \tilde{a}_y}{\partial \tilde{a}_y} = m \\ \frac{\partial Y_0}{\partial \delta_{va}} &= Y_\beta \frac{\partial \beta_p}{\partial \delta_{va}} + Y_\rho \frac{\partial \rho_p}{\partial \delta_{va}} + Y_u \frac{\partial u_a}{\partial \delta_{va}} + Y_\delta = m \frac{\partial \tilde{a}_y}{\partial \delta_{va}} = 0 \end{aligned} \tag{6.152}$$

The same steps can be taken for the yawing moment $N_0(\delta_{va}, \tilde{a}_y)$, getting

$$\begin{aligned} \frac{\partial N_0}{\partial \tilde{a}_y} &= N_\beta \frac{\partial \beta_p}{\partial \tilde{a}_y} + N_\rho \frac{\partial \rho_p}{\partial \tilde{a}_y} + N_u \frac{\partial u_a}{\partial \tilde{a}_y} = 0 \\ \frac{\partial N_0}{\partial \delta_{va}} &= N_\beta \frac{\partial \beta_p}{\partial \delta_{va}} + N_\rho \frac{\partial \rho_p}{\partial \delta_{va}} + N_u \frac{\partial u_a}{\partial \delta_{va}} + N_\delta = 0 \end{aligned} \tag{6.153}$$

In a road vehicle, that is without significant aerodynamic vertical loads, it is reasonable to assume

$$Y_u = N_u = 0 \tag{6.154}$$

if we take β and ρ as state variables to describe the vehicle motion.[12] In other words, Y and N do not change if we modify only u, keeping constant β, ρ and δ_v (cf. (6.53)). It would not be so in Formula cars, that is in cars with aerodynamic devices.

The two equations in (6.152), with $Y_u = N_u = 0$, yield the system of linear equations

$$\begin{cases} Y_\beta \dfrac{\partial \beta_p}{\partial \tilde{a}_y} + Y_\rho \dfrac{\partial \rho_p}{\partial \tilde{a}_y} = m \\ Y_\beta \dfrac{\partial \beta_p}{\partial \delta_{va}} + Y_\rho \dfrac{\partial \rho_p}{\partial \delta_{va}} = -Y_\delta \end{cases} \tag{6.155}$$

and, similarly, from (6.153)

$$\begin{cases} N_\beta \dfrac{\partial \beta_p}{\partial \tilde{a}_y} + N_\rho \dfrac{\partial \rho_p}{\partial \tilde{a}_y} = 0 \\ N_\beta \dfrac{\partial \beta_p}{\partial \delta_{va}} + N_\rho \dfrac{\partial \rho_p}{\partial \delta_{va}} = -N_\delta \end{cases} \tag{6.156}$$

These two systems of equations have the same matrix

$$\begin{bmatrix} \beta_y & \rho_y \\ \beta_\delta & \rho_\delta \end{bmatrix} \begin{bmatrix} Y_\beta \\ Y_\rho \end{bmatrix} = \begin{bmatrix} m \\ -Y_\delta \end{bmatrix} \quad \text{and} \quad \begin{bmatrix} \beta_y & \rho_y \\ \beta_\delta & \rho_\delta \end{bmatrix} \begin{bmatrix} N_\beta \\ N_\rho \end{bmatrix} = \begin{bmatrix} 0 \\ -N_\delta \end{bmatrix} \tag{6.157}$$

whose coefficients are the four components of the *gradients* defined in (6.99)

$$\begin{aligned} \text{grad } \rho_p &= \left(\frac{\partial \rho_p}{\partial \tilde{a}_y}, \frac{\partial \rho_p}{\partial \delta_v} \right) = (\rho_y, \rho_\delta) \\ \text{grad } \beta_p &= \left(\frac{\partial \beta_p}{\partial \tilde{a}_y}, \frac{\partial \beta_p}{\partial \delta_v} \right) = (\beta_y, \beta_\delta) \end{aligned} \tag{6.99'}$$

of the two *steady-state maps* (6.120). After having performed the standard steady-state tests, all these gradient components (already introduced in Sect. 6.7.1) are known functions.

The four *stability derivatives* are the solution of the two systems of Eq. (6.157)

$$\begin{aligned} Y_\beta &= \frac{Y_\delta \rho_y + m\rho_\delta}{\beta_y \rho_\delta - \beta_\delta \rho_y} \qquad Y_\rho = -\frac{Y_\delta \beta_y + m\beta_\delta}{\beta_y \rho_\delta - \beta_\delta \rho_y} \\ N_\beta &= \frac{N_\delta \rho_y}{\beta_y \rho_\delta - \beta_\delta \rho_y} \qquad N_\rho = -\frac{N_\delta \beta_y}{\beta_y \rho_\delta - \beta_\delta \rho_y} \end{aligned} \tag{6.158}$$

Therefore, they are known functions of the *gradient components* and of the *control derivatives* Y_δ and N_δ. This is a fundamental original result, as it shows why steady-

[12] Actually, as discussed right after (6.38), these partial derivatives are not zero if there is roll steer in a double track model. However, they should be very small. See also (6.75).

state data can indeed provide information about the transient behavior, although not in an obvious way.

Moreover, from (6.124) (i.e., $Y_\rho = N_\beta$) and (6.158) we have that

$$\begin{aligned} &\beta_y Y_\delta + \rho_y N_\delta = -m\beta_\delta \\ &\text{which means} \\ &Y_\delta = -\frac{N_\delta \rho_y + m\beta_\delta}{\beta_y} \qquad \text{or} \qquad N_\delta = -\frac{Y_\delta \beta_y + m\beta_\delta}{\rho_y} \end{aligned} \tag{6.159}$$

The transient behavior of the vehicle is characterized by the stability derivatives. This is well known. What is new is that the stability derivatives are strictly related to the gradients of steady-state maps. This result opens up new perspectives in the objective evaluation of the handling of vehicles (cf. [8]).

6.11.2 Equations of Motion

Now, we can go back to the linearized equations of motion (6.141). The stability derivatives can be replaced by the expressions in (6.158), thus obtaining

$$\begin{aligned} mu_a\dot{\beta}_t &= \left(\frac{Y_\delta \rho_y + m\rho_\delta}{\beta_y\rho_\delta - \beta_\delta\rho_y}\right)\beta_t + \left(-\frac{Y_\delta\beta_y + m\beta_\delta}{\beta_y\rho_\delta - \beta_\delta\rho_y} - mu_a^2\right)\rho_t + Y_\delta\delta_{vt} \\ J_z u_a\dot{\rho}_t &= \left(\frac{N_\delta\rho_y}{\beta_y\rho_\delta - \beta_\delta\rho_y}\right)\beta_t + \left(-\frac{N_\delta\beta_y}{\beta_y\rho_\delta - \beta_\delta\rho_y}\right)\rho_t + N_\delta\delta_{vt} \end{aligned} \tag{6.160}$$

where β_t and ρ_t are the shifted coordinates defined in (6.125).

Actually, it would be more systematic to define the generalized control derivatives

$$\hat{Y}_\delta = \frac{Y_\delta}{m} \qquad \text{and} \qquad \hat{N}_\delta = \frac{N_\delta}{J_z} \tag{6.161}$$

thus obtaining

$$\begin{aligned} u_a\dot{\beta}_t &= \left(\frac{\hat{Y}_\delta \rho_y + \rho_\delta}{\beta_y\rho_\delta - \beta_\delta\rho_y}\right)\beta_t + \left(-\frac{\hat{Y}_\delta\beta_y + \beta_\delta}{\beta_y\rho_\delta - \beta_\delta\rho_y} - u_a^2\right)\rho_t + \hat{Y}_\delta\delta_{vt} \\ u_a\dot{\rho}_t &= \left(\frac{\hat{N}_\delta\rho_y}{\beta_y\rho_\delta - \beta_\delta\rho_y}\right)\beta_t + \left(-\frac{\hat{N}_\delta\beta_y}{\beta_y\rho_\delta - \beta_\delta\rho_y}\right)\rho_t + \hat{N}_\delta\delta_{vt} \end{aligned} \tag{6.162}$$

This is quite a remarkable (and original) result. It shows how the equations of motion can be given in terms of data collected in steady-state tests. It is the link between the realm of steady-state gradients and the realm of transient behavior.

6.11.3 Estimation of the Control Derivatives

The control derivatives $\hat{Y}_\delta$ and $\hat{N}_\delta$ can be estimated by means of standard dynamic tests. For instance, let us consider a generalized *step steering input*, that is a sudden increase δ_{vt} of the steering wheel angle δ_v applied to a vehicle in a steady-state (equilibrium) configuration. We say "generalized" since it should and can be done from any steady-state configuration, not necessarily from a straight-line trajectory. Since, by definition $\beta_t(0) = 0$ and $\rho_t(0) = 0$, from (6.162) we obtain

$$\hat{Y}_\delta = \frac{u_a \dot{\beta}_t(0)}{\delta_{vt}} \qquad \text{and} \qquad \hat{N}_\delta = \frac{u_a \dot{\rho}_t(0)}{\delta_{vt}} \tag{6.163}$$

Combining this result with (6.159), we also get that in a step steering input

$$\beta_y \dot{\beta}_t(0) + \frac{J_z}{m} \rho_y \dot{\rho}_t(0) = -\frac{\delta_{vt}}{u_a} \beta_\delta \tag{6.164}$$

6.11.4 Objective Evaluation of Car Handling

The two coefficients $2\zeta\omega_n = -(\lambda_1 + \lambda_2)$ and $\omega_n^2 = \lambda_1\lambda_2$ of the differential equations (6.128), can now be expressed as combinations of steady-state gradient components and control derivatives

$$\begin{aligned} 2\zeta\omega_n &= \frac{1}{u_a(\beta_y\rho_\delta - \beta_\delta\rho_y)} \left[\left(\hat{N}_\delta \beta_y - \hat{Y}_\delta \rho_y \right) - \rho_\delta \right] = -\operatorname{tr}(\mathbf{A}) = n_1(\delta_{va}, \tilde{a}_y) \\ \omega_n^2 &= \frac{1}{(\beta_y\rho_\delta - \beta_\delta\rho_y)} \hat{N}_\delta \left(\rho_y - \frac{1}{u_a^2} \right) = \det(\mathbf{A}) = n_2(\delta_{va}, \tilde{a}_y) \end{aligned} \tag{6.165}$$

Once again, the dynamic features of the vehicle are strictly related to data obtained in steady-state conditions.

Similarly, the two forcing terms F_β and F_ρ in (6.149) can be rewritten as

$$\begin{aligned} F_\beta = -\frac{\hat{N}_\delta}{u_a^2} \left(\frac{\beta_\delta}{\beta_y\rho_\delta - \beta_\delta\rho_y} + u_a^2 \right) \delta_{vt} + \frac{\hat{Y}_\delta}{u_a} \dot{\delta}_v \\ = n_3(\delta_{va}, \tilde{a}_y)\delta_{vt} + n_4(\delta_{va}, \tilde{a}_y)\dot{\delta}_v \end{aligned} \tag{6.166}$$

and

$$\begin{aligned} F_\rho = -\frac{\hat{N}_\delta}{u_a^2} \left(\frac{\rho_\delta}{\beta_y\rho_\delta - \beta_\delta\rho_y} \right) \delta_{vt} + \frac{\hat{N}_\delta}{u_a} \dot{\delta}_v \\ = n_5(\delta_{va}, \tilde{a}_y)\delta_{vt} + n_6(\delta_{va}, \tilde{a}_y)\dot{\delta}_v \end{aligned} \tag{6.167}$$

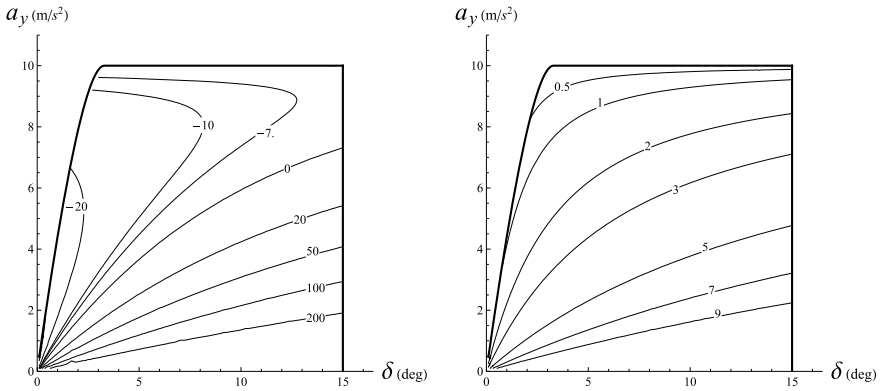

Fig. 6.56 MAP in the plane $(\delta, \tilde{a}_y)$ for F_β, with curves at constant n_3 (left) and constant n_4 (right)

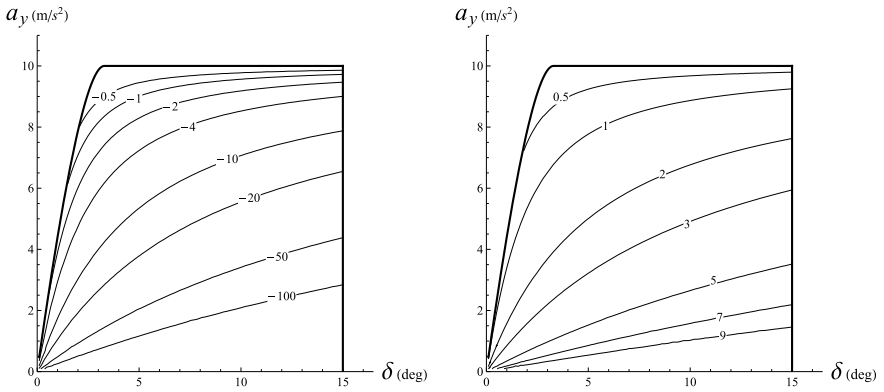

Fig. 6.57 MAP in the plane $(\delta, \tilde{a}_y)$ for F_ρ, with curves at constant n_5 (left) and constant n_6 (right)

Typical patterns are shown in the MAP in Fig. 6.56 for F_β, and in the MAP of Fig. 6.57 for F_ρ.

6.11.4.1 Vehicle "DNA"

Equations (6.165)–(6.167) show that the dynamical behavior of a road vehicle in the neighborhood of any equilibrium point is fully described by six maps $n_i(\delta_{va}, \tilde{a}_y)$. These maps (functions) can be seen as a sort of "DNA" of the vehicle, in the sense that they determine the vehicle transient behavior. To help the reader, these six maps are listed below:

$$
\begin{aligned}
n_1(\delta_{va}, \tilde{a}_y) &= \frac{1}{u_a(\beta_y\rho_\delta - \beta_\delta\rho_y)}\left[\left(\hat{N}_\delta\beta_y - \hat{Y}_\delta\rho_y\right) - \rho_\delta\right] = 2\zeta\omega_n \\
n_2(\delta_{va}, \tilde{a}_y) &= \frac{1}{(\beta_y\rho_\delta - \beta_\delta\rho_y)}\hat{N}_\delta\left(\rho_y - \frac{1}{u_a^2}\right) = \omega_n^2 \\
n_3(\delta_{va}, \tilde{a}_y) &= -\frac{\hat{N}_\delta}{u_a^2}\left(\frac{\beta_\delta}{\beta_y\rho_\delta - \beta_\delta\rho_y} + u_a^2\right) \\
n_4(\delta_{va}, \tilde{a}_y) &= \frac{\hat{Y}_\delta}{u_a} \\
n_5(\delta_{va}, \tilde{a}_y) &= -\frac{\hat{N}_\delta}{u_a^2}\left(\frac{\rho_\delta}{\beta_y\rho_\delta - \beta_\delta\rho_y}\right) \\
n_6(\delta_{va}, \tilde{a}_y) &= \frac{\hat{N}_\delta}{u_a}
\end{aligned}
\tag{6.168}
$$

However, all these quantities are, ultimately, combinations of the following six fundamental "handling bricks":

$$
s_1 = \beta_y, \quad s_2 = \rho_y, \quad s_3 = \beta_\delta, \quad s_4 = \rho_\delta, \quad s_5 = \hat{N}_\delta, \quad s_6 = \hat{Y}_\delta \tag{6.169}
$$

all of them, in general, functions of two variables like, e.g., $\tilde{a}_y$ and δ_v.

Two vehicles with the same s_i, and hence with the same n_i, have *identical transient handling behavior*, notwithstanding their size, weight, etc. In other words, the two vehicles react in exactly the same way to given driver input. Therefore, there is indeed a strong relationship between data collected in steady-state tests and the transient dynamical behavior of a vehicle.

Objective measures of car handling should be based on the quantities defined in (6.168).

On the practical side, we see that the components of the gradients (6.99) of the steady-state maps $\beta_p(\delta_v, \tilde{a}_y)$ and $\rho_p(\delta_v, \tilde{a}_y)$ provide four out of six "handling bricks", the other two being the generalized control derivatives. Basically, we have found a more feasible way, based on the gradient components of the steady-state MAPs, to measure the six stability and control derivatives listed on p. 284.

6.12 Stability (Again)

According to (6.136), an equilibrium point is stable if and only if $\mathrm{tr}(\mathbf{A}) < 0$ and $\det(\mathbf{A}) > 0$. These two conditions, after (6.165), can be expressed in terms of the six fundamental handling bricks (6.169) and the forward speed.

6.13 New Understeer Gradient

Let us discuss in detail the component ρ_y of the new understeer gradient introduced in (6.99). In general it is a function of two variables

$$\rho_y = \rho_y(\delta_{va}, \tilde{a}_y) \tag{6.170}$$

except in some special cases, like the single track model with open differential, where, according to (6.102), $\rho_y = \rho_y(\tilde{a}_y) = -\mathrm{d}f_\rho/\mathrm{d}\tilde{a}_y$.

More explicitly,

$$\rho_y = \frac{\partial \rho_p}{\partial \tilde{a}_y} = \frac{\partial}{\partial \tilde{a}_y}\left(\frac{1}{R}\right) = -\frac{K}{l} \tag{6.171}$$

This is similar to the definition (6.116) of the classical understeer gradient K, but with a few *fundamental differences*.

The definition of ρ_y does not involve any weak concept, like the wheelbase l or the Ackermann steer angle, as discussed in Sect. 6.9. Therefore, it is much more general. This new understeer gradient is defined for *any* vehicle.

Moreover, it is the *correct* measure of understeer/oversteer, while K is not. This may look surprising, but that is the way it is, as will be shown in Sect. 6.14.1 (see in particular Table 6.1).

Of course, the partial derivative in (6.171) requires the steer angle to be kept constant, according to (6.170).[13]

But there are other reasons that support ρ_y as a good handling parameter. Let us consider a *constant steering wheel test* and monitor the yaw rate $r_p = r_p(u_a; \delta_{va})$ as a function of the forward speed u_a, keeping constant the steering wheel angle δ_{va}. For brevity, let $r'_p = \mathrm{d}r_p/\mathrm{d}u_a$. Equation (6.171) can be rewritten as

$$\frac{\mathrm{d}\rho_p}{\mathrm{d}\tilde{a}_y} = \frac{\mathrm{d}(r_p/u_a)}{\mathrm{d}(r_p\, u_a)} = \frac{\mathrm{d}(r_p/u_a)}{\mathrm{d}u_a}\left(\frac{\mathrm{d}(r_p\, u_a)}{\mathrm{d}u_a}\right)^{-1} = \frac{1}{u_a^2}\left(\frac{r'_p u_a - r_p}{r'_p u_a + r_p}\right) = \rho_y \tag{6.172}$$

This general equation provides a way to obtain the critical speed and the characteristic speed. The *characteristic speed* u_{ch} is, by definition, the speed at which $r'_p = 0$. By letting $r'_p \to 0$ in (6.172), we obtain that the characteristic speed must satisfy the following equation

$$\frac{1}{u_a^2} = -\rho_y \qquad \text{that is} \qquad u_{\mathrm{ch}} = \sqrt{-\frac{1}{\rho_y}} \tag{6.173}$$

Similarly, the *critical speed* u_{cr} is, by definition [10, p. 177], the speed at which $r'_p \to \infty$, which means

[13] Tests with constant steer angle are the most general: they can be performed on any kind of vehicle.

$$\frac{1}{u_a^2} = \rho_y \qquad \text{that is} \qquad u_{\text{cr}} = \sqrt{\frac{1}{\rho_y}} \tag{6.174}$$

Summing up:

- ρ_y has been defined without any recourse to weak concepts, like a reference vehicle having Ackermann steering;
- ρ_y can be easily measured in constant steering wheel tests;
- the critical speed and the characteristic speed come out naturally as special cases.[14]

A similar treatment applies to the other gradient component β_y. In this case $v_p = v_p(u_a; \delta_{va})$, thus obtaining

$$\beta_y = \frac{\mathrm{d}\beta_p}{\mathrm{d}\tilde{a}_y} = \frac{\mathrm{d}(v_p/u_a)}{\mathrm{d}(u_a r_p)} = \frac{1}{u_a^2}\left(\frac{v_p' u_a - v_p}{r_p' u_a + r_p}\right) \tag{6.175}$$

In general

$$\beta_y = \beta_y(\delta_{va}, \tilde{a}_y) \tag{6.176}$$

except in cases like the single track model with open differential, where, according to (6.102), $\beta_y = \beta_y(\tilde{a}_y) = -\mathrm{d}f_\beta/\mathrm{d}\tilde{a}_y$.

6.14 The Nonlinear Single Track Model Revisited

The general approach presented in Sect. 6.11, which explains why steady-state data are also relevant for the transient behavior, is applied here to the single track model. The goal is to clarify the matter by a significant worked-out example.

For simplicity, we assume $u = u_a$ and $\dot{u} = 0$ and hence start with the linearized equations of motion (6.141).

In the single track model (with open differential), the *stability derivatives* (6.123) can be obtained directly (cf. (6.88)), taking into account the congruence equations (6.68) and the axle characteristics (6.74)

$$\begin{aligned} Y_\beta &= \frac{\mathrm{d}Y_1}{\mathrm{d}\alpha_1}\frac{\partial\alpha_1}{\partial\beta} + \frac{\mathrm{d}Y_2}{\mathrm{d}\alpha_2}\frac{\partial\alpha_2}{\partial\beta} = -\frac{\mathrm{d}Y_1}{\mathrm{d}\alpha_1} - \frac{\mathrm{d}Y_2}{\mathrm{d}\alpha_2} = -\Phi_1 - \Phi_2 \\ Y_\rho &= \frac{\mathrm{d}Y_1}{\mathrm{d}\alpha_1}\frac{\partial\alpha_1}{\partial\rho} + \frac{\mathrm{d}Y_2}{\mathrm{d}\alpha_2}\frac{\partial\alpha_2}{\partial\rho} = -a_1\frac{\mathrm{d}Y_1}{\mathrm{d}\alpha_1} + a_2\frac{\mathrm{d}Y_2}{\mathrm{d}\alpha_2} = -a_1\Phi_1 + a_2\Phi_2 \end{aligned} \tag{6.177}$$

[14] Actually, the real critical speed can be lower than the value predicted by (6.174), as shown in [7, pp. 216–219]. Basically, (6.174) may not predict the right value because in real vehicles we control the longitudinal force, not directly the forward speed. Therefore, a real vehicle is a system with three state variables, not just two. This additional degree of freedom does affect the critical speed, unless the vehicle is going straight.

and

$$\begin{aligned} N_\beta &= a_1 \frac{\mathrm{d}Y_1}{\mathrm{d}\alpha_1}\frac{\partial \alpha_1}{\partial \beta} - a_2 \frac{\mathrm{d}Y_2}{\mathrm{d}\alpha_2}\frac{\partial \alpha_2}{\partial \beta} = -a_1 \frac{\mathrm{d}Y_1}{\mathrm{d}\alpha_1} + a_2 \frac{\mathrm{d}Y_2}{\mathrm{d}\alpha_2} = -a_1\Phi_1 + a_2\Phi_2 \\ N_\rho &= a_1 \frac{\mathrm{d}Y_1}{\mathrm{d}\alpha_1}\frac{\partial \alpha_1}{\partial \rho} - a_2 \frac{\mathrm{d}Y_2}{\mathrm{d}\alpha_2}\frac{\partial \alpha_2}{\partial \rho} = -a_1^2 \frac{\mathrm{d}Y_1}{\mathrm{d}\alpha_1} - a_2^2 \frac{\mathrm{d}Y_2}{\mathrm{d}\alpha_2} = -a_1^2\Phi_1 - a_2^2\Phi_2 \end{aligned} \tag{6.178}$$

where

$$\Phi_1 = \frac{\mathrm{d}Y_1}{\mathrm{d}\alpha_1} \qquad \text{and} \qquad \Phi_2 = \frac{\mathrm{d}Y_2}{\mathrm{d}\alpha_2} \tag{6.179}$$

are the *slopes* of the axle characteristics *at the equilibrium point*, defined in (6.94). Obviously, $\Phi_i > 0$ in the monotone increasing part of the axle characteristics. These slopes are simple to be defined, but not so simple to be measured directly.

It is also worth noting that

$$Y_\rho = N_\beta \tag{6.180}$$

To proceed further, as already done in (6.50), let

$$\delta_1 = (1+\kappa)\tau\delta_v \qquad \text{and} \qquad \delta_2 = \kappa\tau\delta_v \tag{6.181}$$

thus linking the rear steer angle δ_2 to the front steer angle δ_1 in such a way to keep constant the net steer angle $\tau\delta_v = \delta_1 - \delta_2 = \delta$. To have front steering only it suffices to set $\kappa = 0$.

We can now obtain also the explicit expressions of the *control derivatives*

$$Y_\delta = ((1+\kappa)\Phi_1 + \kappa\Phi_2)\tau, \qquad N_\delta = ((1+\kappa)\Phi_1 a_1 - \kappa\Phi_2 a_2)\tau \tag{6.182}$$

In this vehicle model, all stability derivatives and all control derivatives are functions of $\tilde{a}_y$ only, that is $Y_\beta = Y_\beta(\tilde{a}_y)$, and so on.

The linearized equations of motions (6.141) become

$$\begin{aligned} m(u_a\dot{\beta}_t + u_a^2\rho_t) &= -(\Phi_1+\Phi_2)\beta_t - (\Phi_1 a_1 - \Phi_2 a_2)\rho_t + ((1+\kappa)\Phi_1 + \kappa\Phi_2)\tau\delta_{vt} \\ J_z u_a\dot{\rho}_t &= -(\Phi_1 a_1 - \Phi_2 a_2)\beta_t - (\Phi_1 a_1^2 + \Phi_2 a_2^2)\rho_t + ((1+\kappa)\Phi_1 a_1 - \kappa\Phi_2 a_2)\tau\delta_{vt} \end{aligned} \tag{6.183}$$

Similarly, (6.130) becomes, in this case

$$\begin{aligned} 2\zeta\omega_n = -\operatorname{tr}(\mathbf{A}) &= \frac{1}{u_a}\left(\frac{\Phi_1+\Phi_2}{m} + \frac{\Phi_1 a_1^2 + \Phi_2 a_2^2}{J_z}\right) \\ &= \frac{\Phi_1(J_z + m a_1^2) + \Phi_2(J_z + m a_2^2)}{J_z m u_a} \end{aligned} \tag{6.184}$$

and

$$\omega_n^2 = \det(\mathbf{A}) = \frac{1}{J_z m u_a^2}\left[\Phi_1\Phi_2(a_1+a_2)^2 - m u_a^2(\Phi_1 a_1 - \Phi_2 a_2)\right] \tag{6.185}$$

The damping ratio (6.131) has the following expression

$$\zeta = \frac{(\Phi_1+\Phi_2)J_z + (\Phi_1 a_1^2 + \Phi_2 a_2^2)m}{2\sqrt{J_z m}\sqrt{\Phi_1\Phi_2(a_1+a_2)^2 - m u_a^2(\Phi_1 a_1 - \Phi_2 a_2)}} \tag{6.186}$$

and the natural angular frequency (6.133) becomes

$$\begin{aligned}\omega_s^2 = {} & \frac{\Phi_2 a_2 - \Phi_1 a_1}{J_z} \\ & - \frac{1}{(2J_z m u_a)^2}\Big[(\Phi_1+\Phi_2)^2 J_z^2 + 2(\Phi_2 a_2 - \Phi_1 a_1)^2 J_z m \\ & \qquad - 2(a_1+a_2)^2\Phi_1\Phi_2 J_z m + (\Phi_1 a_1^2 + \Phi_2 a_2^2)^2 m^2\Big]\end{aligned} \tag{6.187}$$

or, equivalently

$$\begin{aligned}\omega_s^2 = {} & -\frac{\Phi_1 a_1}{J_z} + \frac{\Phi_2 a_2}{J_z} \\ & - \Phi_1\Phi_2\left[\frac{J_z^2 - (a_1^2 + 4a_1 a_2 + a_2^2)J_z m + a_1^2 a_2^2 m^2}{2(J_z m u_a)^2}\right] \\ & \qquad - \Phi_1^2\left(\frac{J_z + m a_1^2}{2J_z m u_a}\right)^2 - \Phi_2^2\left(\frac{J_z + m a_2^2}{2J_z m u_a}\right)^2\end{aligned} \tag{6.188}$$

These parameters characterize the handling behavior in the neighborhood of an equilibrium point.

In the single track model, the explicit expressions of the two forcing functions (6.149) can also be obtained

$$\begin{aligned}F_\beta &= \left[\frac{(a_1+a_2)\Phi_1\Phi_2((1+\kappa)a_2 + \kappa a_1)}{J_z m u_a^2} - \frac{(1+\kappa)a_1\Phi_1 - \kappa a_2\Phi_2}{J_z}\right]\tau\delta_{vt} + \frac{(1+\kappa)\Phi_1 + \kappa\Phi_2}{m u_a}\tau\dot{\delta}_v \\ F_\rho &= \frac{(a_1+a_2)\Phi_1\Phi_2}{J_z m u_a^2}\tau\delta_{vt} + \frac{(1+\kappa)a_1\Phi_1 - \kappa a_2\Phi_2}{J_z u_a}\tau\dot{\delta}_v\end{aligned} \tag{6.189}$$

with obvious simplifications if $\kappa = 0$ (only front steering).

All the equations obtained in this section show that for a single track model there are *seven* design parameters

$$\frac{\Phi_1}{m}, \qquad \frac{\Phi_2}{m}, \qquad a_1, \qquad a_2, \qquad \frac{J_z}{m}, \qquad \kappa, \qquad \tau \tag{6.190}$$

in addition to the control parameters u and $\delta_v(t)$, with constant $u = u_a$.

Now, we can relate these design parameters to the *six* fundamental "handling bricks" of (6.169).

The components of the gradients grad β_p and grad ρ_p, defined in (6.99), have been already obtained for the single track model in (6.100)

$$\begin{aligned} \beta_y &= -\frac{m}{l^2}\left(\frac{\Phi_1 a_1^2 + \Phi_2 a_2^2}{\Phi_1 \Phi_2}\right) & \beta_\delta &= \tau\left(\frac{(1+\kappa)a_2 + \kappa a_1}{l}\right) \\ \rho_y &= -\frac{m}{l^2}\left(\frac{\Phi_2 a_2 - \Phi_1 a_1}{\Phi_1 \Phi_2}\right) & \rho_\delta &= \tau\frac{(1+\kappa) - \kappa}{l} \end{aligned} \tag{6.100′}$$

As already stated, all these components can be measured experimentally from standard steady-state tests, without having to bother about Ackermann steer angle and the like.

The generalized control derivatives $\hat{Y}_\delta = Y_\delta/m$ and $\hat{N}_\delta = N_\delta/J_z$ are immediately obtained from (6.182).

Summing up, for the single track model the six "handling bricks" $s_i(\delta_{va}, \tilde{a}_y)$ in (6.169) are

$$\begin{aligned} s_1 &= \beta_y = -\frac{m}{(a_1+a_2)^2}\left(\frac{\Phi_2 a_2^2 + \Phi_1 a_1^2}{\Phi_1 \Phi_2}\right) \\ s_2 &= \rho_y = -\frac{m}{(a_1+a_2)^2}\left(\frac{\Phi_2 a_2 - \Phi_1 a_1}{\Phi_1 \Phi_2}\right) \\ s_3 &= \beta_\delta = \tau\frac{(1+\kappa)a_2 + \kappa a_1}{a_1+a_2} \\ s_4 &= \rho_\delta = \tau\frac{(1+\kappa) - \kappa}{a_1+a_2} = \frac{\tau}{a_1+a_2} \\ s_5 &= \hat{N}_\delta = \tau\frac{(1+\kappa)\Phi_1 a_1 - \kappa\Phi_2 a_2}{J_z} \\ s_6 &= \hat{Y}_\delta = \tau\frac{(1+\kappa)\Phi_1 + \kappa\Phi_2}{m} \end{aligned} \tag{6.191}$$

Therefore, we have six "handling bricks" depending on seven design parameters. This means that there exist infinitely many different vehicles sharing the same handling transient behavior. This observation opens up many new paths of reasoning.

One of these paths of reasoning is worked out in the next section. The results are quite surprising.

6.14.1 Different Vehicles with Identical Handling

As a test of the new theory presented in Sect. 6.14, we are going to compare the transient handling behavior of, say, three linear single track models. These vehicles will be very different, and identical at the same time. How is it possible?

These three vehicles will share exactly the same values of all the six handling bricks listed in (6.191). Therefore, they will have the same handling behavior. However, they need not to be exactly alike, since we can play with seven design parameter to fulfill the six handling requirements.

A good test is to define a first vehicle with front steer only, a second vehicle with also negative rear steer, and a third one with positive rear steer. This can be easily done by means of parameter κ, introduced in (6.181)

$$\delta_1 = (1+\kappa)\tau\delta_v \qquad \text{and} \qquad \delta_2 = \kappa\tau\delta_v \tag{6.181'}$$

Parameter κ controls the amount of rear steer with respect to front steer, while keeping constant the net steer angle $\delta = \tau\delta_v = \delta_1 - \delta_2$. The rear wheels turn opposite to the front wheels if $\kappa < 0$, while both front and rear wheels turn alike if $\kappa > 0$. Typically, $|\kappa| < 0.1$, that is the rear wheels cannot turn as far as the front wheels.

But, let us do some numerical examples. Let us consider a vehicle with front steering only ($\kappa = 0$), with the following features:

- $\tau = 1/20$;
- $m = 1300\,\text{kg}$;
- $J_z = 2000\,\text{kgm}^2$;
- $a_1 = 1\,\text{m}$;
- $a_2 = 1.60\,\text{m}$;
- $\Phi_1 = \Phi_1(0) = 70000\,\text{N/rad}$;
- $\Phi_2 = \Phi_2(0) = 90000\,\text{N/rad}$.

From (6.191) we can compute all six handling bricks s_i for this vehicle, and then use them for the other two vehicles. This way, it is possible to create vehicles that look very different, but which ultimately have exactly the same handling behavior.

The vehicle features for $\kappa \pm 0.1$, that is two very high amounts of rear steer, are shown in Table 6.1. The three vehicles there reported are strikingly different (Fig.. 6.70), yet they have the same handling behavior, and not limited to steady state. For the driver, they behave exactly the same way under any transient conditions.

For instance, starting from a straight trajectory, let us impose a step steering input $\delta_v = 60°$, the forward velocity being $u = 20\,\text{m/s}$. Figures 6.58 and 6.59 show the

Table 6.1 Design parameters of vehicles with different amounts of rear steering κ, but with identical transient handling behavior. Note that the classical understeer gradient K conveys misleading information

κ (−)	Φ_1 (N/rad)	Φ_2 (N/rad)	a_1 (m)	a_2 (m)	J_z (kg m^2)	m (kg)	τ (−)	K (deg/g)	$-\rho_y$ (deg/(mg))
−0.10	86332	73668	0.73	1.86	2000	1300	0.99/20	3.28	1.27
0.00	70000	90000	1.00	1.60	2000	1300	1.00/20	3.30	1.27
+0.10	49065	110935	1.48	1.32	2000	1300	1.08/20	3.55	1.27

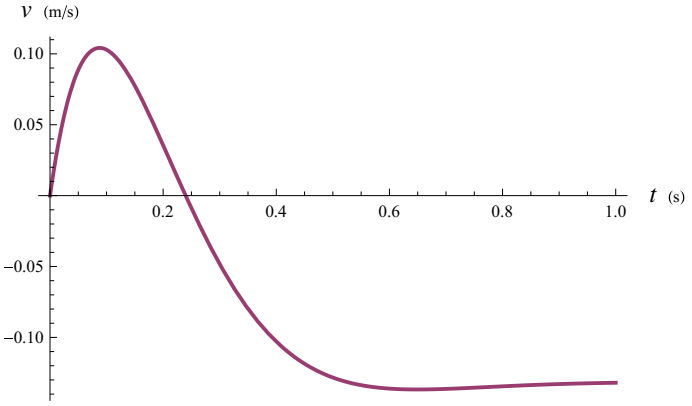

Fig. 6.58 Lateral velocity $v(t)$ of any of the three vehicles after a step steering input

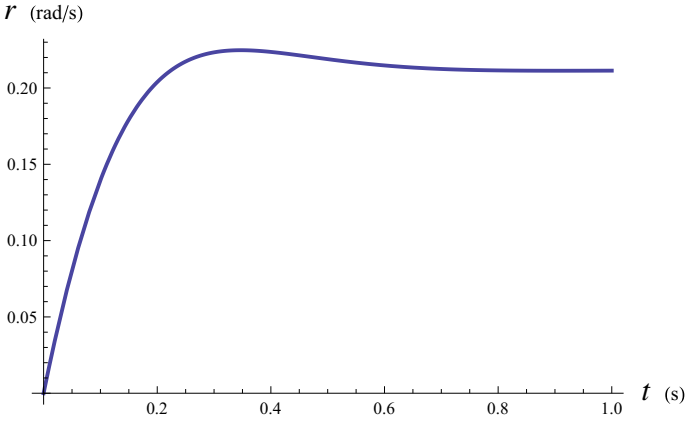

Fig. 6.59 Yaw rate $r(t)$ of any of the three vehicles after a step steering input

lateral velocity $v(t)$ and the yaw rate $r(t)$, respectively. They are identical for the three vehicles, thus confirming the theoretical claims.

Of course, the slip angles are not identical, as shown in Fig. 6.60. The three vehicles are indeed different. It is left to the reader to figure out which curve is for $\kappa = 0.1$, etc.

Just out of curiosity, the most extreme vehicles that can be obtained with this algorithm are shown in Table 6.2. Of course, we are not suggesting that they are feasible vehicles. They are reported here because they provide some rigorous evidence that rear steer must be kept small to have good handling behavior, as intuitively everybody knows.

But perhaps the most astonishing result obtained in this section is that all these vehicles of Tables 6.1 and 6.2, although with identical handling behavior, do not

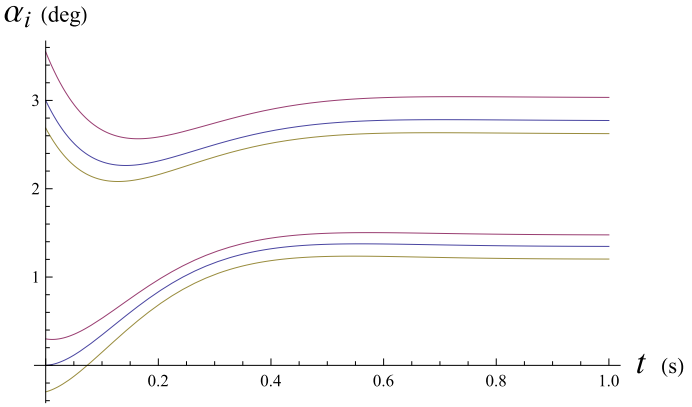

Fig. 6.60 Front and rear slip angles of the three vehicles after a step steering input

Table 6.2 Design parameters of vehicles with extreme amounts of rear steering κ, but with identical transient handling behavior

κ (−)	Φ_1 (N/rad)	Φ_2 (N/rad)	a_1 (m)	a_2 (m)	J_z (kg m^2)	m (kg)	τ (−)	K (deg/g)	$-\rho_y$ (deg/(mg))
−0.60	141316	18684	0.01	4.01	2000	1300	1.55/20	5.10	1.27
0.00	70000	90000	1.00	1.60	2000	1300	1.00/20	3.30	1.27
+0.166	22426	137574	2.73	0.98	2000	1300	1.42/20	4.71	1.27

have the same classical understeer gradient K. Just have a look at the next to last column in Table 6.1. In other words, they would have been classified as very different if evaluated in terms of their classical understeer gradient K.

The conclusion is that the classical understeer gradient is *not* a good parameter and should be abandoned. It should be replaced by the gradient components proposed in (6.99) and discussed in Sect. 6.13, which have proven to really provide a measure of the dynamic features of a vehicle. In particular, the gradient component ρ_y, shown in the last column in Tables 6.1 and 6.2, is the real measure of understeer/oversteer.

6.15 Linear Single Track Model

The simplest dynamical systems are those governed by *linear* ordinary differential equations with *constant* coefficients. The single track model of Fig. 6.20 is governed by the *nonlinear* ordinary differential equations (6.158), unless the axle characteristics are replaced by linear functions

$$Y_1 = C_1\alpha_1 \quad \text{and} \quad Y_2 = C_2\alpha_2 \tag{6.192}$$

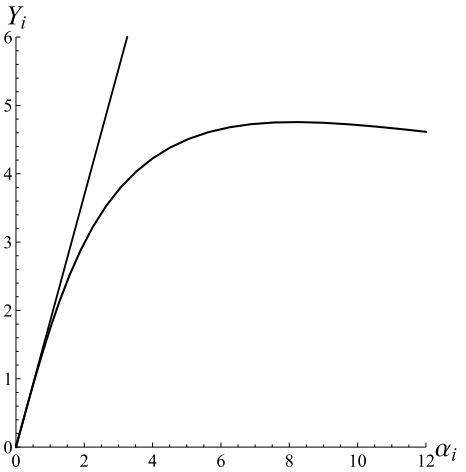

Fig. 6.61 Linear approximation of the axle characteristics

where

$$C_1 = \left.\frac{\mathrm{d}Y_1}{\mathrm{d}\alpha_1}\right|_{\alpha_1=0} = \Phi_1(0) \qquad \text{and} \qquad C_2 = \left.\frac{\mathrm{d}Y_2}{\mathrm{d}\alpha_2}\right|_{\alpha_2=0} = \Phi_2(0) \tag{6.193}$$

The *axle lateral slip stiffness* C_i is usually equal to twice the tire lateral slip stiffness, firstly introduced in (2.91). It is affected by the static vertical load (Fig. 2.25), but not by the load transfer, neither by the amount of grip. The influence of roll steer is quite peculiar (Fig. 6.17).

However, as shown in Fig. 6.61, this linear approximation is acceptable only if $|\alpha_i| < 2°$, that is for very low values of $\tilde{a}_y$.

The main advantage of the *linear* single track model lies in its simplicity, the main disadvantage is that it does not model the vehicle behavior at all, unless the lateral acceleration is really small (typically, $\tilde{a}_y < 0.2g$ on dry asphalt). In some sense, it is a "dangerous" model because one may be tempted to use it outside its range of validity. Indeed, too often it is the only handling model that is presented and discussed in detail.

However, in some cases it is useful to have a model where everything can be obtained analytically. For this reason, the linear single track model is included in this book as well, albeit not in a prominent position.

6.15.1 Governing Equations

The *linear* single track model differs from the more general nonlinear model only in its constitutive equations. However, we list here all relevant equations, that is equilibrium equations (6.4)

$$\begin{aligned} m(\dot{v} + ur) &= Y = Y_1 + Y_2 \\ J_z \dot{r} &= N = Y_1 a_1 - Y_2 a_2 \end{aligned} \tag{6.194}$$

congruence equations (6.68) (with $|\chi| \ll 1$, and often equal to zero)

$$\begin{aligned} \alpha_1 &= \tau_1 \delta_v - \frac{v + r a_1}{u} \\ \alpha_2 &= \chi \tau_1 \delta_v - \frac{v - r a_2}{u} \end{aligned} \tag{6.195}$$

and the just defined *linear* constitutive equations (6.192) [10, Chap. 5]

$$\begin{aligned} Y_1 &= C_1 \alpha_1 \\ Y_2 &= C_2 \alpha_2 \end{aligned} \tag{6.196}$$

Combining congruence and constitutive equations we get

$$\begin{aligned} Y_1 = C_1 \alpha_1 &= C_1 \left(\tau_1 \delta_v - \frac{v + r a_1}{u} \right) \\ Y_2 = C_2 \alpha_2 &= C_2 \left(\tau_1 \chi \delta_v - \frac{v - r a_2}{u} \right) \end{aligned} \tag{6.197}$$

which are linear in v and r, but not in u.

Inserting these equations into the equilibrium equations, we obtain the governing equations, that is two *linear* differential equations

$$\begin{aligned} \dot{v} &= -\left(\frac{C_1 + C_2}{mu} \right) v - \left(\frac{C_1 a_1 - C_2 a_2}{mu} + u \right) r + \frac{C_1 + \chi C_2}{m} \tau_1 \delta_v \\ \dot{r} &= -\left(\frac{C_1 a_1 - C_2 a_2}{J_z u} \right) v - \left(\frac{C_1 a_1^2 + C_2 a_2^2}{J_z u} \right) r + \frac{C_1 a_1 - \chi C_2 a_2}{J_z} \tau_1 \delta_v \end{aligned} \tag{6.198}$$

In matrix notation, (6.198) becomes

$$\dot{\mathbf{w}} = \mathbf{A}\mathbf{w} + \mathbf{b}\delta_v \tag{6.199}$$

where $\mathbf{w}(t) = \big(v(t), r(t)\big)$ is the vector of state variables, the r.h.s. known vector is

$$\mathbf{b}(t) = \tau_1 \begin{bmatrix} \dfrac{C_1 + \chi C_2}{m} \\ \dfrac{C_1 a_1 - \chi C_2 a_2}{J_z} \end{bmatrix} \tag{6.200}$$

and

$$\mathbf{A} = \mathbf{A}(u(t)) = -\begin{bmatrix} \dfrac{C_1 + C_2}{mu} & \dfrac{C_1 a_1 - C_2 a_2}{mu} + u \\ \dfrac{C_1 a_1 - C_2 a_2}{J_z u} & \dfrac{C_1 a_1^2 + C_2 a_2^2}{J_z u} \end{bmatrix} \tag{6.201}$$

is the coefficient matrix. It is important to note that $\mathbf{A}$ depends on the forward speed u, but not on the steer angle δ_v, which multiplies the known vector $\mathbf{b}$.

6.15.2 Solution for Constant Forward Speed

As well known, the general solution $\mathbf{w}(t)$ of (6.199) is given by the solution $\mathbf{w}_o$ of the homogeneous equation plus a particular solution $\mathbf{w}_p$

$$\mathbf{w}(t) = \mathbf{w}_o(t) + \mathbf{w}_p(t) \tag{6.202}$$

Unfortunately, analytical solutions are not available if $u(t) \neq \text{const}$.

If u is *constant* ($\dot{u} = 0$), the system (6.199) has constant coefficients and the homogeneous solution must fulfill

$$\dot{\mathbf{w}}_o = \mathbf{A}\mathbf{w}_o \tag{6.203}$$

with a *constant* matrix $\mathbf{A}$. Assuming constant u is therefore a very relevant assumption. We look for a solution among the exponential functions

$$\mathbf{w}_o(t) = \big(v_o(t), r_o(t)\big) = \mathbf{x}\mathrm{e}^{\lambda t} \tag{6.204}$$

which implies $\dot{\mathbf{w}}_o(t) = \lambda \mathbf{x}\mathrm{e}^{\lambda t}$, and consequently yields an eigenvalue problem for the matrix $\mathbf{A}$

$$\mathbf{A}\mathbf{x} = \lambda \mathbf{x} \tag{6.205}$$

The eigenvalues are the solutions of the characteristic equation

$$\det(\mathbf{A} - \lambda \mathbf{I}) = 0 \tag{6.206}$$

which, for a (2×2) matrix, becomes

$$\lambda^2 - \mathrm{tr}(\mathbf{A})\lambda + \det(\mathbf{A}) = 0 \tag{6.207}$$

The two eigenvalues λ_1 and λ_2 are

$$\lambda_{1,2} = \frac{\mathrm{tr}(\mathbf{A}) \pm \sqrt{\mathrm{tr}(\mathbf{A})^2 - 4\det(\mathbf{A})}}{2} = -\zeta\omega_n \pm \omega_n\sqrt{\zeta^2 - 1} \tag{6.208}$$

If the discriminant is negative, that is if $\zeta < 1$, the dynamical system is underdamped and the eigenvalues are complex conjugates.

From (6.201) we get the trace

$$\mathrm{tr}(\mathbf{A}) = -\frac{1}{u}\left(\frac{C_1 + C_2}{m} + \frac{C_1 a_1^2 + C_2 a_2^2}{J_z}\right) < 0 \tag{6.209}$$

and the determinant

$$\det(\mathbf{A}) = \frac{1}{u^2 m J_z}\left[C_1 C_2 (a_1 + a_2)^2 - m u^2 (C_1 a_1 - C_2 a_2)\right] \tag{6.210}$$

These two quantities are very important because they provide handy information about the two eigenvalues λ_1 and λ_2 of $\mathbf{A}$, since

$$\mathrm{tr}(\mathbf{A}) = \lambda_1 + \lambda_2 \tag{6.211}$$

$$\det(\mathbf{A}) = \lambda_1 \lambda_2 \tag{6.212}$$

These two relationships can be obtained easily writing the characteristic equation as $(\lambda - \lambda_1)(\lambda - \lambda_2) = 0$.

Once the two eigenvalues have been obtained, we can compute the two eigenvectors $\mathbf{x}_1$ and $\mathbf{x}_2$.

Therefore, the solution of the homogeneous system is

$$\mathbf{w}_o(t) = \gamma_1 \mathbf{x}_1 \mathrm{e}^{\lambda_1 t} + \gamma_2 \mathbf{x}_2 \mathrm{e}^{\lambda_2 t} \tag{6.213}$$

where γ_1 and γ_2 are constants still to be determined. In components we have

$$\begin{aligned} v_o(t) &= \gamma_1 x_{11} \mathrm{e}^{\lambda_1 t} + \gamma_2 x_{12} \mathrm{e}^{\lambda_2 t} \\ r_o(t) &= \gamma_1 x_{21} \mathrm{e}^{\lambda_1 t} + \gamma_2 x_{22} \mathrm{e}^{\lambda_2 t} \end{aligned} \tag{6.214}$$

where $\mathbf{x}_1 = (x_{11}, x_{21})$ and $\mathbf{x}_2 = (x_{12}, x_{22})$.

The particular integral $\mathbf{w}_p(t) = (v_p(t), r_p(t))$ depends on the known vector $\mathbf{b}$ and on the steering wheel angle $\delta_v(t)$. The simplest case is for constant δ_v, but analytical solutions are available also when $\delta_v(t)$ is a polynomial or trigonometric function.

Summing up, the general solution of the system (6.199) is

$$\mathbf{w}(t) = \mathbf{w}_o(t) + \mathbf{w}_p(t) = \gamma_1 \mathbf{x}_1 \mathrm{e}^{\lambda_1 t} + \gamma_2 \mathbf{x}_2 \mathrm{e}^{\lambda_2 t} + \mathbf{w}_p(t) \tag{6.215}$$

in which the two constants γ_1 and γ_2 are to be determined from the initial conditions $\mathbf{w}(0) = (v(0), r(0))$, that is solving the system

$$\mathbf{S}\mathbf{y} = \mathbf{w}(0) - \mathbf{w}_p(0) \tag{6.216}$$

where $\mathbf{y} = (\gamma_1, \gamma_2)$ and $\mathbf{S}$ is the matrix whose columns are the two eigenvectors of $\mathbf{A}$.

6.15.3 Critical Speed

The two parts $\mathbf{w}_o$ and $\mathbf{w}_p$ of the general solution have distinct physical meanings. The particular integral is what the vehicle does asymptotically, that is basically at steady-state. The solution of the homogeneous system shows how the vehicle behaves before reaching the steady-state condition, if the vehicle is stable.

As already discussed in Sect. 6.10.4, the stability of the vehicle is completely determined by the two eigenvalues λ_1 and λ_2, or better, by the sign of their real parts $\mathrm{Re}(\lambda_1)$ and $\mathrm{Re}(\lambda_2)$. The rule is very simple: the system is asymptotically stable if and only if both eigenvalues have negative real parts

$$\text{stability} \quad \Longleftrightarrow \quad \mathrm{Re}(\lambda_1) < 0 \quad \text{and} \quad \mathrm{Re}(\lambda_2) < 0 \tag{6.217}$$

If just one eigenvalue has a positive real part, the corresponding exponential solution grows without bound in time, and the system is unstable.

Fortunately, we can check the stability without computing the two eigenvalues explicitly, but simply looking at (6.211) and (6.212). To have an asymptotically stable vehicle it suffices to check that

$$\text{stability} \quad \Longleftrightarrow \quad \mathrm{tr}(\mathbf{A}) < 0 \quad \text{and} \quad \det(\mathbf{A}) > 0 \tag{6.218}$$

From (6.209) we see immediately that $\mathrm{tr}(\mathbf{A}) < 0$ is always fulfilled. Stability is therefore completely due to the second condition in (6.218). Setting $\det(\mathbf{A}) = 0$ in (6.185) yields an equation in the unknown forward speed u, whose solution, if it exists, is the *critical speed* u_{cr}

$$u_{\mathrm{cr}} = \sqrt{\frac{C_1 C_2 l^2}{m(C_1 a_1 - C_2 a_2)}}. \tag{6.219}$$

Beyond the critical speed the vehicle becomes unstable. It is worth noting that u_{cr} does not depend on J_z.

In the linear single track model, the critical speed exists if and only if

$$C_1 a_1 - C_2 a_2 > 0 \tag{6.220}$$

that is, if the vehicle is oversteer. In this vehicle model (which, we recall, has a very limited range of applicability), the critical speed is not affected by the steer angle.

6.15.4 Transient Vehicle Behavior

It may be of some interest to know how the eigenvalues evolve as speed changes. To this end, it is useful to plot $\mathrm{tr}(\mathbf{A})$ vs $\det(\mathbf{A})$, which, according to (6.209) and (6.210),

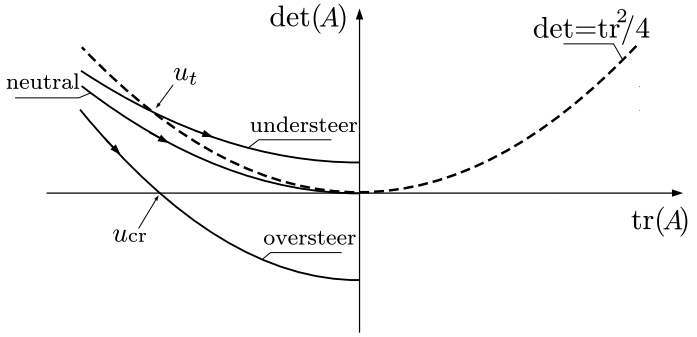

Fig. 6.62 Evolution of $\det(A)$ and $\mathrm{tr}(A)$ when u grows

can be compactly expressed as[15]

$$\det(\mathbf{A}) = \frac{\alpha}{u^2} + \beta, \qquad \mathrm{tr}(\mathbf{A}) = -\frac{\gamma}{u} \tag{6.221}$$

where α and γ are always positive, while $\beta = (C_2a_2 - C_1a_1)/J_z$ can be either positive or negative, depending on the vehicle being understeer or oversteer, respectively.

Both functions are monotone increasing in u (if $u > 0$). They can be combined to get

$$\det(\mathbf{A}) = \frac{\alpha}{\gamma^2}\,\mathrm{tr}(\mathbf{A})^2 + \beta. \tag{6.222}$$

Moreover, it is easy to show that

$$\lim_{u\to+\infty} \mathrm{tr}(\mathbf{A}) = 0^-, \qquad \lim_{u\to+\infty} \det(\mathbf{A}) = \beta \tag{6.223}$$

Therefore, as u grows, we draw parabolas, as shown in Fig. 6.62, up to their vertex in $(0, \beta)$.

Also plotted in Fig. 6.62 is the parabola $\det = \mathrm{tr}^2/4$. According to (6.208), it corresponds to the points where $\lambda_1 = \lambda_2$. Below this parabola the two eigenvalues are real, whereas above it they are complex conjugates.

It can be shown that

$$\left(\frac{\alpha}{\gamma^2} = \frac{C_1C_2k^2l^2}{[k^2(C_1+C_2) + C_1a_1^2 + C_2a_2^2]^2}\right) \le \frac{1}{4} \tag{6.224}$$

where $J_z = mk^2$. Since it attains its maximum value $1/4$ when $C_1a_1 = C_2a_2$ (neutral vehicle) and $J_z = ma_1a_2$, we see that all vehicles at sufficiently low speed have real negative eigenvalues.

[15] Here α, β and γ are just constants. They have no connection with slip and camber angles.

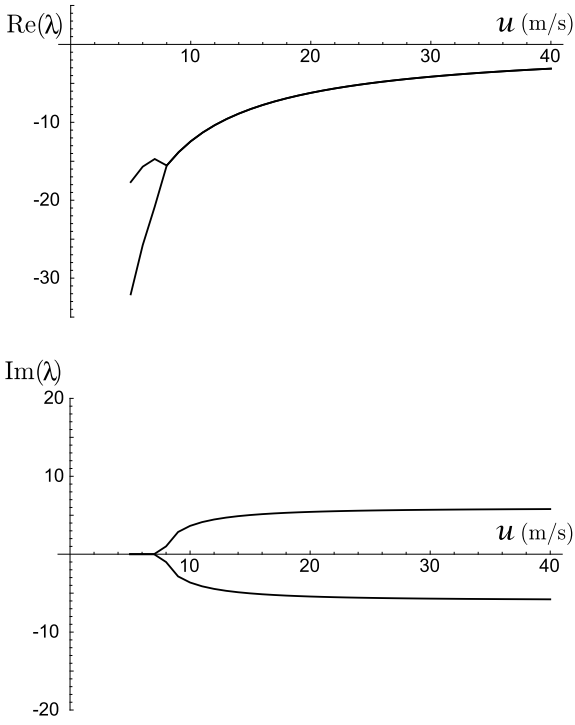

Fig. 6.63 Evolution of the real part and of the imaginary part of λ_1 and λ_2 as functions of the forward speed u, for an understeer vehicle

As the speed increases, the following evolutions are possible. An oversteer vehicle (actually, an oversteer linear single track model) has always two real eigenvalues. When the parabola in Fig. 6.62 crosses the horizontal axis (det $= 0$), one eigenvalue becomes positive and the vehicle becomes unstable. That happens for $u = u_{\text{cr}}$.

An understeer vehicle has two negative real eigenvalues at low speed. For speeds higher than $u = u_t$, they become complex conjugate with negative real parts (Fig. 6.62): $\lambda_1 = -\zeta\omega_n + i\omega_n\sqrt{1-\zeta^2}$, $\lambda_2 = -\zeta\omega_n - i\omega_n\sqrt{1-\zeta^2}$. Therefore, at sufficiently high speed, the transient motion is a damped oscillation (very damped, indeed). The speed u_t is given by

$$u_t = \sqrt{\frac{\gamma^2 - 4\alpha}{4\beta}} = \sqrt{\frac{[J_z(C_1 + C_2) + m(C_1 a_1^2 + C_2 a_2^2)]^2 - 4J_z m C_1 C_2 l^2}{4m^2 J_z(C_2 a_2 - C_1 a_1)}} \tag{6.225}$$

From Fig. 6.63, we see that the imaginary part of the eigenvalues, that is the angular frequency $\omega_s = \omega_n\sqrt{1-\zeta^2}$, is almost constant up to relatively high speeds. This is typical and makes the classical sine sweep test quite insensitive to the selected speed.

The general solution is given by (6.215). However, when the eigenvalues are complex conjugates, also the eigenvectors $\mathbf{x}_1$ and $\mathbf{x}_2$ and the constants γ_1 and γ_2 are

complex conjugates. Having to deal with so many complex numbers to eventually get a real function $\mathbf{w}(t)$ is not very convenient. Fortunately, we can rearrange it in a way that it involves only real numbers. As well known, $e^{(\zeta+i\omega)t} = e^{\zeta t}[\cos(\omega t) + i\sin(\omega t)]$, and the general solution can be written as

$$\begin{aligned}\mathbf{w}(t) &= \mathbf{w}_o(t) + \mathbf{w}_p(t)\\ &= \gamma_1\mathbf{x}_1 e^{\lambda_1 t} + \gamma_2\mathbf{x}_2 e^{\lambda_2 t} + \mathbf{w}_p(t)\\ &= e^{-\zeta\omega_n t}[(\gamma_1\mathbf{x}_1 + \gamma_2\mathbf{x}_2)\cos(\omega_s t) + i(\gamma_1\mathbf{x}_1 - \gamma_2\mathbf{x}_2)\sin(\omega_s t)] + \mathbf{w}_p(t)\\ &= e^{-\zeta\omega_n t}[\mathbf{z}_1\cos(\omega_s t) + \mathbf{z}_2\sin(\omega_s t)] + \mathbf{w}_p(t)\end{aligned} \tag{6.226}$$

where $\omega_s = \omega_n\sqrt{1-\zeta^2}$.

To obtain $\mathbf{z}_1$ and $\mathbf{z}_2$ we can proceed as follows. Vector $\mathbf{z}_1$ is simply obtained setting $t = 0$ in the last expression in (6.226)

$$\mathbf{z}_1 = \mathbf{w}(0) - \mathbf{w}_p(0) \tag{6.227}$$

where $\mathbf{w}(0)$ is the vector of the initial conditions. To obtain the other vector, just consider that

$$\dot{\mathbf{w}}_o(0) = \mathbf{A}\mathbf{w}_o(0) = -\zeta\omega_n\mathbf{z}_1 + \omega_s\mathbf{z}_2 = \mathbf{z}_1 \tag{6.228}$$

and hence

$$\mathbf{z}_2 = \frac{1}{\omega_s}(\mathbf{A} + \zeta\omega_n\mathbf{I})\mathbf{z}_1 \tag{6.229}$$

6.15.5 Steady-State Behavior: Steering Pad

As already stated, the particular integral $\mathbf{w}_p(t) = (v_p(t), r_p(t))$ is determined, in this linear model, by the known vector $\mathbf{b}$, and hence by the function $\delta_v(t)$. The simplest case is when $\delta_v = \text{const}$.

Keeping the steering wheel in a fixed position and driving at constant speed makes the vehicle go round in a circle. This is called steering pad. To obtain the steady-state solution, we have to solve the system

$$-\mathbf{A}\mathbf{w}_p = \mathbf{b}\delta_v \tag{6.230}$$

thus getting

$$
\begin{aligned}
v_p &= \frac{[C_1C_2l(a_2+a_1\chi)-mu^2(C_1a_1-C_2a_2\chi)]u}{C_1C_2l^2-mu^2(C_1a_1-C_2a_2)}\tau_1\delta_v,\\
r_p &= \frac{C_1C_2l(1-\chi)u}{mJ_zu^2\det(\mathbf{A})}\tau_1\delta_v = \frac{C_1C_2l(1-\chi)u}{C_1C_2l^2-mu^2(C_1a_1-C_2a_2)}\tau_1\delta_v.
\end{aligned}
\tag{6.231}
$$

Once we have obtained v_p and r_p, we can easily compute all other relevant quantities, like the vehicle slip angle β_p and the curvature ρ_p

$$
\begin{aligned}
\beta_p &= \frac{v_p}{u} = \left(\frac{a_2+a_1\chi}{l}\right)\tau_1\delta_v - \frac{m}{l^2}\left(\frac{C_1a_1^2+C_2a_2^2}{C_1C_2}\right)\tilde{a}_y = \frac{S_p}{R_p}\\
\rho_p &= \frac{r_p}{u} = \left(\frac{1-\chi}{l}\right)\tau_1\delta_v - \frac{m}{l^2}\left(\frac{C_2a_2-C_1a_1}{C_1C_2}\right)\tilde{a}_y = \frac{1}{R_p}
\end{aligned}
\tag{6.232}
$$

According to (6.195), we can compute the steady-state front and rear slip angles

$$
\begin{aligned}
\alpha_{1p} &= \tau_1\delta_v - \frac{v_p+r_pa_1}{u} = \frac{ma_2}{lC_1}\tilde{a}_y\\
\alpha_{2p} &= \chi\tau_1\delta_v - \frac{v_p-r_pa_2}{u} = \frac{ma_1}{lC_2}\tilde{a}_y
\end{aligned}
\tag{6.233}
$$

A non-zero lateral speed v_p at steady state may look a bit strange, at first sight. It simply means that the trajectory of G is not tangent to the vehicle longitudinal axis. As shown in Fig. 6.32a, at low lateral acceleration we have very small slip angles α_{1p} and α_{2p} and, as a consequence, β_p has the same sign as δ_v. At high lateral acceleration, the large slip angles cause β_p to become of opposite sign with respect to δ_v, as shown in Fig. 6.32b.

The speed u_β that makes $\beta_p = v_p = 0$ is given by (6.231) and is equal to (if $\chi = 0$)

$$
u_\beta = \sqrt{\frac{C_2a_2l}{a_1m}}
\tag{6.234}
$$

It is called *tangent speed* [10, p. 174].

6.15.6 Lateral Wind Gust

It is of some practical interest to study the behavior of a vehicle (albeit a very linear one) when suddenly subjected to a lateral force, like the force due to a lateral wind gust hitting the car when, e.g., exiting a tunnel. As shown in Sect. 6.15.7, the same mathematical problem also covers the case of a car going straight along a banked road.

We have only to modify the equilibrium equations (6.194) by adding a lateral force $\mathbf{F}_l = -F_l\,\mathbf{j}$, applied at a distance x from G

$$\begin{aligned} m(\dot{v} + ur) &= F_{y_1} + F_{y_2} - F_l \\ J_z \dot{r} &= F_{y_1} a_1 - F_{y_2} a_2 - F_l x. \end{aligned} \tag{6.235}$$

where $x > 0$ if $\mathbf{F}_l$ is applied between G and the front axle. The other equations are not affected directly by $\mathbf{F}_l$.

The equations of motion are like in (6.199), with the only difference that the term

$$\mathbf{b}_F = -\begin{bmatrix} 1/m \\ x/J_z \end{bmatrix} F_l \tag{6.236}$$

must be added to the known vector.

If we assume $\delta_v = 0$, the steady-state conditions $\mathbf{w}_p$ are obtained, as usual, by solving the system of equations $-\mathbf{A}\mathbf{w}_p = \mathbf{b}_F$, with $\mathbf{A}$ as given in (6.201). Accordingly, we have the following quantities at steady-state

$$\begin{aligned} v_p &= \frac{[x(C_1 a_1 - C_2 a_2 + mu^2) - (C_1 a_1^2 + C_2 a_2^2)]u}{C_1 C_2 l^2 - mu^2(C_1 a_1 - C_2 a_2)} F_l, \\ r_p &= \frac{[C_1 a_1 - C_2 a_2 - x(C_1 + C_2)]u}{C_1 C_2 l^2 - mu^2(C_1 a_1 - C_2 a_2)} F_l = -(x - e)\frac{(C_1 + C_2)u}{C_1 C_2 l^2 - mu^2(C_1 a_1 - C_2 a_2)} F_l, \end{aligned} \tag{6.237}$$

where

$$e = \frac{C_1 a_1 - C_2 a_2}{C_1 + C_2} \tag{6.238}$$

Should the steer angle be non-zero, it suffices to superimpose the effects. This is legitimate because of the linearity of the equations.

This quantity e in (6.238) is often called *static margin*. The yaw rate is zero, that is $r_p = 0$, if and only if the lateral force is applied at a distance e from G. This is the distance that makes the vehicle translate diagonally under the action of a lateral force, as shown in Fig. 6.64. The point N_p on the axis of the vehicle at a distance e from G is called *neutral steer point*.

Obviously, the condition $r_p = 0$ with $\delta_v = 0$ is equivalent to $\alpha_{1p} = \alpha_{2p} = \alpha_p$. Inserting this condition into (6.235) we get

$$\begin{aligned} 0 &= (C_1 + C_2)\alpha_p - F_l \\ 0 &= (C_1 a_1 - C_2 a_2)\alpha_p - F_l e, \end{aligned} \tag{6.239}$$

which provide another way to obtain e.

An oversteer vehicle has $e > 0$, whereas $e < 0$ in an understeer vehicle.

If $\delta_v = 0$, the steady-state distance R_p is

$$R_p = \frac{u}{r_p} = \frac{C_1 C_2 l^2 - mu^2(C_1 a_1 - C_2 a_2)}{-(x - e)(C_1 + C_2)F_l}. \tag{6.240}$$

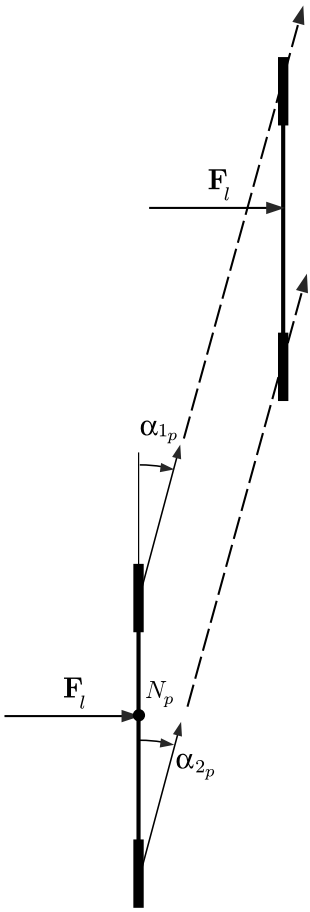

Fig. 6.64 Lateral force applied at the neutral point N_p (i.e., $x = e$)

The numerator is always positive if $u < u_{\text{cr}}$. Therefore, $R_p > 0$ if $x < e$, and vice versa.

If the point of application of the lateral force is located ahead of the neutral point N_p, the vehicle behaves like in Fig. 6.65, turning in the same direction as the lateral force. This is commonly considered good behavior.

If the point of application of the lateral force is behind the neutral point N_p, the vehicle behaves like in Fig. 6.66. This is commonly considered bad behavior.

Of course, since an oversteer vehicle has the neutral point N_p ahead of G, the likelihood that a wind gust applies a force behind the neutral point is higher, much higher, than in an understeer vehicle.

To understand why the first case is considered good, while the second is considered bad, we have to look at the lateral forces that the tires have to exert. In the first case, the inertial effects counteract the wind gust, thus alleviating the tire job. In the second case, the inertial effects add to the lateral force, making the tire job harder.

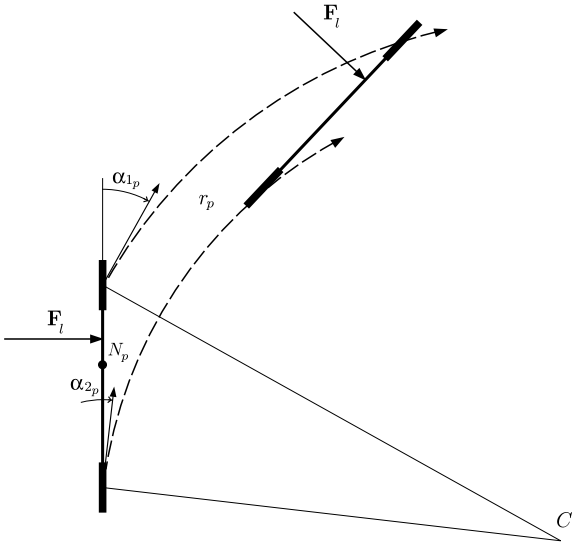

Fig. 6.65 Lateral force applied at a point ahead of the neutral point ($x > e$)

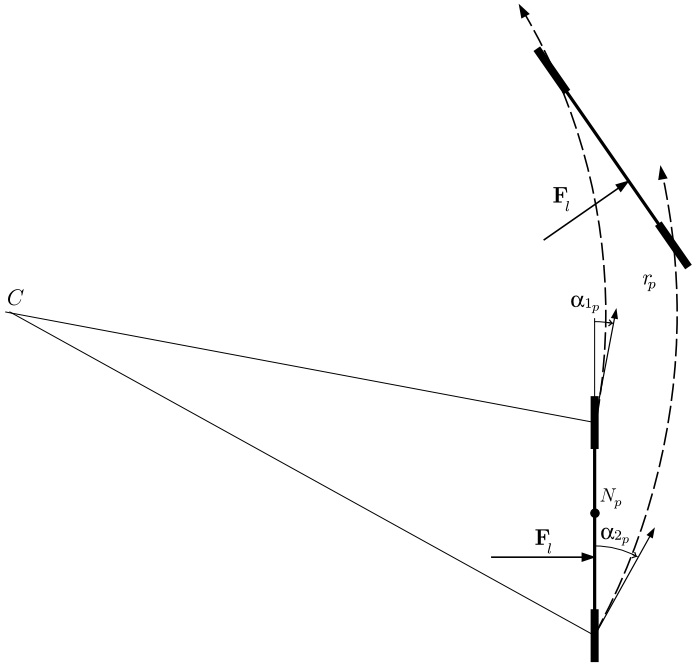

Fig. 6.66 Lateral force applied at a point behind the neutral point ($x < e$)

Fig. 6.67 Lateral force applied by means of a rocket (General Motors Corporation, circa 1960)

Figures 6.65 and 6.66 show a lateral force constantly perpendicular to the vehicle axis, pretty much like if a rocket were strapped on the side of the car. Indeed, in some cases a rocket has been really employed as shown in Fig. 6.67, taken from a presentation by Tom Bundorf at the SAE Automotive Dynamics and Stability Conference (2000).

6.15.7 Banked Road

A car going straight on a banked road is subject to a lateral force due to its own weight. Therefore, it is a situation somehow similar to a lateral wind gust, but not equal. The main difference is that the lateral force is now applied at G.

Understeer and oversteer vehicles behave differently, as shown in Fig. 6.68. Both axles must exert lateral forces directed uphill to counteract the weight force $mg \sin \varepsilon$. Therefore, both must work with positive slip angles α_1 and α_2, if the banking is like in Fig. 6.68. However, due to the different locations of the neutral point N_p with respect to G, the two front axles cannot have the same slip angle. To go straight, we must steer the front wheels uphill in an understeer vehicle and (apparently) downhill in an oversteer vehicle, as shown in Fig. 6.68. More precisely, in both cases $\alpha_1 - \delta_1 = \alpha_2$, where $\delta_1 > 0$ if the vehicle is understeer, while $\delta_1 < 0$ if the vehicle is oversteer.

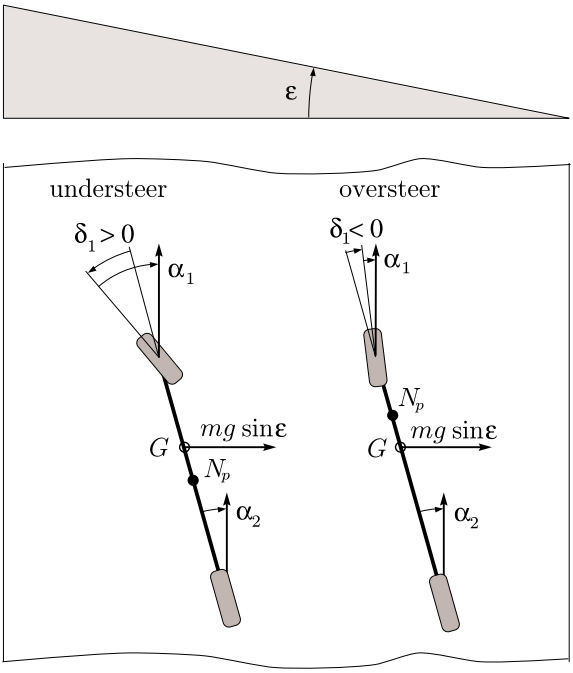

Fig. 6.68 Understeer and oversteer vehicles going straight on a banked road

6.16 Compliant Steering System

Many modern cars use rack and pinion steering mechanisms. The steering wheel turns the pinion gear, which moves the rack, thus converting rotational motion into linear motion. This motion applies steering torque to the front wheels via tie rods and a short lever arm called the steering arm.

So far we have assumed the steering system to be perfectly rigid, as stated on p. 67 and 232. More precisely, Equation (3.198) have been used to relate the steer angles δ_{ij} of each wheel to the angle δ_v of the steering wheel.

In the single track model (Fig. 6.20) we have taken a further step, assuming that the left and right gear ratios of the steering system are almost equal, that is

$$(\tau_{11} = \tau_{12}) = \tau_1 \qquad \text{and} \qquad (\tau_{21} = \tau_{22}) = \tau_2 \tag{6.49'}$$

thus getting (6.50)

$$\begin{aligned} (1 + \chi)\delta = \delta_1 = \tau_1 \delta_v \\ \chi \delta = \delta_2 = \tau_2 \delta_v \end{aligned} \tag{6.50'}$$

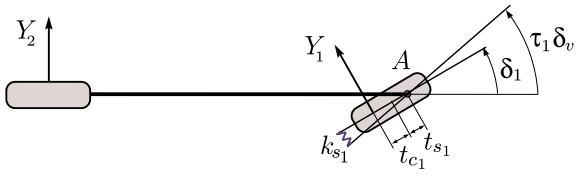

Fig. 6.69 Single track model with compliant steering system

Now, in the framework of the *linear* single track model, we relax the assumption of rigid steering system. This means to make a few changes in the congruence equations (6.195), since δ_1 and $\tau_1\delta_v$ are no longer equal to each other.

6.16.1 Governing Equations

As shown in Fig. 6.69, the steering system now has a finite angular stiffness k_{s_1} with respect to the axis about which the front wheel steers. In a turn, the lateral force Y_1 exerts a vertical moment with respect to the steering axis A because of the pneumatic trail t_{c_1} and also of the trail t_{s_1} due to the suspension layout (see Fig. 3.1). The effect of this vertical moment $Y_1(t_{c_1} + t_{s_1})$ on a compliant steering system is to make the front wheel steer less than $\tau_1\delta_v$. More precisely, we have that (Fig. 6.69)

$$\delta_1 = \tau_1\delta_v - \frac{Y_1(t_{c_1} + t_{s_1})}{k_{s_1}} \tag{6.241}$$

The computation of the pneumatic trail t_{c_1} is discussed on p. 490.

Accordingly, the congruence equations (6.195) of the linear single track model become

$$\begin{aligned} \alpha_1 &= \delta_1 - \frac{v + ra_1}{u} \\ \alpha_2 &= \chi\tau_1\delta_v - \frac{v - ra_2}{u} \end{aligned} \tag{6.242}$$

with the additional equation (6.241).

On the other hand, the equilibrium equations

$$\begin{aligned} m(\dot{v} + ur) &= Y = Y_1 + Y_2 \\ J_z\dot{r} &= N = Y_1a_1 - Y_2a_2 \end{aligned} \tag{6.194'}$$

and the constitutive equations

$$\begin{aligned} Y_1 &= C_1\alpha_1 \\ Y_2 &= C_2\alpha_2 \end{aligned} \tag{6.196'}$$

do not change at all.

6.16.2 *Effects of Steer Compliance*

Equation (6.241) can be rewritten taking the first equation in (6.196) into account

$$\delta_1 = \tau_1 \delta_v - \frac{C_1(t_{c_1} + t_{s_1})}{k_{s_1}} \alpha_1 = \tau_1 \delta_v - \varepsilon \alpha_1 \tag{6.243}$$

where

$$\varepsilon = \frac{C_1(t_{c_1} + t_{s_1})}{k_{s_1}} \tag{6.244}$$

The first congruence equation becomes

$$(1 + \varepsilon)\alpha_1 = \tau_1 \delta_v - \frac{v + a_1 r}{u} \tag{6.245}$$

which leads naturally to define a fictitious slip angle

$$\tilde{\alpha}_1 = (1 + \varepsilon)\alpha_1 \tag{6.246}$$

and, consequently, a fictitious slip stiffness

$$\tilde{C}_1 = \frac{C_1}{1 + \varepsilon} \tag{6.247}$$

Summing up, the linear single track model with *compliant* steering system is governed by the set of equations

$$\begin{aligned} m(\dot{v} + ur) &= Y = Y_1 + Y_2 \\ J_z \dot{r} &= N = Y_1 a_1 - Y_2 a_2 \\ \tilde{\alpha}_1 &= \tau_1 \delta_v - \frac{v + r a_1}{u} \\ \alpha_2 &= \chi \tau_1 \delta_v - \frac{v - r a_2}{u} \\ Y_1 &= \tilde{C}_1 \tilde{\alpha}_1 \\ Y_2 &= C_2 \alpha_2 \end{aligned} \tag{6.248}$$

which is formally identical to the set governing the single track model with rigid steering system. Therefore, the analysis developed in Sect. 6.15 applies entirely, provided we take into account that $C_1 \to \tilde{C}_1$ and $\alpha_1 \to \tilde{\alpha}_1$.

Since $\tilde{C}_1 < C_1$, a compliant steering system makes the vehicle behavior more understeer.

6.17 Road Vehicles with Locked or Limited Slip Differential

The handling of cars equipped with either a locked or a limited-slip differential is addressed in Sect. 7.5, that is in the chapter devoted to the handling behavior of race cars. This has been done because the limited-slip differential is a peculiarity of almost all race cars, whereas very few road cars have it.

6.18 Exercises

6.18.1 Camber Variations

As shown in (6.18) *and in Fig.* 6.7*, camber variations due to vehicle roll motion are determined by some suspension parameters. Given the track length* t_i*, find the values of* c_i *to have*:

1. $\Delta\gamma_i/\phi_i^s = -1$;
2. $\Delta\gamma_i/\phi_i^s = 0$;
3. $\Delta\gamma_i/\phi_i^s = 1$.

Solution

It is a simple calculation to obtain

1. $c_i = t_i/4$;
2. $c_i = t_i/2$;
3. $c_i = +\infty$.

Quite a big difference.

6.18.2 Ackermann Coefficient

According to (6.19)*, and assuming* $\delta_1^0 = 0$, $l = 2.6\text{m}$, $t_1 = 1.6\text{m}$, *and* $\varepsilon_1 = 1$ *(Ackermann steering), compute* δ_{11} *and* δ_{12} *when* $\tau_1\delta_v$ *is equal to* $5°$, $10°$, *and* $15°$.

Solution

It is a simple calculation to obtain

1. $\delta_{11} = 5.13°$, $\delta_{12} = 4.87°$;
2. $\delta_{11} = 10.54°$, $\delta_{12} = 9.46°$;
3. $\delta_{11} = 16.21°$, $\delta_{12} = 13.79°$.

We see that the Ackermann correction is relevant, with respect to parallel steering, only for not so small steer angles.

6.18.3 Toe-In

Repeat the previous calculations now with 1° *of toe-in.*

Solution

1. $\delta_{11} = 4.13^\circ$, $\delta_{12} = 5.87^\circ$;
2. $\delta_{11} = 9.54^\circ$, $\delta_{12} = 10.46^\circ$;
3. $\delta_{11} = 15.21^\circ$, $\delta_{12} = 14.79^\circ$.

Quite influential.

6.18.4 Steering Angles

With reference to (6.50)*, obtain the relationship between* χ *and* κ *for any steering system.*

Solution

From the following system of equations

$$\begin{aligned} (1+\kappa)\tau &= \tau_1 \\ \kappa\tau &= \chi\tau_1 \end{aligned} \tag{6.249}$$

we obtain

$$\chi = \frac{\kappa}{1+\kappa} \tag{6.250}$$

6.18.5 Axle Characteristics

Axle characteristics are very important in vehicle dynamics. In Sect. 6.5.3*, the effects of the following set-up parameters were discussed (not in this order):*

1. *roll stiffness;*
2. *static camber angles;*
3. *roll camber;*
4. *roll steer;*
5. *toe-in/toe-out.*

Some of these parameters have similar effects on the axle characteristics. Before going back to Sect. 6.5.3*, think about the physics of each parameter and try to figure out the similarities.*

Solution

Have a look at Sect. 6.5.3.

6.18.6 Playing with Linear Differential Equations

Find out how to go from (6.126) to (6.128), that is, from a system of two first-order linear differential equations with constant coefficients to two second-order equations.

Solution

Like in (6.126), the starting point is

$$\begin{aligned} \dot{\beta}_t &= a_{11}\beta_t + a_{12}\rho_t \\ \dot{\rho}_t &= a_{21}\beta_t + a_{22}\rho_t \end{aligned} \tag{6.251}$$

where a_{ij} are the entries of matrix $\mathbf{A}$, as in (6.144).

We can see (6.251) as a system of two algebraic equations and solve it with respect to $\dot{\beta}_t$ and β_t, thus getting

$$\begin{aligned} \beta_t &= \frac{-a_{22}\rho_t + \dot{\rho}_t}{a_{21}} \\ \dot{\beta}_t &= \frac{(a_{12}a_{21} - a_{11}a_{22})\rho_t + a_{11}\dot{\rho}_t}{a_{21}} \end{aligned} \tag{6.252}$$

Differentiating the first equation in (6.252) and setting it equal to the second equation in (6.252) provides the sought second-order linear differential equation

$$\ddot{\rho}_t - (a_{11} + a_{22})\dot{\rho}_t + (a_{11}a_{22} - a_{12}a_{21})\rho_t = 0 \tag{6.253}$$

exactly like in (6.128).

6.18.7 Static Margin

Compute the static margin for the single track model defined on p. 306.

Solution

To compute the static margin we have to use (6.238). The result is $e = -0.46\,\text{m}$. A negative value is typical of understeer vehicles.

6.18.8 Banked Road

The same vehicle is travelling on a straight road with 6° of banking. Compute the steering wheel angle required to have a trajectory parallel to the road (that is to go straight ahead).

Solution

With the aid of Fig. 6.68, we see that the rear axle has to counteract a lateral force $Y_2 = mg\sin(6^\circ)a_1/l = 452.8\,\text{N}$. That means that the rear axle operates with a slip angle $\alpha_2 = Y_2/\Phi_2(0) = 0.29^\circ$.

Similarly, the front axle has to balance a force $Y_1 = mg\sin(6^\circ)a_2/l = 724.4\,\text{N}$, which needs a slip angle $\alpha_1 = Y_1/\Phi_1(0) = 0.59^\circ$.

Therefore, the front steer angle has to be $\delta_1 = 0.59 - 0.29 = 0.3^\circ$. The steering wheel angle is $\delta_v = 20 \times 0.3 = 6^\circ$.

Of course, the vehicle slip angle is $\beta = -\alpha_2 = -0.29^\circ$.

6.18.9 Rear Steer

Repeat the calculations of the banked road for the two vehicles with rear steer whose features are listed in Table 6.1.

Solution

First we consider the vehicle with $\kappa = -0.1$. We have $Y_2 = 331.8\,\text{N}$ and hence $\alpha_2 = 0.26^\circ$. Similarly, $Y_1 = 845.4\,\text{N}$, and $\alpha_1 = 0.56^\circ$.

To obtain the net steer angle δ we have to solve the equation

$$\alpha_1 - (1+\kappa)\delta = \alpha_2 - \kappa\delta \tag{6.254}$$

with $\kappa = -0.1$, which provides $\delta = 0.3^\circ$, and hence a steering wheel angle $\delta_v = 0.3 \times 20/0.99 = 6.0^\circ$.

The vehicle slip angle is $\beta = -(0.26 + 0.1 \times 0.3) = -0.29^\circ$.

Then we consider the vehicle with $\kappa = 0.1$. We have $Y_2 = 622.2\,\text{N}$ and hence $\alpha_2 = 0.32^\circ$. Similarly $Y_1 = 555.0\,\text{N}$, and $\alpha_1 = 0.65^\circ$.

To obtain the net steer angle δ we have to solve (6.254), with $\kappa = 0.1$, which provides $\delta = 0.33^\circ$, and hence a steering wheel angle $\delta_v = 0.3 \times 20/0.99 = 6.0^\circ$.

The vehicle slip angle is $\beta = -(0.32 - 0.1 \times 0.33) = -0.29^\circ$.

As expected, for the driver the three vehicles behave exactly the same way: same steer wheel angle δ_v, same vehicle slip angle β. The three vehicles also have the same static margin $e = -0.46\,\text{m}$.

6.18.10 Wind Gust

Are the three vehicles of Table 6.1 fully equivalent with respect to a lateral wind gust?

Solution

These three vehicles are compared in Fig. 6.70. The point of application of a lateral force F_l due to a wind gust depends on the shape of the vehicle. However, we can

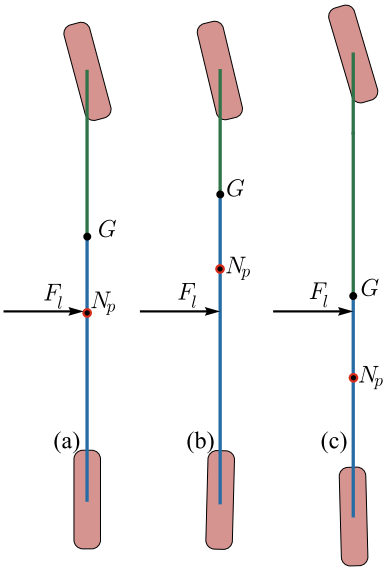

Fig. 6.70 Comparison of the three vehicles of Table 6.1 under a lateral wind gust

reasonably assume F_l be applied like in Fig. 6.70. Should this be the case, the three vehicles would behave very differently.

Vehicle (a), which has $\kappa = 0$, would do like in Fig. 6.64. Vehicle (b), which has $\kappa = -1$, would do like in Fig. 6.66. Vehicle (c), which has $\kappa = 1$, would do like in Fig. 6.65.

Therefore, the three vehicles are not equivalent with respect to a lateral wind gust. Actually, their behaviors can be completely different.

6.19 Summary

Road cars are characterized by having an open differential and no significant aerodynamic downforces. These two aspects allow for some substantial simplifications of the vehicle model. With the additional assumption of equal gear ratios of the steering system for both front wheels, we have been able to formulate the single track model.

Quite contrary to common belief, we have shown that the axle characteristics can take into account many vehicle features, like toe in/out, roll steering, camber angles and camber angle variations.

The steady-state analysis has been carried out first using the classical handling diagram. Then, the new global approach MAP (Map of Achievable Performance), based on handling maps on achievable regions has been introduced and discussed in detail. This new approach shows the overall vehicle behavior at a glance.

Stability and control derivatives have been introduced to study the vehicle transient behavior. Moreover, the relationship between data collected in steady-state tests and vehicle transient behavior has been thoroughly analyzed in a systematic framework. To prove the effectiveness of these results, a number of apparently different vehicles with the same handling characteristics have been generated.

6.20 List of Some Relevant Concepts

p. 213 — road cars are normally equipped with an open differential;
p. 231 — to go from the double track to the single track model we need the following additional assumption: the left and right gear ratios of the steering system are almost equal;
p. 243 — the main feature of the single track model is that the two wheels of the same axle undergo the same apparent slip angle;
p. 230 — some steady-state quantities are functions of the lateral acceleration only because of the open differential and no significant downforces;
p. 275 — some "fundamental" concepts in classical vehicle dynamics are indeed very weak if addressed with open mind;
p. 291 — the understeer gradient is not a good parameter and should be dismissed.

6.21 Key Symbols

a_1	distance of G from the front axle
a_2	distance of G from the rear axle
a_n	centripetal acceleration
a_t	tangential acceleration
a_x	longitudinal acceleration
a_y	lateral acceleration
$\tilde{a}_y$	steady-state lateral acceleration
C	velocity center
C_i	lateral slip stiffness of ith axle
C_x, C_y, C_z	aerodynamic coefficients
d	diameter of the inflection circle
F_l	lateral force (wind gust)
$F_{x_{ij}}$	tire longitudinal force
$F_{y_{ij}}$	tire lateral force
$F_{z_{ij}}$	tire vertical force
g	gravitational acceleration
G	center of mass
h	height of G
J_x, J_y, J_z	moments of inertia

K	acceleration center
K	classical understeer gradient
k_ϕ	total roll stiffness
k_{ϕ_i}	global roll stiffness of ith axle
$k_{\phi_i}^p$	tire roll stiffness
$k_{\phi_i}^s$	suspension roll stiffness
l	wheelbase
m	mass
N	yaw moment
N_β, N_ρ	stability derivatives
N_δ	control derivative
q_1	height of the front no-roll center
Q_1	front no-roll center
q_2	height of the rear no-roll center
Q_2	rear no-roll center
r	yaw rate
R	lateral coordinate of C
r_i	rolling radii
S	longitudinal coordinate of C
S_a	frontal area
t_1	front track
t_2	rear track
u	longitudinal velocity
v	lateral velocity
X	longitudinal force
X_a	aerodynamic drag
Y	lateral force
Y_i	lateral force on the ith axle
Y_β, Y_ρ	stability derivatives
Y_δ	control derivative
Z	vertical force
Z_i	vertical load on ith axle
Z_i^0	static vertical load on ith axle
Z_i^a	aerodynamic vertical load on ith axle
ΔZ	longitudinal load transfer
ΔZ_i	lateral load transfer on ith axle
α_{ij}	tire slip angles
β	ratio v/u
$\hat{\beta}$	vehicle slip angle
β_t	shifted coordinate
(β_y, β_δ)	gradient components
γ_{ij}	camber angles
δ_{ij}	steer angle of the wheels

δ_v	steering wheel angle of rotation
ε_1	Ackermann coefficient
ζ	damping ratio
η_h	internal efficiency of the differential housing
ρ	ratio r/u
ρ_a	air density
ρ_t	shifted coordinate
(ρ_y, ρ_δ)	gradient components
$\sigma_{x_{ij}}$	tire longitudinal slips
$\sigma_{y_{ij}}$	tire lateral slips
τ	steer gear ratio
ϕ	roll angle
Φ_i	slope of the axle characteristics
φ_{ij}	spin slips
ψ	yaw angle
ω_{ij}	angular velocity of the rims
ω_n	natural angular frequency
ω_s	damped natural angular frequency

References

1. Abe M (2009) Vehicle handling dynamics. Butterworth-Heinemann, Oxford
2. Bastow D, Howard G, Whitehead JP (2004) Car suspension and handling, 4th edn. SAE International, Warrendale
3. Dixon JC (1991) Tyres, suspension and handling. Cambridge University Press, Cambridge
4. Font Mezquita J, Dols Ruiz JF (2006) La Dinámica del Automóvil. Editorial de la UPV, Valencia
5. Frendo F, Greco G, Guiggiani M, Sponziello A (2007) The handling surface: a new perspective in vehicle dynamics. Vehicle Syst Dyn 45:1001–1016
6. Gillespie TD (1992) Fundamentals of vehicle dynamics. SAE International, Warrendale
7. Guiggiani M (2007) Dinamica del Veicolo. CittaStudiEdizioni, Novara
8. Mastinu G, Ploechl M (eds) (2014) Road and Off-Road Vehicle System Dynamics Handbook. CRC Press, Boca Raton
9. Meywerk M (2015) Vehicle dynamics. Wiley, New Jersey
10. Milliken WF, Milliken DL (1995) Race car vehicle dynamics. SAE International, Warrendale
11. Pacejka HB (1973a) Simplified analysis of steady-state turning behaviour of motor vehicles, part 1. handling diagrams of simple systems. Vehicle Syst Dyn 2:161–172
12. Pacejka HB (1973b) Simplified analysis of steady-state turning behaviour of motor vehicles, part 2: Stability of the steady-state turn. Vehicle Syst Dyn 2:173–183
13. Pacejka HB (1973c) Simplified analysis of steady-state turning behaviour of motor vehicles, part 3: More elaborate systems. Vehicle Syst Dyn 2:185–204
14. Popp K, Schiehlen W (2010) Ground vehicle dynamics. Springer, Berlin
15. Schramm D, Hiller M, Bardini R (2014) Vehicle dynamics. Springer, Berlin
16. Wong JY (2001) Theory of ground vehicles. Wiley, New York